Università degli studi di Roma "La Sapienza"

FACOLTÁ DI INGEGNERIA

Laurea specialistica in Ingegneria per l'ambiente ed il territorio

Tesi di Laurea specialistica sperimentale

The effect of weathering on slope instability

The Marbrière versant, Grasse, Alpes Maritimes, France

Stage svolto presso :

Geoscience Azur

CENTRE NATIONAL DE LA RECHERCHE SCIENTIFIQUE

Université Nice Sophia-Antipolis

Relatore all' estero :	Relatore in sede :	Candidata :
Prof.	Prof.	Valeria Ida
Thomas Lebourg	Giuseppe Sappa	Silvestri Demandt

ANNO ACCADEMICO 2009/2010

INDEX:

LIST OF FIGURES:

LIST OF TABLES:

INTRODUCTION

Landsliding is worldwide considered as a phenomenon of great risk and is the cause of major catastrophes due to the lack of identification ability. Therefore its study and comprehension is of crucial importance for risk management on a scale of territorial politics. The Maritime Alps in southern France are particularly affected by this phenomenon and are closely monitored by the BRGM (Bureau de recherches géologiques et minières) and Géoazur which is the sector of the CNRS (Centre national de la recherche scientifique) which studies the dynamics of the lithosphere. In this area a zone of special vulnerability and interest is the Marbrière Versant which presents characteristic deformations of gravitational slope movements like topographic anomalies as crevasses, steep slopes and cliffs, superficial slides, subsidence, rock falls, collapses and vegetal and morphologic alignments which make strongly suppose that this sector is affected by the re activation in gravitational dynamics of a series of major faults. In the framework of the study of Zerathe, (2009), which concerns the deep seated gravitational slope deformation (DSGSD) hazard in this extremely vulnerable area an anomaly has been observed in one of the lower levels of the stratigraphic log: The Dolomite of the Hettangien. This series presents a brittle and soil like behaviour on the studied versant in opposition to the sane rock of which it is composed elsewhere. Especially in proximity of one of the major faults which represents a sort of lateral boundary of the slope movement the alteration of the dolomite is in a very advanced state and can easily been studied thanks to a huge cliff face that crops out in this series.

In this study the relationship between the extreme alteration of this dolomite rock of the Hettangien and its mechanical properties is investigated.

- On the one hand the relation weathering-mechanical properties is studied in **time:** How much are the different states of progressive weathering altering the rock properties and which are these properties?
- On the other hand this relation of weathering-mechanical properties is studied in **space:** Is this extremely high grade of weathering caused by the proximity of the fault and how does it affect the mechanical properties ?

This leads to the question of how much influence these changing mechanical parameters will have on gravitational movements and on slope stability?

In order to answer these questions index and engineering design tests have been carried out in situ on the first 20m of the outcropping cliff face and in the laboratory on its drilled rock cores and its collected soil samples. The following tests have been performed:

- Electric resistivity tomography (ERT)
- Apparent Joint Separation (AJS)
- Schmidt Hammer Test (SHRV)
- Triaxial compression strength (TCS)
- Uniaxial compressive strength (UCS)
- Density
- Effective porosity
- Rock Quality Designation (RQD)
- Image analysis of thin slices

During this investigation a simple means for determining rock strength was studied since it came out that laboratory testing for the determination of mechanical strength of rock is very laborious, time consuming and expensive.

To describe the studied area, the problematic, the performed analysis and to discuss the results of all the tests, their relations amongst each other, and their role on slope instabilities, and the conclusions that can be made, this work has been structured in six chapters:

- The first chapter is an introduction to slope instabilities describing the predisposing, preparing and triggering factors of landslides, pointing out the important role that weathering plays in the destabilisation of versants and the kinematics of its action.

- The second chapter introduces the studied area: The geo-morphological properties of the Marbrière Versant and of the studied cliff face are described.

- In the third chapter the problematic of the study is introduced and discussed: The deep seated gravitational slope deformation of the Marbrière versant, the pre-cutting of the versant by a network of major faults and their reactivation are discussed and the following chapters of analysis are presented.

- In the fourth chapter every test is singularly discussed and the investigating methods are described in terms of the theory on which they are based, their bibliographic references, the test protocols, the analysis of the results in relation to the distance from the fault and a preliminary conclusion is presented.

- In Chapter 5 a Principal Component Analysis is carried out with the results of the performed tests trying to correlate them among each other. A law of correlation between the parameters of SHRV and UCS is proposed in order to make the determination of mechanical parameters of shear strength with a smaller spacing throughout the whole versant and with less temporary and pecuniary effort. An electric resistivity tomography of the cliff face is analysed and its results discussed in comparison to the other test results.
  Afterwards some physical and mechanical parameters of the dolomite rock of the studied cliff face are confronted with those of the same rock on other parts of the versant. The influence of the fault and a syndiagenetic cause of this variation are discussed.
  With the mechanical parameters determined by the engineering design tests in this study a stability calculus of the security factor of the versant is carried out for several scenarios of different saturation and the different time depending results are discussed.

- In chapter 6 the guideline questions of this study are answered and the conclusions are made. Propositions of further investigations to deepen the knowledge on the role that weathering plays on slope instabilities are made. Also a further study of the use of the Schmidt Hammer as a simple mean to determine mechanical parameters of this peculiar lithology on the Marbrière versant is proposed in order to confirm the found law. Finally the instrumental equipment that will be installed in key sectors of the versant that face a particular risk of instability are presented.

Chapter 1 : Slope instabilities; Bibliographic approach

1.1 *Intervening factors in the instability process:*

The generic term "Landslide" defines the displacement of a volume of rock, soil or debris on a slope. This definition puts a multitude of more or less known and defined phenomenons into a frame. The factors that control these movements are extremely various (gradient, lithologie, hydrogeologic and climatic conditions, structural heritage ...) as well as the cinematic of the phenomenon. As summarised by Jomard (2006) and El Bedoui (2009) cinematically a landslide can broadly be divided in 3 distinct phases:

- **preparatory phase** (also called the phase of generation)
- **rupture and propagation** (phases of acceleration and deceleration) better known as paroxysm
- **phase of relaxation** or deposition in which the movement stops

These three phases are the more distinct between each other the faster the phenomenon is.
For a better comprehension and predictability of landslides the preparatory phase has to be studied, and when possible monitored and analysed.

The preparatory phase is that phase in which the rock mass passes from a stable state to an active instable one. It is the result of the action of the **preparing factors** which brings the slope to rupture, started by the action of the so called **triggering factors.**

Two destabilising processes can so be defined:

- **Slow phenomenons** which require a long period of time to affect the stability of the slope (tectonics, alteration...) These are the preparing factors.
- **Fast phenomena** with a very short action time which take part in the rupture (earthquakes, extreme climatic events as heavy rainfalls or snow, atrophic development). These are the triggering factors.

Gravity is the principal agent in slope instabilities: Stability can simply be defined as the ratio of the forces that tend to start a movement and those that are opposed. The breakdown of the equilibrium of a massif is therefore defined by the modification of a stabilising parameter or the addition of destabilising parameters. Therefore the question that has to be answered is: "which are those parameters that allow the modification of one or the other stabilising or destabilising parameters?

1.1.1. Pre-disposing factors:

The predisposing factors come from the structure of the rock massif resulting from its geological history:

- **Lithologie:** an alternation of layers with different mechanical behaviours (ex: limestone vs marl) predispose a slope to flow-creep. The orientation of the stratification in relation to the morphologic gradient might for example lead to a bank on bank sliding.
- **The rock fabric** is a source of mechanical discontinuities in case of stratification, schistosities or foliation.
- **Discontinuities** (fractures, joints, faults, diaclasts...) and their density, layout and orientation within the massif lead the way for the preparing factors which drive to rupture.

1.1.2. Preparing factors:

Gravitational movements result from a long, slow and progressive preparation of the slope. This preparation is generally much longer and important for the destabilisation of rock material than for soils (which derive majorly from the alteration of rocks) In any case the preparation of a versant consists in diminishing the rock resistance along existent anisotropies or in affecting the structure itself of the massif.

- **Geological factors:**

  - **The geologic material**: Certain materials are subject to the degradation of their mechanical properties in time due to the influence of solicitations as for example water or vibrations , and will so concentrate their deformations in certain points.
  - **Tectonic movements**: they modify the characteristics of the rock due to the displacement, throw and heave of the fault or the formation of bends. These actions can play an important role both in the short and in the long term evolution in tectonically active areas. (Figure 27,a)
  - **Alteration and weathering**: The alteration is defined as the transformation of rock material due to external actions. It can lead either to a consolidation (patina) or to a fragmentation or better called macro-mechanic alteration which modifies the rock structure, grinds it, forming grains and which is at the origin of the diminution of the resistance of rock materials. (ex: Figure 27) The effects of alteration on slope instabilities have been studied by many authors (a resume of their results is displayed in chapter 1.3.) and are also a key factor of the present work and will largely be analysed and discussed in the following parts. An extra chapter (1.2) has been dedicated to the physical and chemical weathering agents and their effects on rock structure and strength.

- **Morphologic and geomorphologic factors:**

  - **The creation and modification of morphologic gradients**: The tectonic or isostatic surrection of a massive is at the origin of the increase of the slope gradient. The incision of valleys is as well a modification of the slope morphology. The return to an equilibrium slope gradient can be an either slow

or fast phenomenon of compensation due to erosion and is largely considered as responsible for ground movements

- **Erosion**: Majorly erosion is due to the action of water, through dissolution or canalisation. The subtraction of material from the base of a slope is caused by the mechanical action of fluviatile circulation, of ocean-tide cycles and of the action of waves. The variation of the plant cover in function of climatic fluctuations or fire is a supplemental factor which contributes to erosion.

- **Permanent and punctual physical factors**:

  - **Gravity** is the only physical permanent factor and it is the origin of the majority of gravitational movements. It is at the same time a preparatory and a triggering factor.
  - **Punctual physical factors** are normally very intense but do not directly lead to rupture. These can be extreme climatic conditions as intense precipitations, exceptional floods, tempests, etc. or geological punctual solicitations as seisms or volcanic eruptions.

- **Antrophic factors:**

  Human activity can sometimes be an additional factor in the evolution of slopes towards rupture. Normally these movements are of small amplitude and only exceptionally of big magnitude. Nevertheless some cases of catastrophic movements caused by anthropic activity can be cited:
  - **Mineral activity** for the Elm and Frank catastrophes
  - **Hydraulic causes** for the Vajont
  - **Pastoral and agricultural causes** for the Mayunmarca slide in Peru.

  Frequently the origin of movements of small to middle amplitude is the misreading and the failed anticipation of overpressures, overloads or incorrect drainage.

1.1.3. Triggering factors (and/or accelerating factors):

Ground movements are started by external triggering actions which increment the shear stress or diminish the resistance of the material. The triggering external solicitations are the same than the punctual physical factors of preparation.

- **Seismic and volcanic solicitations**:

  Our days it is clearly demonstrated that the tremors of the earth are the major source of gravitational movements in active zones. The shear stress resistance of soils and rock diminish due to the augmentation of interstitial pressure and react strongly to the solicitations ported by S-waves.
  - The action of volcanic activity is more complex but often leads equally to destabilisations and earth movements. Soil inflations, hydrothermal activity, explosions and seismes can all be caused by volcanic activity.

- **Climatic solicitations:**

Climatic factors are normally responsible for the destabilisation of small volumes , but they can be very numerous. The actions of water, which will be discussed in the next paragraph, and of tempests generally induce many superficial movements and can equally be the origin of movements of great amplitude in case of long and/or repetitive solicitations.

- **Overload:**

Overloading a versant modifies its equilibrium. It can have different sources: gravitational movements on top, infiltration of water, overload of glacial material, volcanic depositions, anthropic activity.

1.1.4. A global and particular factor: Water

As cited in the work of Jomard (2006) it is found that from 250 slides described in specialised literature in France, 52% are of hydraulic origin. In fact we have seen that water intervenes in the same time as a preparing and as a triggering factor in the preparation of a slope towards rupture. The action of water can be chemical or mechanical and constitutes an aggravating phenomenon coupled with other solicitations.

1.1.4.1 Origin of water within the versant:

- **Superficial water:**

This is the water that did not penetrate into the versant and is divided into different types:

- **streaming water**
- **evapotranspiration**
- **storage** of water under the form of snow or ice

- **Underground water:**

- **Infiltration of superficial water**: In normal times the soil is saturated only to a certain level (piezometric level). Over this level water can be retained by capillary forces. An input of water from the surface can fill the voids and generate filtration, the speed of this infiltration is controlled by the porosity and permeability on the one hand and by the network of fractures on the other hand. (ex: karst) In the case of this study an important bringing in of water could come from a rupture of the Foulon channel which crosses the whole versant as shown in Figure 6.
- **External alimentation** as water drained from one or several geologic structures from one to another basin.
- **Fossil origin** as storage of water in closed aquifers that date from previous hydrologic cycles.
- **Geothermal origin**
- **Water derived from the global warming**

1.1.4.2 Action of water on the stability of the versant:

- **Superficial water** can have two main effects:

  - **Streaming** acts as a modification factor of the morphology. It can remove material which determines the stability from the foot of the versant. It intervenes as well as a rheological modification of superficial formations in removing fine particles.
  - **Storage** of water under the form of snow and ice can increase the charge and act as an overload.

- **Underground water** induces mechanical and chemical phenomenons which can be grouped in four types:

  - **Effects on the ground properties**: Infiltrations or rising of the ground water level affect the security factor of a versant by an increase of the volumic mass. Moreover the replacement of the gases that are contained in the pores by liquid will diminish the phenomenon of suction, therefore diminish the cohesion. This is called decrease of capillary forces.
  - **Hydrostatic effects**: During the augmentation of the piezometric level, an augmentation of the hydrostatic pressure takes place in the ground. This augmentation of pressure (ΔU) leads to a modification of the stress state of the grains and to a shift of the moor circle towards the envelop-rupture curve (in case of a weak behaviour). (Figure 1) The capillary effect described above is maintained.
  -

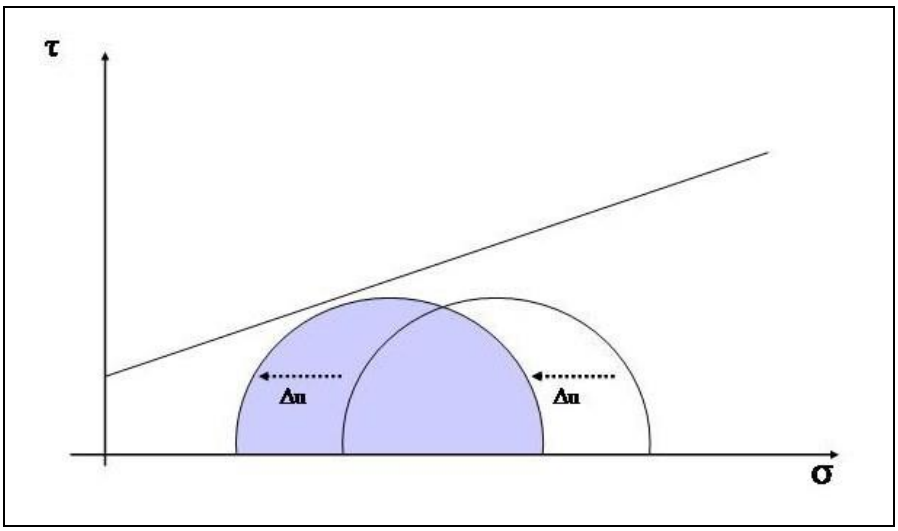

Figure 1 : Modification of the intergranular stress represented on the Mohr circle (Desvarreux in Lebourg, 2000)

  - **Hydrodynamic effects**: The flow of water through rocks produces a thrust on the crossed material. On one hand the transport of fine particles can increase permeability by percolating forces, on the other hand the filling of the pores by the deposition of the fine particles in case of an inefficient flow leads to a diminution of permeability and with it a diminution of the hydraulic capacity. This modification of the hydraulic conditions might allow an augmentation of

the charge/load of water (=charge d'eau) and so of the interstitial pressure of the versant. It comes back to a hydrostatic effect.

- **Chemical effects** are essentially dissolution phenomenons, which lead to a diminution of intergranular bonds and so of the cohesion of soils and rocks. (ex: gypsum, limestone...). Also flocculation phenomenons could take place, of inflation of clays. Mineral transformations, especially in clays could as well change the hydraulic conditions of a versant for example by creating impermeable horizons.

1.1.5. Conclusion:

Alteration is the principal preparing factor for slope instability. Whether it is caused by geologic, morphologic, geomorphologic etc. factors or by water, it is the most important factor in the degradation of the mechanical properties of rock and the instabilisation of rock material. Therefore a more precise definition of physical and chemical weathering will be presented in the next paragraphs. A resume of the results of other authors on how weathering affects slope instabilities is as well presented in paragraph 1.3.

1.2 *Weathering*

Weathering is the breakdown and alteration of rocks and minerals at or near the Earth's surface into products that are more in equilibrium with the conditions found in this environment. The destruction of rocks is the primary source of soil material. This phenomenon concerns igneous, metamorphic and sedimentary rocks. The process of weathering can broadly be divided in two principal mechanisms:

1. **Mechanical or Physical** weathering causes the breakdown of rock material into smaller fragments with no, or only a little change in the chemical composition of the material. The rock fragmentation is caused by the following physical agents:

   - **Temperature variations** cause expansion and contraction : submitted to incessant variations of volume the rock fissures and then breaks.

   - **Frost disintegration** : This type of weathering is common in mountain areas where the temperature is around freezing point. Frost induced weathering, is caused by the expansion of freezing water captured in pores and cracks.

   - **Salt crystallization**: causes disintegration of rocks when saline solutions seep into cracks and joints in the rocks and evaporate, leaving salt crystals behind. These salt crystals expand as they are heated up, exerting pressure on the confining rock.

   - **Pressure release**: also known as unloading, overlying materials (not necessarily rocks) are removed (by erosion, or other processes), which causes underlying rocks to expand and fracture parallel to the surface.

   - **Other types** : Cracking of rocks by plant roots and burrowing animals.

2. **Chemical weathering** is the breakdown of rocks by chemical agents. It involves the change in the composition of rocks, often leading to a 'break down' in its form. This is done through a combination of water and various chemicals to create an acid which directly breaks down the material. Chemical weathering is a gradual and ongoing process as the mineralogy of the rock adjusts to the near surface environment. New or *secondary minerals* develop from the original minerals of the rock.

   - **Dissolution**: Rainfall is acidic because atmospheric carbon dioxide dissolves in the rainwater producing weak carbonic acid. In unpolluted environments, the rainfall pH is around 5.6. Acid rain occurs when gases such as sulphur dioxide and nitrogen oxides are present in the atmosphere. These oxides react in the rain water to produce stronger acids and can lower the pH to 4.5 or even 3.0. Sulphur dioxide, SO_2, comes from volcanic eruptions or from fossil fuels, can become sulphuric acid within rainwater, which can cause solution weathering to the rocks on which it falls.

   - **Carbonatation**: One of the most well-known solution weathering processes is carbonatation process in which atmospheric carbon dioxide leads to solution weathering. Carbonation occurs on rocks which contain calcium carbonate, such as limestone and chalk. This takes place when rain combines with carbon dioxide or an organic acid to form a weak carbonic acid which reacts with calcium carbonate (the limestone) and forms calcium bicarbonate. Calcium bicarbonate is soluble so therefore the rock is dissolved and carried away. This type of weathering can produce landforms such as caves, limestone pavements and sinkholes
     The reactions as follows:

     $CO_2 + H_2O \rightarrow H_2CO_3$
     carbon dioxide + water -> carbonic acid
     $H_2CO_3 + CaCO_3 \rightarrow Ca(HCO_3)_2$
     carbonic acid + calcium carbonate -> calcium bicarbonate

     Carbonation on the surface of well-jointed limestone produces a dissected limestone pavement which is most effective along the joints, widening and deepening them.

   - **Hydration** : Mineral hydration is a form of chemical weathering that involves the rigid attachment of H+ and OH- ions to the atoms and molecules of a mineral. When rock minerals take up water, the increased volume creates physical stresses within the rock.

   - **Hydrolysis** is the destruction of the minerals caused by water, it can be total or partial. In total hydrolysis the mineral is decomposed in its smallest structures (hydroxides and ions) whereas partial hydrolysis is an incomplete degradation of the minerals.

- **Oxidation**: Within the weathering environment chemical oxidation of a variety of metals occurs. The most commonly observed is the oxidation of Fe^{2+} (iron) and combination with oxygen and water to form Fe^{3+} hydroxides and oxides such as goethite, limonite, and hematite. This gives the affected rocks a reddish-brown coloration on the surface which crumbles easily and weakens the rock.

The different types of weathering listed above are in reality strictly interrelated among each other and are in the mean time amplified by and amplifying factor of the other weathering types. In the initial stages of weathering opening of grain boundaries, micro-fracturing and development of inter-granular porosity generally take place. Granular disintegration prepares the rock for chemical attack. Water penetrates into the discontinuities in the rock and begins to cause chemical alteration widening the fractures and penetrating deeper in the rock. In this vicious circle a dense network of closely spaced alteration zones is then produced. (Calcatera and al., 2005, Le Pera and al., 2000.)

1.3 *The effects of Weathering on slope instabilities*

Weathering processes as mechanical, micro-mechanical and chemical are very important as predisposing factors to slope instabilities. In fact pronounced weathering conditions determine meaningful reductions in shear strength and therefore a reduction of the safety factor of the bed rock and a consequent increase in possible slope failures Many authors studied the relationship of weathering with slope instabilities mainly in crystalline rocks (plutonic and metamorphic). (Borelli and al. 2007, Jaboyedoff and al. 2004, Calcaterra and al. 2005, Shengwen and al. 2009, Pellegrino and al. 2006, Durgin 1977).
Borrelli et al. (2007) propose a control procedure consisting of field observations and simple index tests to survey weathering and confirm with their results the relationship between rock weathering grades and slope instability.
Calcaterra & Parise (2005) find that it is extremely difficult to draw a straightforward relationship between landslides and weathering but indicate that over 50% of the slope movements of the Serre massif in Calabria (crystalline rock) occur in weathering grades IV and IV-V according to the classification scheme of the Geotechnical Control Office in Hong Kong. Nevertheless a third of the mass movements occur in weathering grades II-IV which is believed to result from the presence of significant discontinuities in the bedrock.
Jaboyedoff et al. (2004) demonstrate that the effect of chemical weathering coupled with saturation-unsaturation cycles of granite-gneisses plays an important role in slope instabilities.
Durgin (1977) states that the engineering properties of granitic rock change as weathering continues. Granitoids break down progressively from massive blocks to a deep layer of clay-size particles. Therefore, the disciplines of both rock mechanics and soil mechanics are useful for investigating the slope stability of such materials. The shear strength and critical slope angle decrease as a granitic rock mass weathers. Each stage of weathering is susceptible to specific slope-stability hazards. If the stage of weathering is identified at a site, it will provide clues to the engineering properties of the material and help the engineering geologist predict the slope-stability hazards of proposed actions.

Weathering processes rocks undergo can present heterogeneous characteristics in outcrop and in depth, from a mineralogical, physical and mechanical point of view. Therefore rock mass characterization is one of the most basic and important tasks in rock mechanics and engineering. Literature review indicates that although there are many publications available on weathering as a predisposing factor for landslides, there are only few reports of weathered

dolomite and limestone and generally on sedimentary rocks and their mechanical properties. This work presents a case study of characterizing a group of highly weathered dolomite rocks in an area in which the landslide hazard is very severe, and will therefore be monitored by the public authorities and by Geoscience Azur, Research and Development unity of the CNRS of Nice, Sophia Antipolis. A geological and geotechnical mechanical analysis is carried out in order to find the relationship of the heterogeneous weathering of this rock mass with the slope instability hazard.

1.4 *Cinematic Aspect:*

The concept of rupture in geology has been studied by geotechnicians and geologists since many years, but just up to some years ago these studies were concentrated on post rupture observations and analysis. The structural heterogeneities as for example stratigraphic surfaces , foliation, faults and fractures, their consistence and interconnection justify the pre-cutting of a sliding surface that individualises a mobile mass.
But as largely analysed by El Bedoui (2009) it is extremely rare for a volume of rock that is bigger than some m^3 that a network of discontinuities individualizes a surface of rupture and isolates an unstable rock mass. However, it is not about bringing into question the fact that a structural pre cutting of the versant favours the localisation of the deformations of the versant and eases destabilisation. Nevertheless the generation of a surface of rupture within a pre-cut rocky medium involves most of the time the propagation of the fracture network within the rock bridges. (Figure 2)
The concept of progressive rupture can therefore be preliminarily defined as the propagation of the internal fracturing of the versant in time.

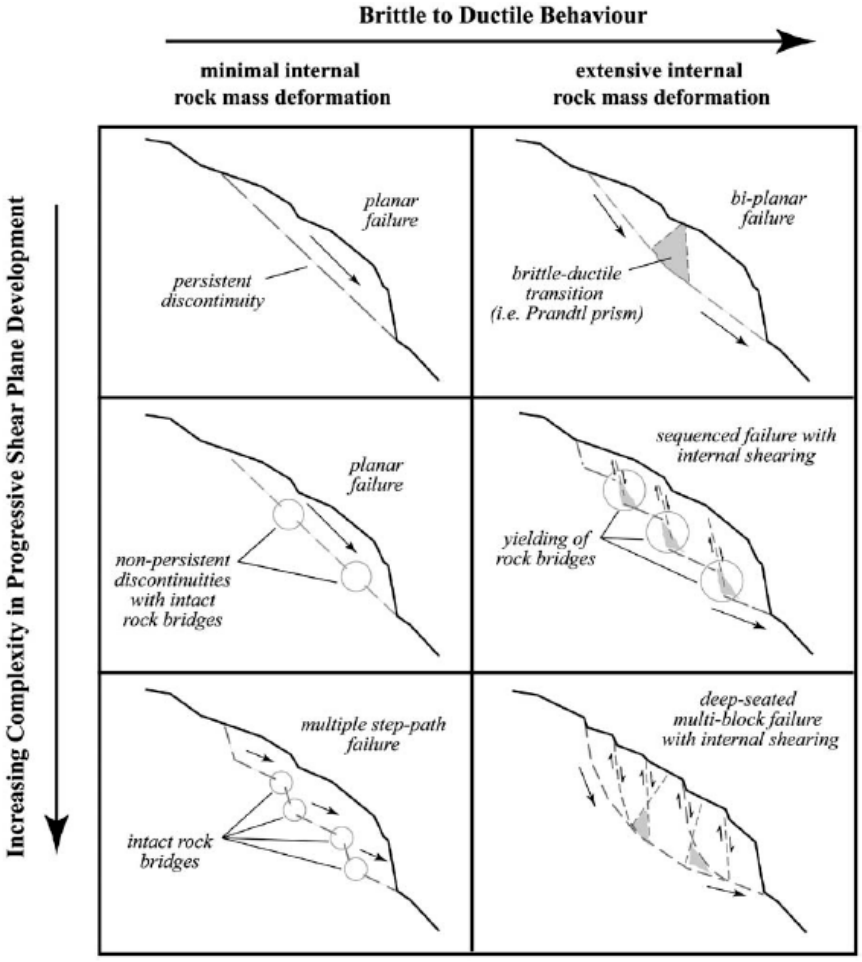

Figure 2 : rupture mechanism of a rocky versant in function of its geologic discontinuities that pre-cut the massif, Eberhardt and al, 2004, in El Bedoui, 2009)

The kinematics of the genesis of the rupture surface is controlled by the mechanisms of fracturing of the rock bridges. This explains the extremely long periods (some thousands of years) that are needed to undermine the stability of a versant before the sudden start (in geologic scale) of a catastrophic movement. The evolution in time of a potential rupture surface cannot be considered as linear. During the progression of the fracturing of this sliding surface the deformations will progressively be concentrated on this week surface which will lead to a progressive acceleration of the phenomenon of rupture just to reach the state of so called "bifurcation". This progressive rupture weakens the mechanical resistance of the versant to the shearing stresses.

Because of this spoiling progressively smaller external solicitations (climatic or tectonic) can accelerate or provoke the destabilisation of the massive.(Figure 3a) In Figure 3b different scenarios for a rock-mass subject to progressive rupture are proposed: (i) a final acceleration that leads to rupture, (ii) a stationary state, (iii) a stabilisation. These different evolutions are dependent on the internal conditions of the versant and on the external solicitations.

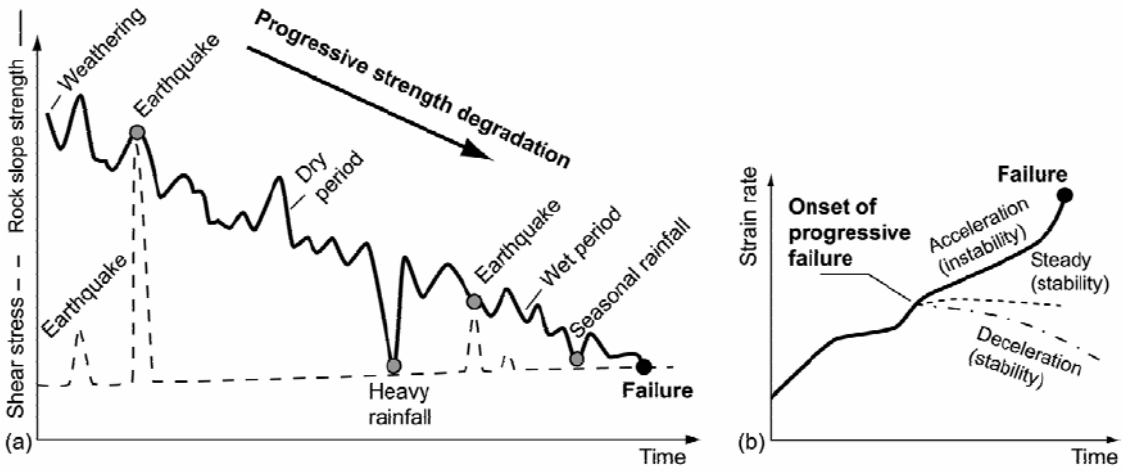

Figure 3 : (a) conceptual evolution of the mechanical resistance of a versant during the progressive rupture, (b) Evolution curve of the tax of deformation in function of time for a versant submitted to progressive rupture. (after Finlayson and Staham, 1980 in El Bedoui, 2009)

Weathering plays a fundamental role in this advancing destabilisation. It is considered as a preparing factor in the rupture process and slowly, during long (geologic) periods, undermines the mechanical resistance of rocks preparing the versant for rupture, that is finally provoked by one or more triggering factors. In this study a deeply weathered dolomite is analysed and the relation of weathering in relation to the distance of the nearest major fault is investigated. The versant, which overlies this weathered layer is slowly travelling his way towards rupture, and the time plays a key factor in the destabilisation of this rock mass.

Chapter 2 : Presentation of the studied area

2.1 *Grasse and the Marbrière Versant*

2.1.1. Morphological aspects

The studied sector is the Rioucougourde Valley which cuts the versant of the Marbrière together with other two valleys: the St Christophe Valley and the Bouillides Valley. The Marbrière is located at the North-Eastern extremity of the city of Grasse, situated 15km north from the coast of Cannes and 30km North-West from Nice in the Department of the Alps Maritimes in the region 'Provence – Alpes – Cote D'Azur ' in southern France.

Figure 4 : Department of the Maritime Alps: The Coastline (source: Google Earth) In the inset: France

Morphologically this Versant has a general orientation of N°40 spread over an altitude from 300 to 900m, with a mean slope between 30° and 40°. The versant is bordered by plateaus levelled up to 1400m which represent the first limestone relieves in the North, and by an extensive depression from 200 to 100 m of altitude in the south. Its particularity consists in the fact that it is considered "the first erosion front of the southern Alps"

Concerning the development of the territory, this sector has been submitted to an intense antropisation in the last 50 years (factor 2 or 3). A considerable urbanisation has developed on the whole lower part of the versant (Figure 5), increasing strongly the vulnerability.

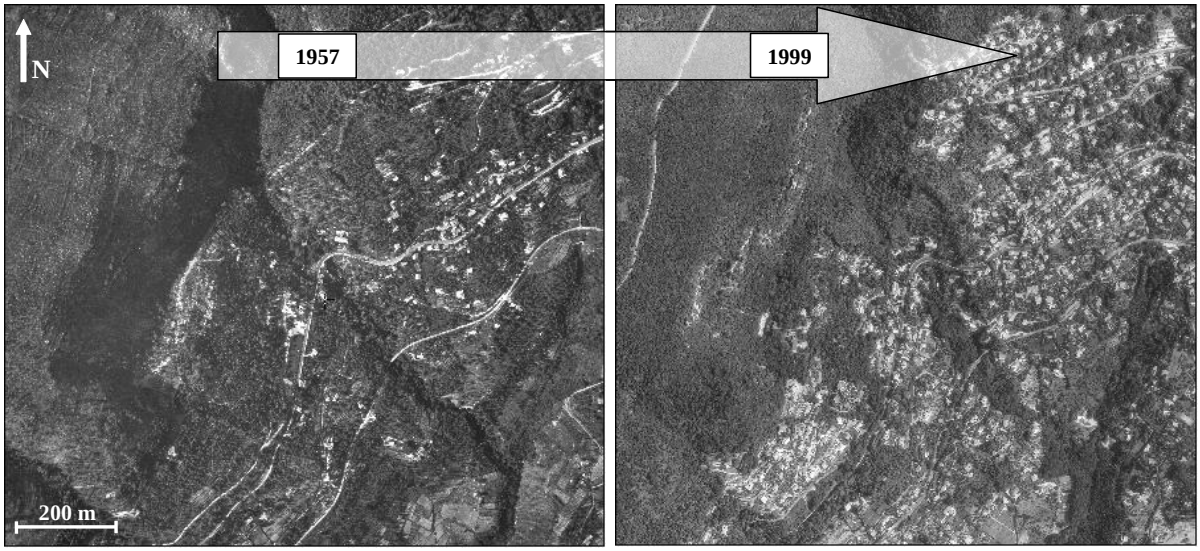

Figure 5 : Couple of aerial photos : (50 years of interval) showing the antropisation of the sector Hautes Chauves (north eastern foot of the Marbrière Versant) (in Zerathe, 2009)

Another particularity of this sector is the aqueduct of Foulon, which crosses the whole versant. (Figure 6)

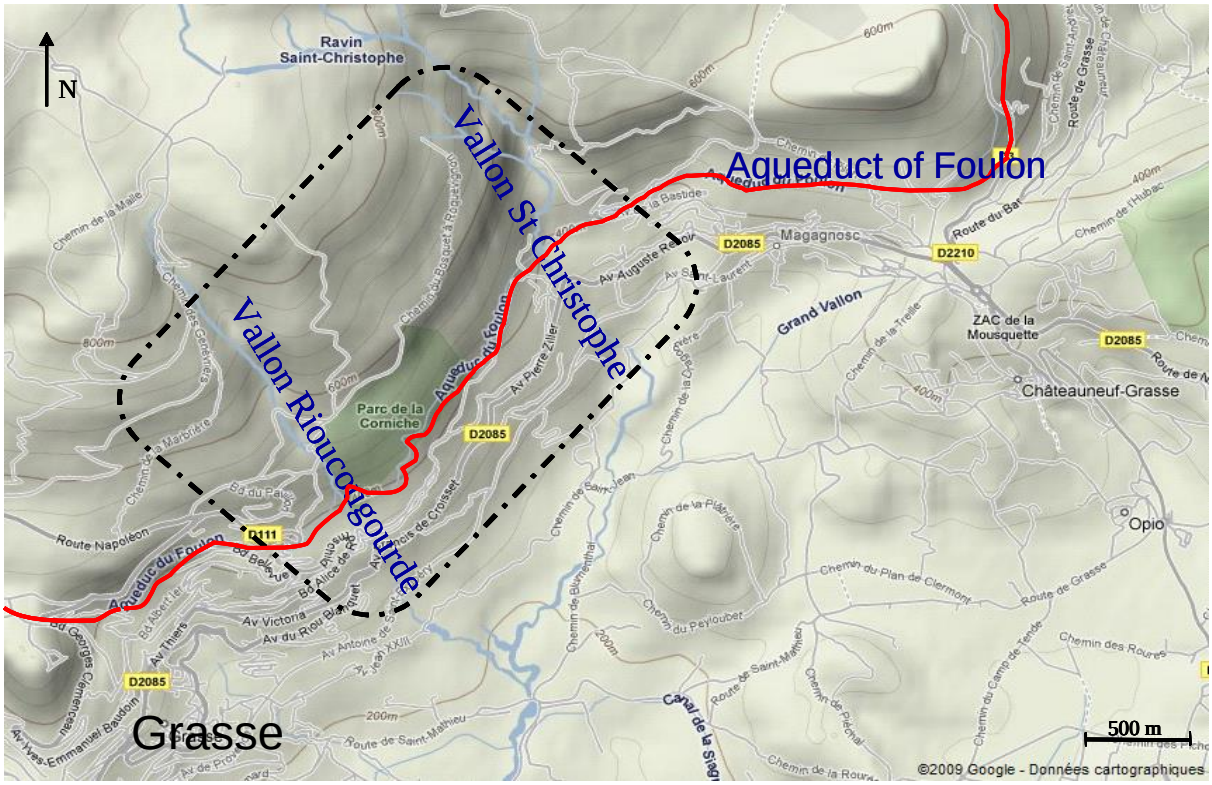

Figure 6 : Localisation of the Marbrière versant with its valleys : Vallon Rioucougourde and Vallon St. Christophe (source Google Maps)

It is the principal aqueduct which aliments the Community of Grasse with drinkable water. It is constantly charged with 400 to 500 m^3/h. This channel can be considered as a vulnerability factor (Alimentation with drinkable water for 120 000 habitants) and meantime as a triggering factor for a big movement of a versant in urban area. The breaking or a major leakage of the channel would flow directly in the versant and in its major faults.

2.1.2. Geological setting

This area constitutes the southern border of the southern sub alpine chain.
The geology of the area is essentially composed by sedimentary ground which has its origins between the Triassic (Middle Muschelkalk -220Ma) and the Lias (Hettangian -190Ma)
Three families of fractures N 20-40°, N 70-90° and N 120-140° are generally present in this area. These deformations are an expression of an important phase of alpine compression, in direction North-South which took place from the Miocene to the Pliocene.
A particularity of the versant is the fact that it is posed on a Triassic basis, composed by clay, marls and gypsum. This series has a great contrast of stiffness with the Jurassic limestone of the versant. The series has also acted as a "soap layer" for the alpine overlapping, could play a similar role in the deep seated gravitational slope deformation that affects the versant.

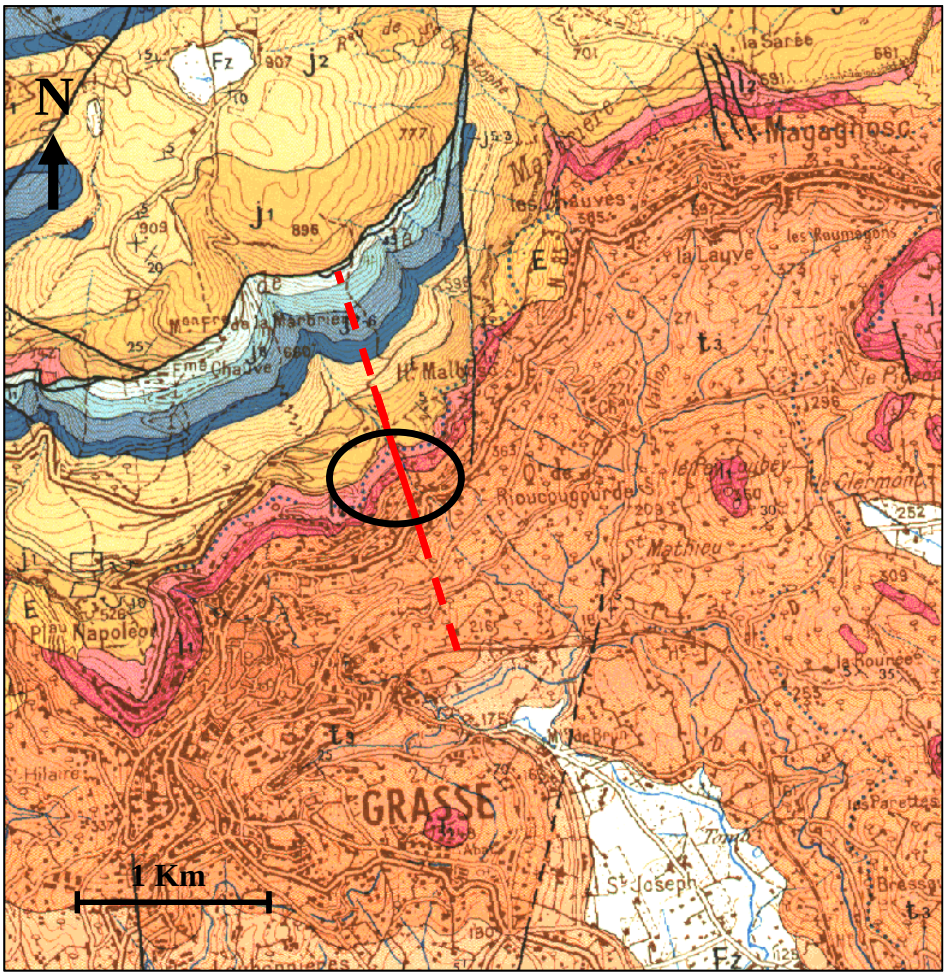

Figure 7 : Geological map of Grasse (BRGM, Cannes Grasse)

<u>Stratigraphy :</u>

Presentation of the different lithologies found on the sector are (source: BRGM, 1983 and Spini, 1978).

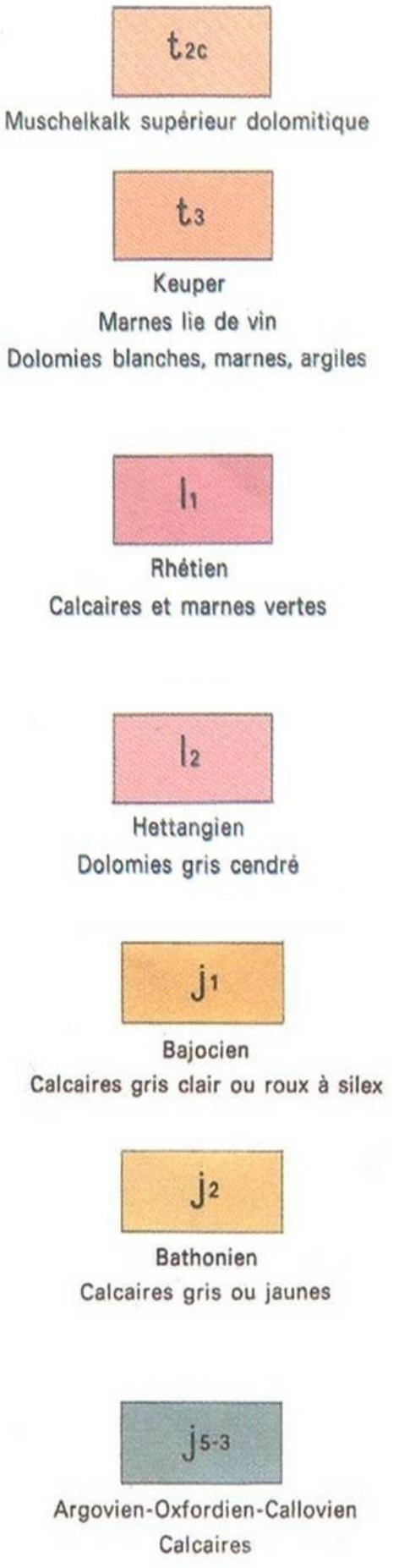

- Middle Trias – Muschelkalk

Represented by limestone-dolomitic banks, whitish and massive 20 – 60 m thick, it constitutes the oldest level that is visible in the Grass basin.

- Superior Trias – Keuper

The Keuper formations are not differentiated on the geologic map Cannes- Grasse of the BRGM. They are described from the bottom to the top as white dolomites intercalated with marls plastic clay stone which can reach 50m of thickness, followed by cellular dolomites, big parallelepipedic white dolomites and finally gypsum layers.
Together the group could be thicker than 100m.

- Inferior Lias – Rhétien

The Rhétien is composed of a base of grey shale yellow platy parting marly-limestone overcome by dolomitic limestone banks which are thicker and ripple-marks. The transition between the dolomitic limestone and the underlying shale is continuous. The thickness of the formation is about 20m

- Superior Lias – Hettangien

This is the formation of the studied cliff face. It is a stratigraphic stage of the lower Jurassic and it is represented by ash grey dolomites in thick banks and well stratified, and parallelepipedic disintegration and separated by green or yellow shale in the upper part of the formation. Together they have a thickness of about 40m.

- Middle Jurassic – Bajoncien

It concerns a light grey or ginger limestone which is disposed in metric banks with a fine stratification. The characteristic base is surmounted by an oolithic niveau that contains many organic debris.

- Middle Jurassic – Bathonien

The Bathonien is represented by 50 to 60m of grey or honey-yellow limestone, with shaly interpositions containing Brachiopodes, Bryozoaires and debris of shells. The base of the formation consists of a layer of purplish and oxidated fire clay and shale which thickness can reach up to several meters.

- Superior Jurassic - Callovien/Oxfordien

It concerns about 20m of limestones light colored and with a lightly lumpy split (de couleur claire et à la cassure légèrement grumeleuse), containing numerous little shells

Table 1 : Lithologies of the Geological map of Grasse (BRGM, Cannes Grasse) (Figure 7)

2.2 *Rioucougourde Valley and the Cliff face*

As mentioned before the Marbrière Versant is cut by three valleys and various faults. There where one of these faults, which usually is not visible on the ground cuts the Rioucougourde valley a cliff face crops out of the versant. (Figure 8)

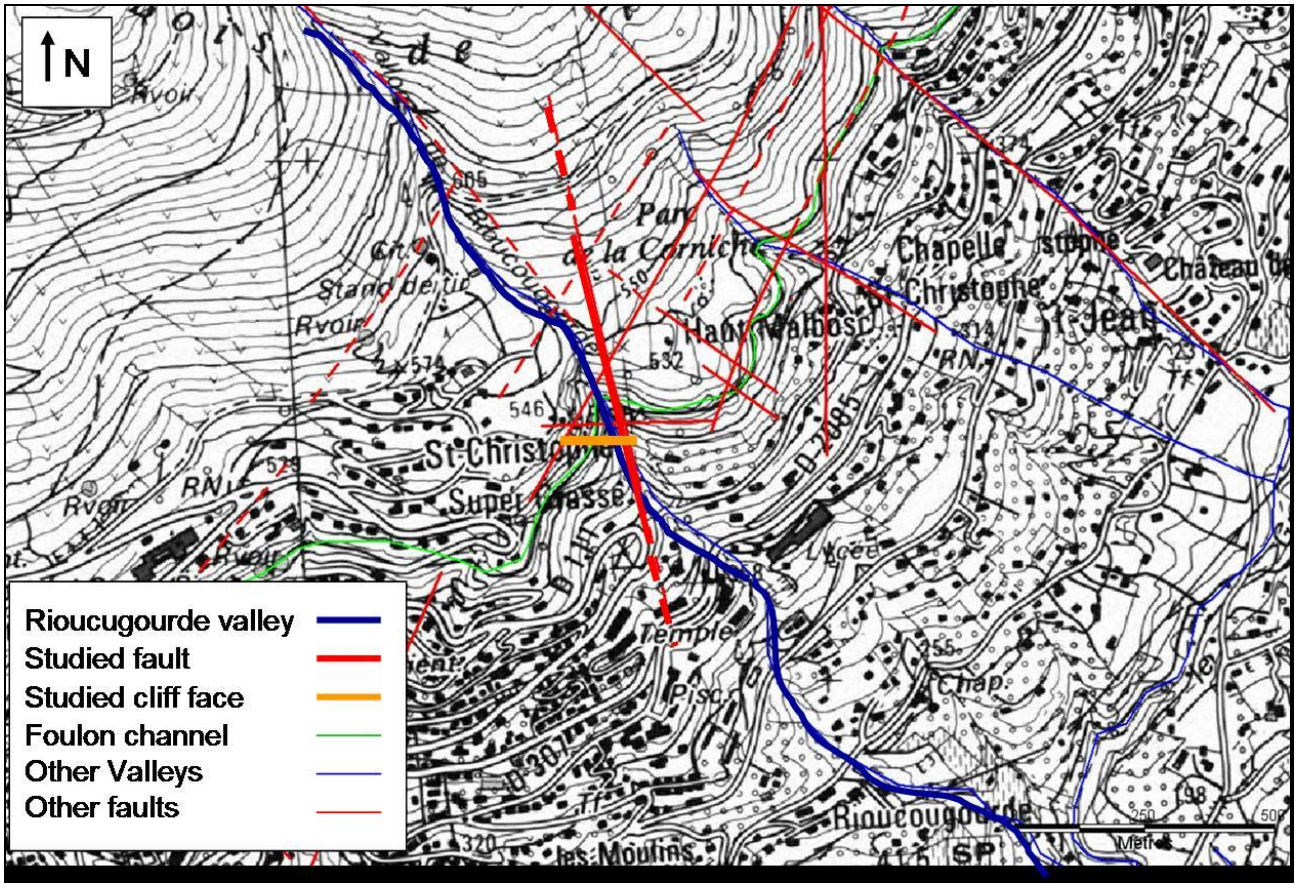

Figure 8 : The studied sector with its Valleys, faults, the cliff face and the Foulon channel.

2.2.1. Morphological aspect

The cliff face is approximately 20m high, and 30m long.(Figure 9) At that place the fault is clearly visible and its opening is between 60 et 100 cm. Two main families of fractures are visible on the cliff face: (Figure 10) The first one is almost parallel to the orientation of the cliff face and vertical: 96.9° N 86.7 and the other one is parallel to the fault direction and almost vertical but not always straight. The fractures are "flower-formed": For the first 1 to 2 m from the ground the fractures have a mean orientation of: 175° E 80 , are good visible and isolated with an opening up to 15cm, filled by fine grained material framed by very solid rock with good mechanical properties. In this context we find the hard layer that will be studied. Over 1, 5 m of height the fractures open themselves in more fractures with different orientations. There where

the main fracture families cut the rock: (ex: 6-7m c.a., 9m c.a., 13m c.a.) the rock is totally reduced to soil on the weathered layer while it remains solid on the hard layer. (Figure 20)

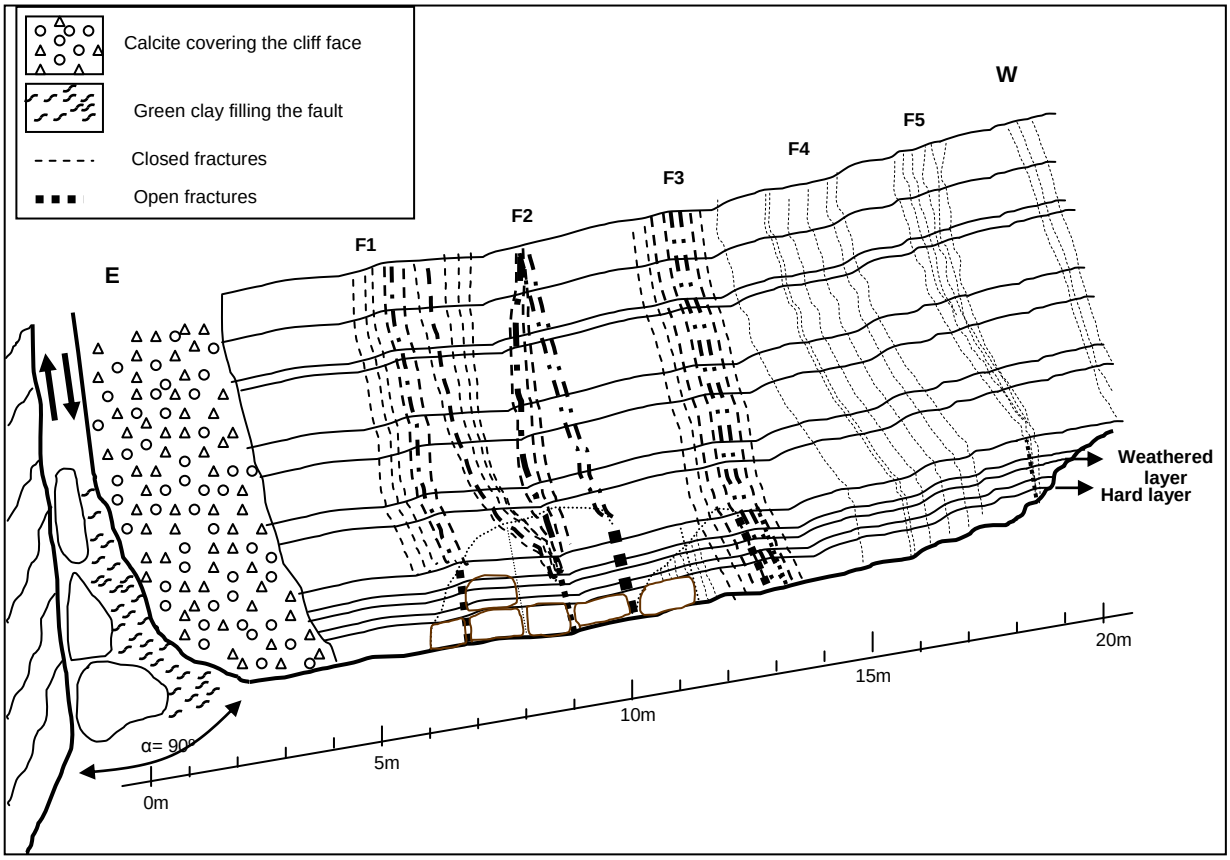

Figure 9 : Scheme of the studied the cliff face in the Rioucougourde Valley

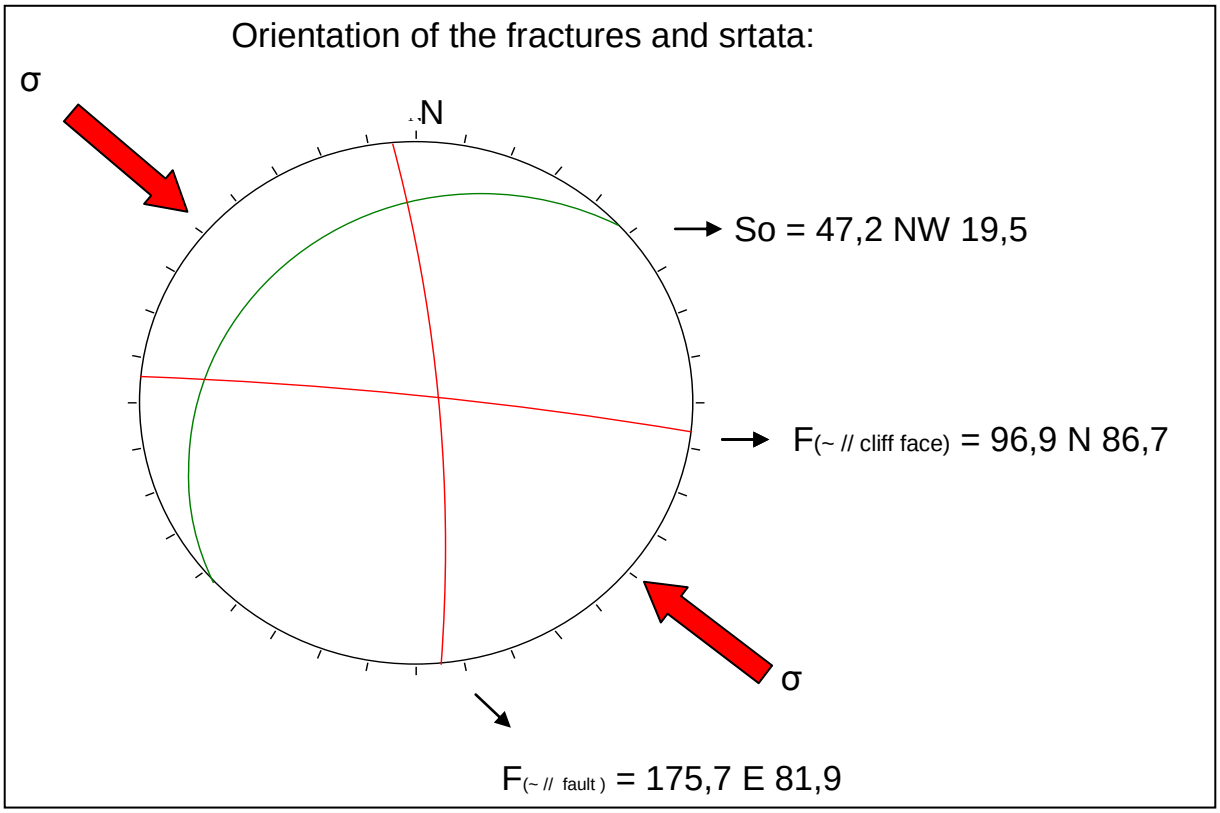

Figure 10 : Stereo plot of mean orientation of fractures and strata of the cliff face on Wulf canvas, lower hemisphere.

2.2.2. Geological setting

Geologically the cliff face it is situated in the lower Jurassic, the Hettangien and is formed by the ash grey well stratified dolomites (47.2° NW 19.5) with thin interpositions of dark-red, brownish clay with thickness in the order of some mm. The thickness of the layer is contained between some centimetres and some decimetre, and does not remain constant following a single stratum along the cliff face. This and the presence of fine stratigraphic lenses indicates that the formation of this dolomite has taken place in a paleo environment of a basin with channels of current which reorganized the fine mud of calcite and dolomite crystals. It is possible to follow the same layer for 20m along the cliff face; afterwards the topographic gradient differs too much from the inclination of the strata. For this reason the tests have been carried out along the cliff face for 20m. Furthermore Imposa et al. (2004) found that the local amplification of ground motion is negligible from 20m distance from the fault on.
The layers have very different properties and over very small distances the mechanical parameters can totally change. The differences are immediately visible: in certain places it is possible to observe a very weak, poor rock mass, totally destructed and reduced to debris and soil just beneath a perfectly integral and resistant rock. The fault is filled mostly with green clay and blocks of dolomite rock.

Chapter 3 Problematic:

3.1 *The frame of this study: Deformation of the Marbrière Versant*

Since many years the gravitational risk in the mountains is closely studied in the department of the Maritime Alps. More than 150 active gravitational movements are identified and recognized in the database of the *BRGM (*Bureau de recherches géologiques et minières) which reflects essentially the hazards with high vulnerability, that means which have been identified as zones with a high risk **(**Roquebillière, La Clapière, ...). During a preliminary study of analysis and cartography of gravitational hazards (Lebourg 2008) J'AI PAS LE TITRE POUR LA BIBLIO on the slopes of the Basin of Grasse and of the near Vallée du Loup, several slope movements of different ages (ancient and present ones) have been identified. This area is affected by deep seated deformations with volumes bigger than 10^6 m^3 for which the structural and morphological context plays a major role in the process of rupture (intense tectonic cutting, confluence of local major faults)
In this area the attention has been focalised on a key sector : the Marbrière Versant which presents clues of characteristic deformations of great movements of versants: topographic anomalies as crevasses, steep slopes and cliffs and some particularly active zones with superficial slides, subsidence, rock falls, collapses. Additionally, vegetal and morphologic alignments that can be observed on aerial photographs make strongly suppose that this sector is affected by the re activation in gravitational dynamics of a series of major faults (Zerathe, 2009)

3.1.1. Electric Resistivity Tomography of the Rioucougourde valley and the fault

In the frame of a geophysical campaign of electric tomography in the key sectors and the modelling of these results which allows confirming the interpretation of the electric profiles for a

better understanding of the gravitational morphologies and the deep deformations the fault in the Rioucougourde valley has been studied. A profile has been made along the Foulon channel in the Hettangien series, perpendicularly to the fault which passes in the centre of the profile, in order to study its morphology and its depth. (Profile ERT3 in Figure 11)

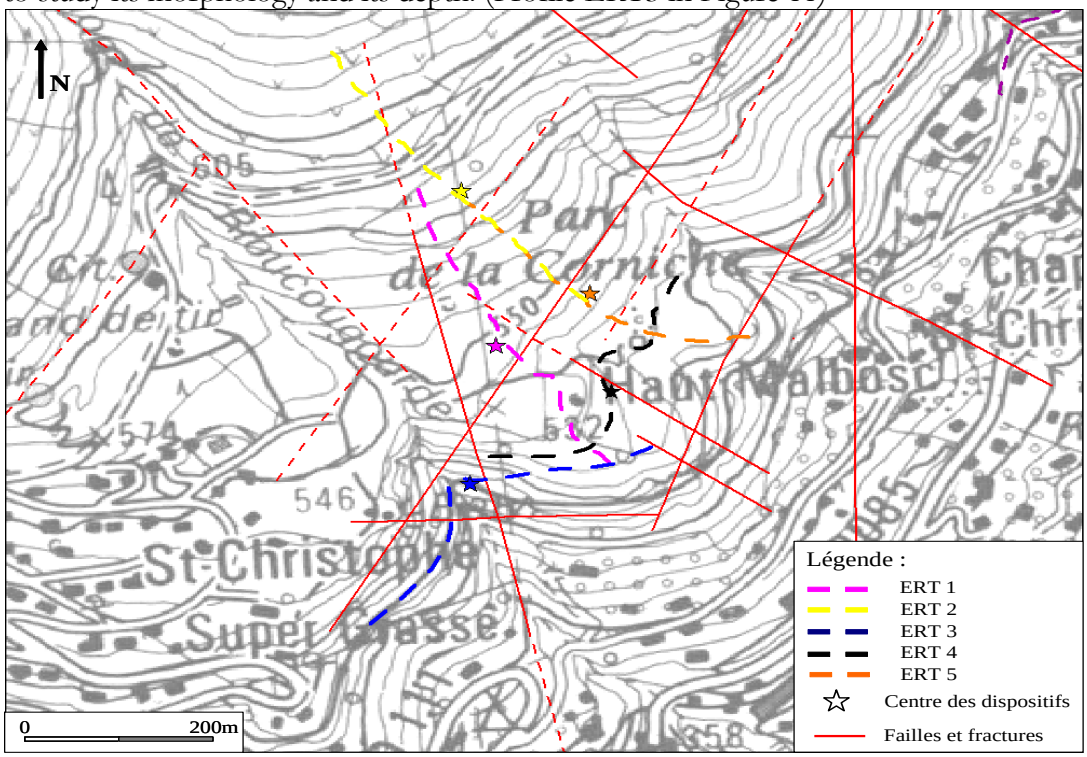

Figure 11 : Localisation of the electrical profiles on the Marbrière versant (ERT3 is the studied profile) and localisation of the faults and fractures.

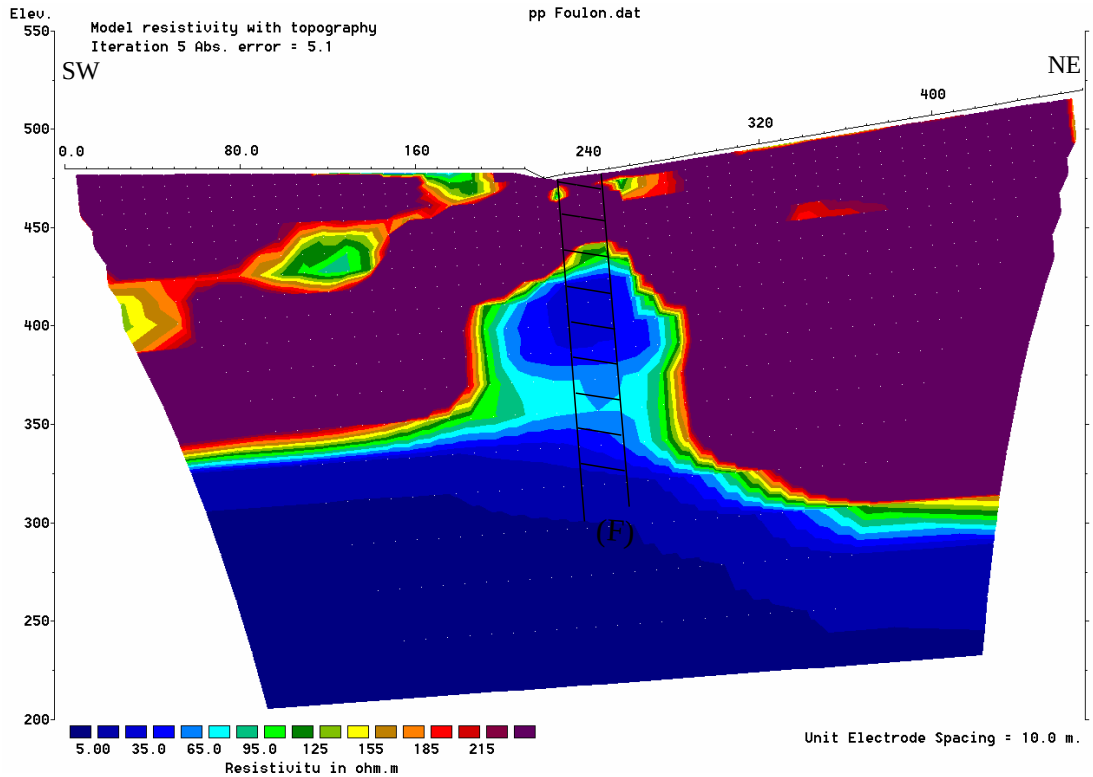

Figure 12 : Inversed electric profile, ERT 3 (Rms = 5.1%).

The theory and physical principles on which electric resistivity tomography is based are explained in § 4.2. for a structural reason of this work. Nevertheless the test protocol for obtaining the electric profile presented in Figure 12 is described below and its result is analysed and discussed.

3.1.1.1 Test protocol:

The protocol used for this study was previously tested in Jomard et al., 2007a giving accurate results in the higher part of a landslide. The same protocol has been followed in this study. The key acquisition and inversion parameters are described below.
Measurements were undertaken with a multi-electrode 2D device, using the Syscal R1 Plus imaging system (IRIS Instrument). The 2D devices are composed of 48 electrodes separated by 10 m (limit of the system). ERT making a total length of 480m. Pole-pole and dipole-dipole arrays have been acquired. Each acquisition point is stacked 3 to 5 times and the obtained value is deleted if the quality factor (corresponding to a deviation between the injected power and received signal) is not null. For pole-pole arrays, the location of infinite electrodes has been done with respect to recommendations mentioned in Robain et al. (1999). In particular, infinite electrodes are placed symmetrically on both sides of the in-line electrodes with a spread angle of more than 30°. However, the length of 'infinite lines' does not reach more than 7 to 10 times the greatest 'in line' electrode distance because of problems introduced by the shape of this mountainous steep terrain. This limitation can introduce an almost homogeneous under evaluation of the deepest measurements as proposed by Robain et al., 1999. This problem is partly addressed by the very consistent correlation observed between resistivity ranges obtained for dipole-dipole and pole-pole arrays in previous works (Jomard et al., 2007a).
The presented ERT is only pole-pole arrays because other geometric configurations hadn't allowed reaching a depth consistent with the assumed position of the failure surface. The resolution of the acquired profiles is a function of the number of acquisition points; a grid of about 10x10 (in meters) was created in agreement with the geological settings scale. It corresponds to about 1000 measurement points for each ERT and should allow probing theoretically down to a 250 m calculated depth (Edwards, 1977).

Inversion of the data is then required to obtain a vertical true resistivity section through the underlying structure (Loke and Barker, 1996). The field data were inverted with software $RES_{2D}INV$ written by Loke (1997). Constraints provided by the topographic variations have been incorporated in the inversion processing. The results of the inversion process are presented in Figure 12.
According to the relative basement homogeneity for ERT, we will be able to associate resistivity contrasts not to the lithological variations, but to the coupling between rocks mechanical weathering, saturation and fracturing. In general, resistivity variations can be explained by (Jongmans and Garambois, 2007):

- The water content. In the same geological formation resistivity variation is a function of the ratio saturation/porosity of the rock,
- The rock weathering. It can be considered in two ways: chemical weathering and mechanical weathering. Chemical (hydrolysis) weathering induces an increase content of clay and the decreasing of the permeability. Mechanical weathering followed by gravitational movements induces a porosity increasing in a destructed medium. Both weathering types are characterized by a resistivity increase ??????????????????

ERT 3 will also be dependent to lithological variations at depth.

JE NE LES AI PAS LU, EST CE QUE JE DOIS LES CITER DANS LA BIBLIO ???????????

3.1.1.2 Analysis and interpretation of the Electric Resistivity Tomography:

In this profile (Figure 12) globally two superposed compartments are found: a superior part with resistivity ϱ1 > 500 Ωm which corresponds to the Hettangien/Rhetien and a lower part with resistivity ϱ2 < 20 Ωm
Corresponding to the Keuper. From the height of 190m to the height of 260m a vertical band of low resistivity which cuts the compartment of ϱ1 can be observed (ϱ3 < 50 Ωm). It is 60m broad and does not reach the surface. In accordance with the cartographic data this anomaly is the expression of the fault.

Moreover, important water sources at the level of the cliff face that means about 50 m under the profile, shows the draining character of the fault: the band of low resistivity corresponds to this damaged zone saturated with water. But this damaged zone, the cliff face, is just 20m broad and not 60 as on the profile. This difference could depend from two factors:
Either it could depend from the non linearity of the profile which is V-shaped due to the topography of the Valley or it is an over estimation which depends directly from the inversion.

Furthermore a vertical shift of about 20m (±5m) is clearly recognisable between the South-western and the North-eastern block which indicates that this last one has been subjected to subsidence in relation to the South-western block.

3.1.1.3 Conclusion:

As a results of these studies strong spatial and geometrical relations have been found between the gravitational morpho-structures and two big networks of strike-slip faults (N20 - 40° ; 90° et N160-170° ; 80°E).(Figure 11) These relations have been observed on the surface and in the underground, where these deformations are strongly coupled with the fault network (200-300m). The Hettangien level (level of the studied cliff face) is especially cut by deformations and makes up a marker of the deformations of the versant.
Two types of behaviours/ kinematics acting at different levels of the versant have been proposed:

-tensional openings of fractures and faults in the lower part of the versant (recognizable by the open crevasses)
-vertical movements along the fracture network N20-40° in the upper part of the versant (marked by steep slopes and topographic berms)

An overall view of the results suggests a first hypothesis of deformational model at the scale of the whole versant but which depth of the investigation of the electric tomography has its boundaries in the Keuper. It concerns a deep movement, clearly controlled from behind by the fracture network N20-40° and N90° with a hypothetic amortisation in the Triassic lithologies.
(Figure 13)
The conjugated N160-170° cuttings (the grey outer surface of Figure 13) allows lateral adjustments, differential movements among lateral compartments, and represents the lateral boundary of the movement. The studied fault of the Rioucougourde Valley is one of these lateral cuttings of the versant. It is one of the major eastern boundaries of the slope movement in the sense that the sector on the West side of the fault is relatively stable whereas the sector on the

East side of the fault is the studied instable slope. The Rioucougourde valley fault allows the differential evolution of these sectors.

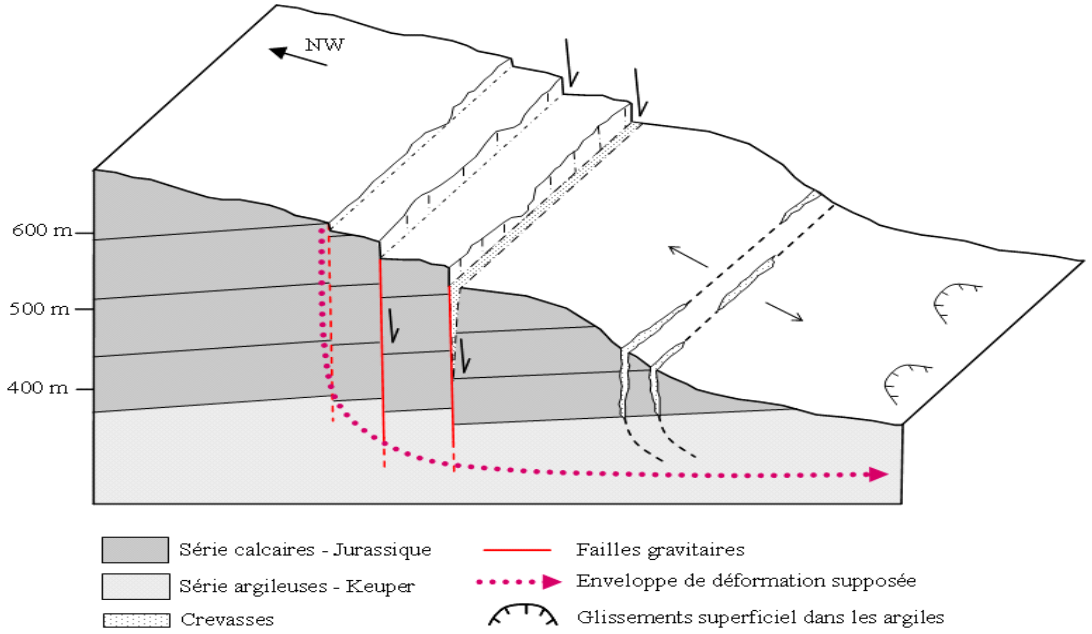

Figure 13 : Conceptual block diagram illustrating the big scale deformation of the Marbrière versant

3.2 *Presentation of the study:*

In this context of gravitational slope deformation the strike-slip fault (N175° ; 80°E) adjacent to the studied cliff face in the Rioucougourde Valley plays a major role as described above. In this study the focus is put on this fault zone and more precisely on the cliff face that crops out just beneath the fault. This outcrop is highly weathered and it presents very heterogeneous characteristics from a physical and a mechanical point of view as the presence of parts with both hard-rock and soil-like behaviour.

Some questions are the guidelines of this study:

a. Is this extremely high grade of weathering caused by the proximity of the fault?
b. Which are the mechanical properties of this material and how much are they affected by the weathering process?
c. How much influence has the change of the mechanical properties on the gravitational movement and on slope stability?
d. Are there any simple means to characterize the mechanical properties of the rock?

Up to now most studies on weathering processes and their relationship with slope instabilities have been carried out on crystalline rocks (plutonic and metamorphic) (§1.3) because the effects of weathering are particularly intense on these types of rocks, and not many on sedimentary rocks. Most of the papers available on the weathering of sedimentary rocks are especially about geochemical and mineralogical weathering and do not concern mechanical weathering.

Also the change of mechanical properties in relation of the distance from the fault has only been carried out on crystalline rocks.(Greco et al. 2005, Tansi et al. 2000) and most studies of the mechanical behaviour carried out on weathered rock in proximity of faults are concern only fault gauges and breccias and the bimrocks (block in matrix rocks) or Kakirites (Buergi et al.2001 , Buergi et al.1999, Kahraman et al., 2008, Kahraman et al.,2006, Habimana et al. 2002) but do not consider the damage zone just after the fault zone. In this damage zone the intense jointing of the rock mass facilitates weathering and accelerates the alteration process.

In this study the damage zone adjacent to the fault is analyzed and its macro and micro mechanical properties are investigated:

In Chapter 4 the investigating methods are described and every test is singularly discussed: The following tests have been carried out:

- Electric resistivity tomography (ERT)
- Apparent Joint Separation (AJS)
- Schmidt Hammer Test (SHRV)
- Triaxial compression strength (TCS)
- Uniaxial compressive strength (UCS)
- Density
- Effective porosity
- Rock Quality Designation (RQD)
- Image analysis of thin slices

In Chapter 5 a Principal Component Analysis is carried out and the various test results are correlated with each other. A law of correlation between the parameters of SHRV and UCS is proposed in order to make the determination of mechanical parameters of shear strength with less temporary and pecuniary effort.
An electric resistivity tomography of the cliff face is analysed and its results discussed in comparison to the other test results.
Afterwards some physical and mechanical parameters of the dolomite rock of the studied cliff face are confronted with those of the same rock on other parts of the versant. The influence of the fault and a diagenetic cause of this variation are discussed.
Finally a stability calculus of the security factor of the versant is carried out for various scenarios using the mechanical parameters that were determined in this study and the different time depending results are discussed.
Cette partie devrait être aussi dans l'introduction …..les 20 lignes avant

Chapter 4 : Analysis and methodology

4.1 *Introduction:*

In the frame of the study of the gravitational deformation of the Marbrière Versant a key site has been analysed with particular attention: The cliff face in the Rioucougourde valley. The Marbrière versant is one of the sectors affected by the re activation in gravitational dynamics of a series of major faults (Zerathe, 2009) The fault and fracture network N160-170° which represents both the lateral boundaries and the subdivision between various sectors of the landslide and which allows lateral adjustment.

The cliff face in the Rioucougourde valley shows signs of extremely advanced weathering and alteration. Now the first two guideline-questions (3.2) that arise are:

- Is this extreme weathering caused or at least favoured by the closeness of the fault?

  This is a licit question since this particular fault has permitted a vertical shift of about 20m (±5m) between the South-western and the North-eastern block of the versant. That means that the rock adjacent to the fault has suffered great shearing stresses and in addition it is exposed to mayor fluid circulation due to the draining character of the fault.

- Which are the mechanical properties of the rock and how are they affected by weathering or rather by the closeness of the fault?

To find an answer to these questions field observations together with laboratory and in situ tests that have been carried out on the dolomite cliff face adjacent to the fault. The tests have been conducted on a total horizontal length of 20m, starting from the fault. After 20m is it not possible anymore to follow the same stratigraphic layer because the topography has a higher gradient than the immersion of the stratigraphy (Figure 9). However the execution of the tests for 20m should be enough to notice a variation of the rock properties in function of the distance, if there are any variations. Additionally Imposa et al. (2004) state that the local amplification of ground motion is negligible from 20m distance from the fault on.

4.1.1. Presentation of the tests:

The following tests have been performed on the outcropping rock:

Index Tests:

- Performed in situ:
  - Apparent Joint Separation (AJS)
  - Schmidt hammer Rebound Value (SHRV)
- Performed in the laboratory:
  - Rock Quality Designation (RQD)
  - Bulk density
  - Effective porosity
  - Image analysis (thin slices)

Engineering design test:

- Performed in situ:
  - Electric resistivity tomography
- Performed in the laboratory:
  - Triaxial compression tests:
    - Effective cohesion (c')
    - Effective angle of internal friction (φ')
  - Uniaxial compressive strength (UCS)

In Figure 14 the tests are represented in an organization chart in order to point out what they measure, and what influence their values. The mechanical rock properties are affected by jointing,

weathering and by a syndiagenetic lithological difference. AJS and RQD measure the Jointing, the TCS supplies c' and φ' which are influenced by weathering, ERT, UCS and SHRV are influenced by both, the jointing and the weathering. Furthermore the SHRV is influenced by the compressive strength of rock. Bulk density and Porosity are influenced by weathering and by the lithologie and with the image analysis lithologic differences are found and the porosity is evaluated.

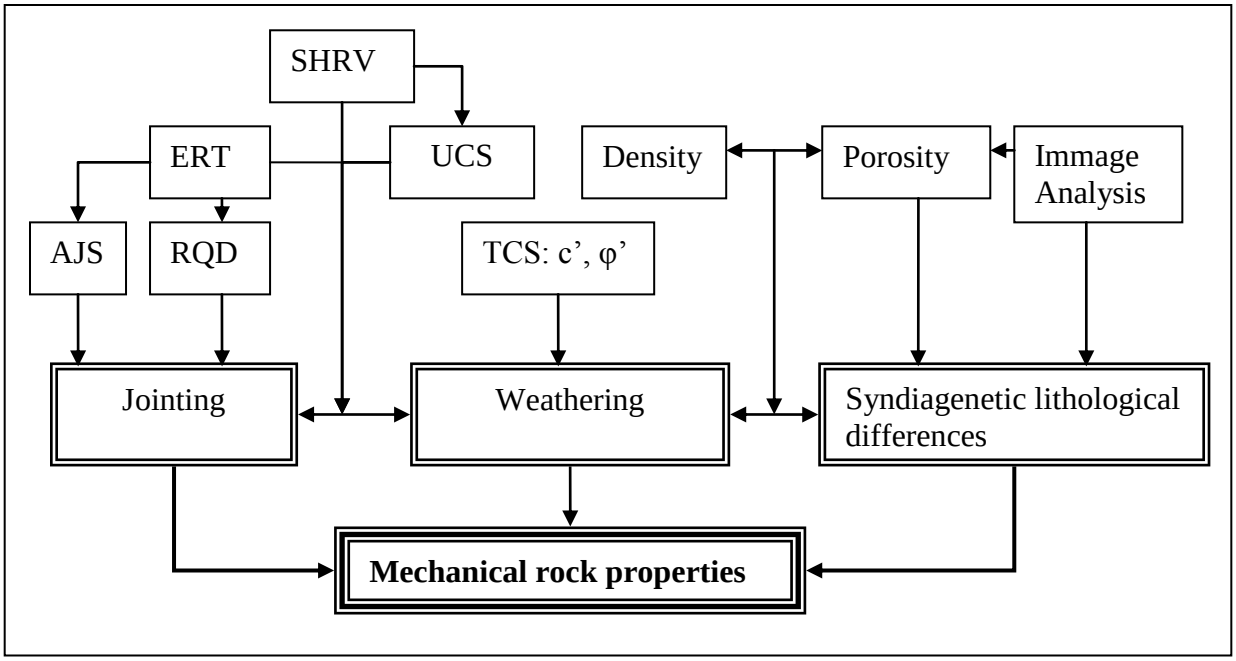

Figure 14 :Organization chart of the different tools, their interaction, their purpose

The second purpose is to provide sufficient and adequate mechanical parameters of the dolomite rock for the modelling of the gravitational phenomenon that slowly destroys the versant
.LA DEVO ANCORA FA STA PARTE???????

4.1.2. Problems:

Some difficulties came up during the tests:

- The first 3 meters starting from the fault were strongly covered with calcite. On the very first meter thick pockets of calcite have been observed, whereas a layer of about a cm covers the cliff face from meter 1 to 3. This does not only complicate the measurement of the SHRV, but it also hides the fractures and micro-fractures of the rock, which makes the evaluation of the apparent joint separation impossible on the first meters. To overcome this inconvenience on the first meter the calcite has been removed on various spots with the geological pick, uncovering a cataclastic rock. A matrix of totally altered, from orange to red and very porous rock material is crossed by small veins of calcite and contains discoloured blocks in which the original mass structure is still visible. The geological pick easily indents in the reddish matrix which can as well be easily crumbled by hand, whereas the discoloured bocks do not crumble by hand and the point of the geological pick scratches the surface but does not easily indent.

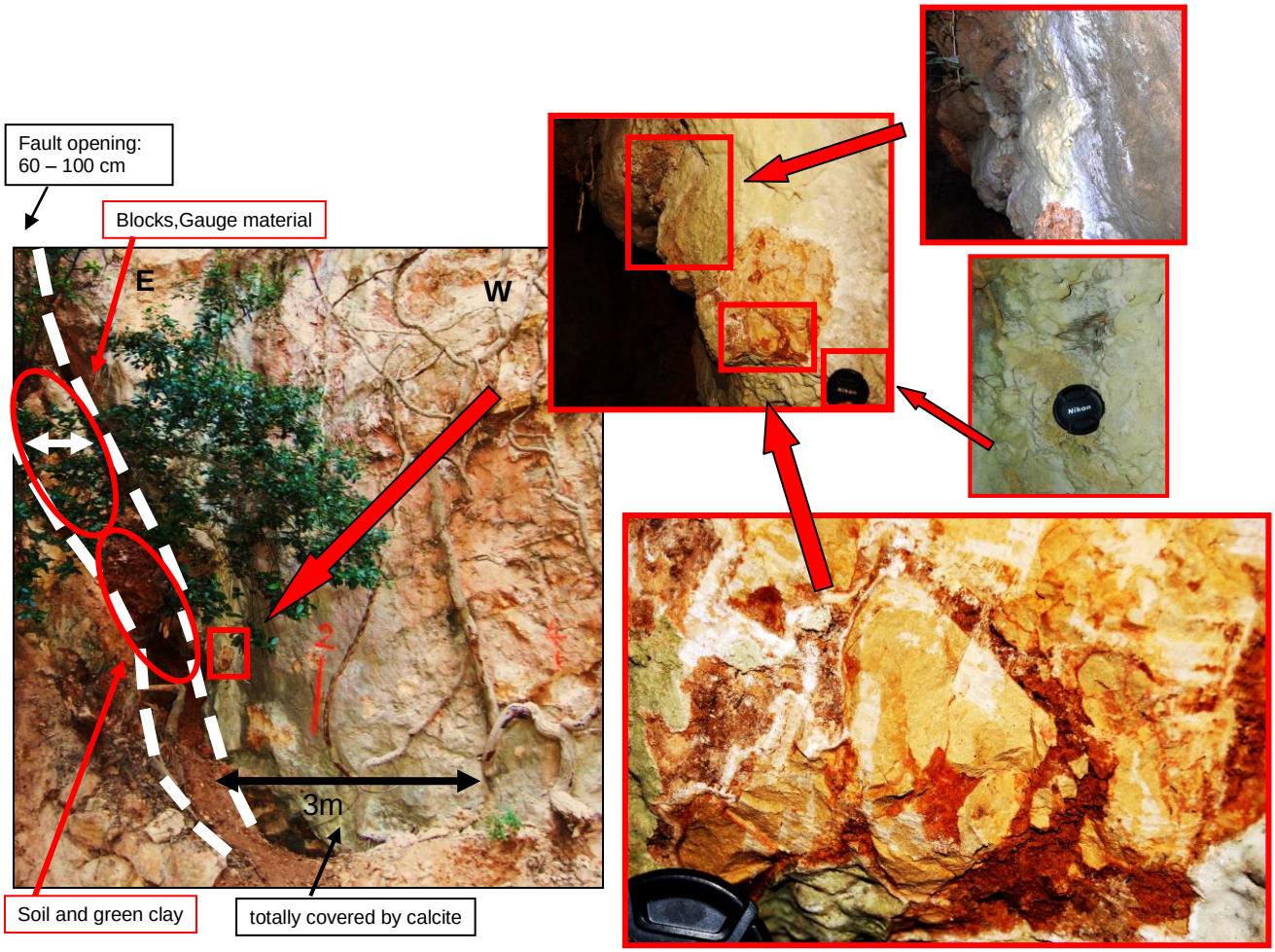

Figure 15 : Visual description of the fault and the first 4m of the cliff face which are completely covered by calcite

4.2 *Horizontal Electrical Resistivity Tomography (ERT)*

4.2.1. Theory

Electric resistivity tomography is one of the geophysical methods that have proved to be important at a large scale, especially for pre-investigation at a feasibility stage. This is a relatively old method which has developed greatly during the last 20 years. The method is relatively fast and coast efficient compared to other profiling methods e.g. seismic refraction. In order to interpret the data certain knowledge of the geological setting is important. Electric tomography is used for measuring the spatial variation in the resistivity of the subsurface. The resistivity of the different geological materials differs greatly from about $10^{-6}\Omega$m in minerals such as graphite to more than $10^{12}\Omega$m for dry quartzitic rocks. Most rock forming minerals are insulators so the resistivity of rocks depends largely on the amount and quality of water bearing fractures or degree of weathering of the rock. Therefore rock without water bearing fractures has a considerably lower resistivity. When electrical resistivity measurements are made a direct current is transmitted between two electrodes (A and B) and the potential difference is measured between two other electrodes (M and N) following different dispositions (Figure 16). The measurement results in an apparent resistivity value that depends on the subsurface conditions. The convention today is to perform a large number of four electrode measurements along profiles.

The result from this type of resistivity measurements is a set of apparent resistivities with corresponding midpoint and pseudo depth that can be presented as a pseudo section. (Figure 16b)
This data can give an estimate of the resistivity distribution in the ground but does not show the true distribution. For an estimate of the actual resistivity distribution it is necessary to perform inverse modelling on the measured data. The root mean square (RMS) indicates the difference between the pseudo section of the apparent resistivity (measures) and the recalculated resistivity (real) of the inversed pseudo section. Techniques for acquisition and interpretation of resistivity data have been developed continuously during the last century and now there are advanced methods available for creating two dimensional as well as three dimensional resistivity models of the subsurface.
Generally the depth of investigation of the method increases with increasing electrode distance. As a rule of thumb the penetration depth of a Schlumberger array is L/4 where L is the distance between the two outermost active current electrodes. (Figure 16a)

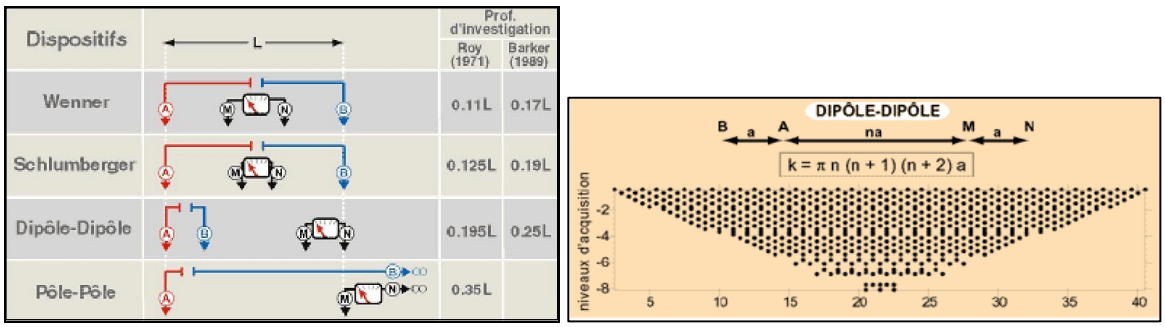

Figure 16 : a(Left side): principal dispositifs and their investigation depth. b(Right side): a model of a pseudo section

4.2.2. Test and Analysis:

To investigate the fracturing in the depth of the cliff face horizontal electric tomography (pole-pole, pole-dipole, dipole-dipole) has been tried. The electrodes were put in horizontal wholes that have previously been bored and then fixed with cement in order to improve the contact and consequently the electric conductivity from the electrode to the rock. The distance between the electrodes is of 1m and a total number of 24 electrodes have been planted.
The obtained values of apparent resistivity have been inversed by means of the Res2Dinv program. The pole-dipole gave the best result in terms of RMS. Despite the data has been filtered and various iterations of filtering have been carried out the RMS remains very high: RMS=74%. This is a not acceptable value and the profile cannot be used to demonstrate and prove anything. Nevertheless an interpretation of the results and an explanation of the errors can be attempted:

A first reason for the high RMS could be the fact that the profile was made in the second half of June when the ground is extremely dry and therefore the electric current is not properly transmitted in the ground. In addition to that the contact between the electrodes and the rock was not very good. Normally the electrodes are planted in the humid soil and the current passes very well but the contact electrode-rock is not perfect and this is even worsened by the fact that this contact is established by means of the cement. So all in all the electric current does not circulate very well despite the attempt to wet the zone where the electrodes are planted which improved the circulation a little but apparently not enough.

Another reason for the bad result might be the inadequacy of inversion program: Not too much time has passed since these programmes have been developed and they are still in constant evolution to be improved. Nevertheless they are still far away from perfection. The data registered in deep layers is influenced by the overlying layers, so more errors and outliers are present in deeper layers. To interpret this data the program takes mean values of more points. In this way the error is reduced at the expense of resolution because fewer points are available in taking the mean values.
In addition to the loss of resolution this program has been developed for vertical profiles and probably the modification of deep values influenced by the superficial ones is different in a vertical and a horizontal disposition.

Although all these problems cause a too high RMS an interpretation of the profile is proposed:

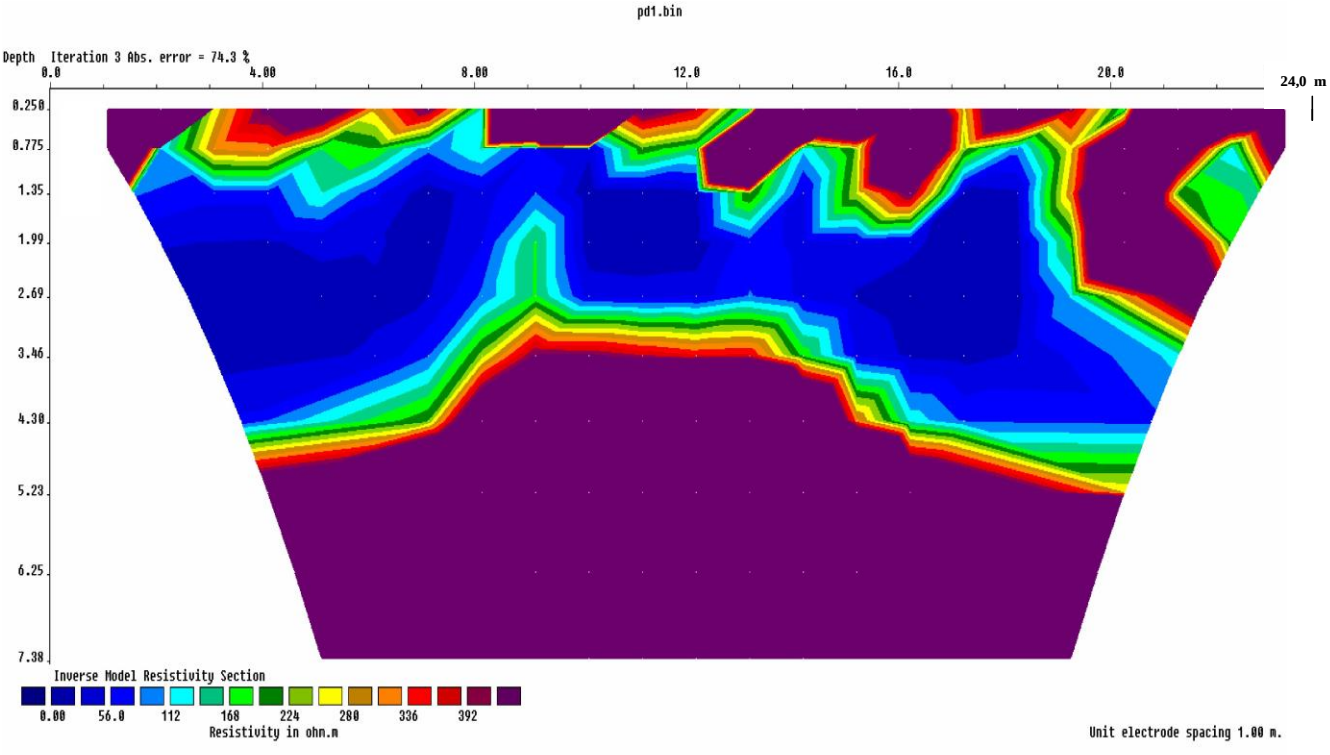

Figure 17 : Inversed horizontal electric profile on the cliff face. (Rms=74,3%)

The first thing that can be seen on the profile (Figure 17) is a great band which is parallel to the surface of the cliff face (W-E) of very low resistivity, $\varrho 1 < 60\ \Omega m$. This band is 1 to 4m thick. To possible interpretations are proposed: It is the expression of the fracturing W-E and represents a decompression of the massif: In the weathering process vertical parallel layers peel off the cliff face thanks to an important decrease of pressure that has taken place when the cliff face has actually become an outcrop. In this fractured decompressed zone fluid circulation is favoured and the zone is more humid than the compact rock, which results in a drop of resistivity.
Another less probable interpretation for this band with $\varrho 1$ is the fact that the profile is not perfectly horizontal and does probably as well not follow perfectly the same layer, since the stratification of the massive is So=47,2° NW 19,5 °. The current tends to descend to lower heights, and not to stay perfectly horizontal. This phenomenon happens when current is injected with horizontally planted electrodes. The well stratified dolomite of this cliff face has some

interpositions of Marls of some mm of thickness. So it might be possible that in this configuration it takes the current several m to go through the Marls which results in this band of resistivity ϱ1 of some m of thickness.

The second particularity of this profile is the very superficial variation of resistivity which can be interpreted as an expression of the fracturing N°175. (Blocks of ϱ3>400 Ωm cut by zones of ϱ2 = 150 – 400 Ωm) Diminutions of resistivity can be observed from3 to 4m, 5,5 to 6,5m, 7,5 to 8m, from 11 to 13m, at 17 and from 19 to 20m. It was hoped to see an expression of these fractures in the depth of the massif but unfortunately they are visible only on the superficial 1,5m. A possible explanation could be the fact that the massif is more compressed starting from a horizontal depth of 3/5m from the surface which is expressed through the uniform resistivity ϱ3. The fractures might exist but are closed and dry and therefore not visible on the profile. In addition to that it has to be remembered that resolution is lost with growing deepness, so it is very difficult to see a closed, dry fracture which has the same lithology on its both sides.

A third particularity is the more resistive point (ϱ up to 230Ωm in the band of ϱ1<60 Ωm) at about 9-10 m from the fault and 1,5 – 3,5 m in the interior of the massive. It might be a more compact, resistant part of the rock or a harder block between two fractured and altered zones.

These interpretations are re-discussed at the light of the other test results in §5.2.1 and most of them are confirmed.

4.3 *Apparent joint separation: s*

4.3.1. Bibliography:

Sorriso-Valvo et al. (1996) found that high intensity jointing alongside major faults influences both the frequency and the typology of mass movements, causing flow types to be more frequent. Greco and al. (2005) studied the intensity of jointing to investigate how the apparent separation of jointing varies according to the distance from faults, and how the mechanical properties of rock masses depend on this distance and jointing density. Such relationships have relevant implications in engineering geology (e.g., in the analysis of landslide susceptibility and hazard, in urban and lifeline planning..). Observations and theoretical studies make assume that the intensity of jointing that accompanies faulting tends to diminish with distance from the faults, but this assumption has been tested only by few researchers. Tansi et al. (2000) used regression analysis to study how jointing depends on faulting, and Greco and al. (2005) found, on a study carried out on Granites that the relationship between apparent joint separation (s) and average distance (d) from the closest fault can be roughly expressed by the formula:

$$s = 0.013\sqrt{d}$$ **(Equation 1)**

4.3.2. Test Protocol:

The number of joints (n) was counted along a straight line, following the layer on both layers every 30cm (L).(**Figure 18**) Its value is obtained dividing the length L by the number of joints crossed by the measure scale.

The apparent separation is expressed in m. $s = \frac{L}{n}$ **[m] (Equation 2)**

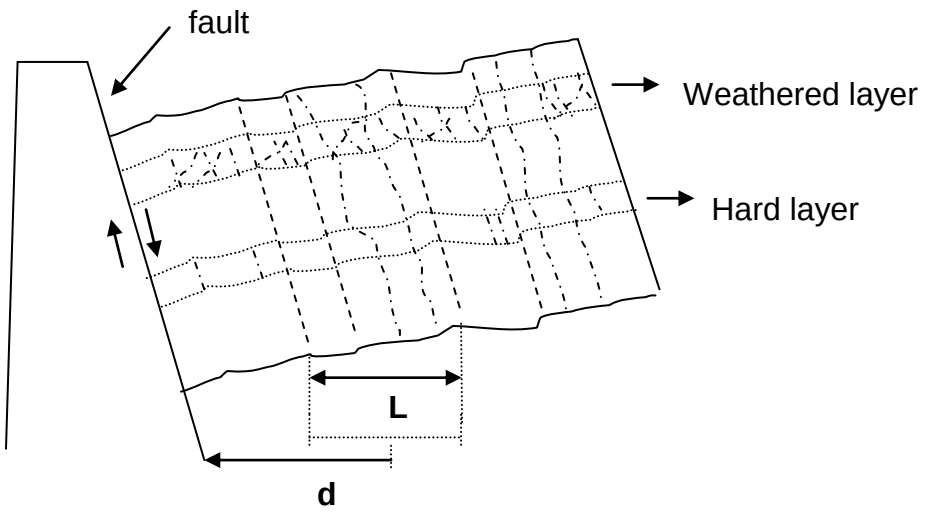

Figure 18: Schematic illustration of the measuring method.

As described in the section of the difficulties it was not always easy to count the number of joints: for the first 4 meters the cliff face is covered with calcite and the joints are not visible, at some points the rock is so fractured and reduced to powder that an extreme limit number has been taken.

4.3.3. Analysis

In this graph the mean value out of three adjacent values has been calculated for each plotted point: The aim of this study is to show a trend, because of this it is not really important to interpret each single measurement, which would provoke too much confusion due to the extreme variability of all parameters measured on the cliff face.
It is immediately evident how the properties of the two layers are not the same. Sometimes they have the same trend and at times they are even in opposition to each other.

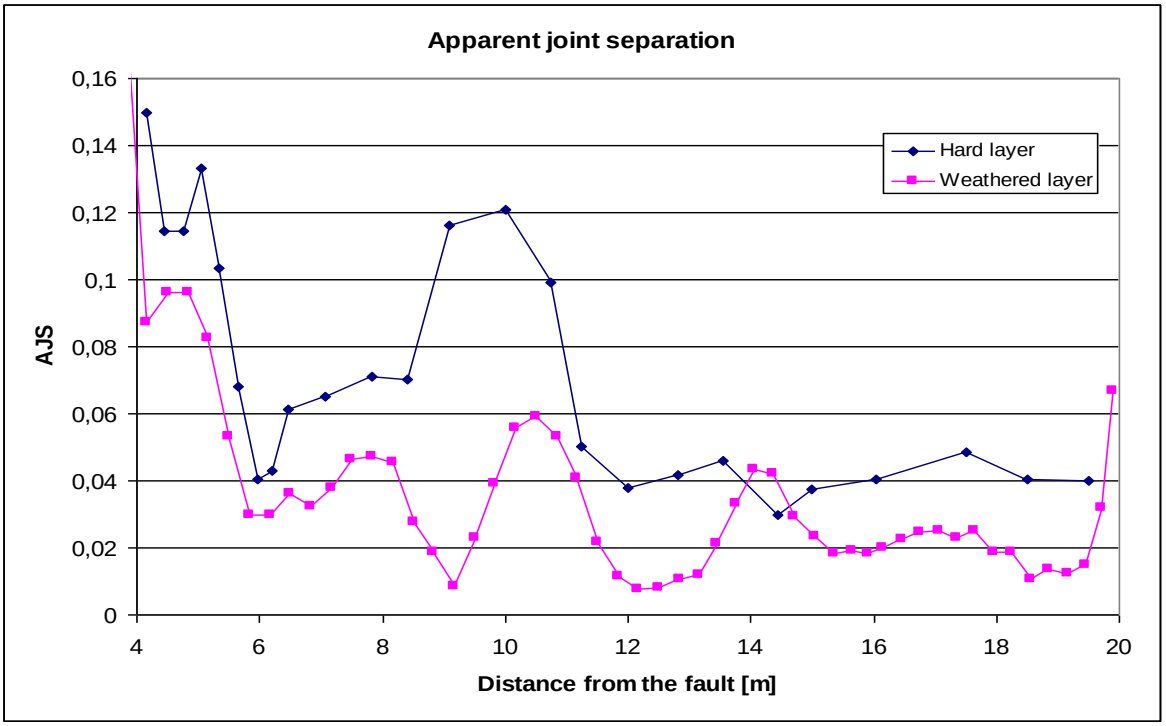

Figure 19 : Apparent Joint Separation in function of the distance from the fault

On the first 4m starting from the fault no value was taken because of the heavy calcification which makes it impossible to see the fractures.
Observing the AJS of the weathered layer the fracture families (175ºN) present on the cliff face are immediately visible: At about 6m the first big fracture family F1 drops the AJS of almost one order of magnitude. F2 is clearly recognizable towards 9m, F3 at about 11- 13m and other two fracture families, F4 and F5 at about 16 and 19m respectively. These last two are not as evident as the first ones: From 15m on the rock is crossed by so many micro-fractures that it hard to recognize the different families. In fact the mean value from 15 m on is lower than on the first 15m, which is absolutely opposite to the expected result of this test.
The AJS of the hard layer is globally higher than that of the weathered layer (0,07m versus 0,057m) F1 is visible in the same way, F2 is not expressed in the hard layer, F3 influences the AJS but not as much as on the weathered layer and F5 at 19m as well. F4 does not determine a drop of AJS.

The opposite trend from 8 to 10m is explainable by the "flower-formed" fractures: the hard layer is cut in blocks (visible surface c.a. 50x50cm^2) by the fractures but is not further altered, whereas the weathered layer is more affected by the micro-fractures which spread from about 1,5m of altitude towards the top of the cliff face, and is almost reduced to soil. (Figure 20)
No certain explanation has been found for the opposition of trends at 14m. The reason might be a different history of this area, or maybe it has been re-calcified differentially by fluid circulation after fracturing.

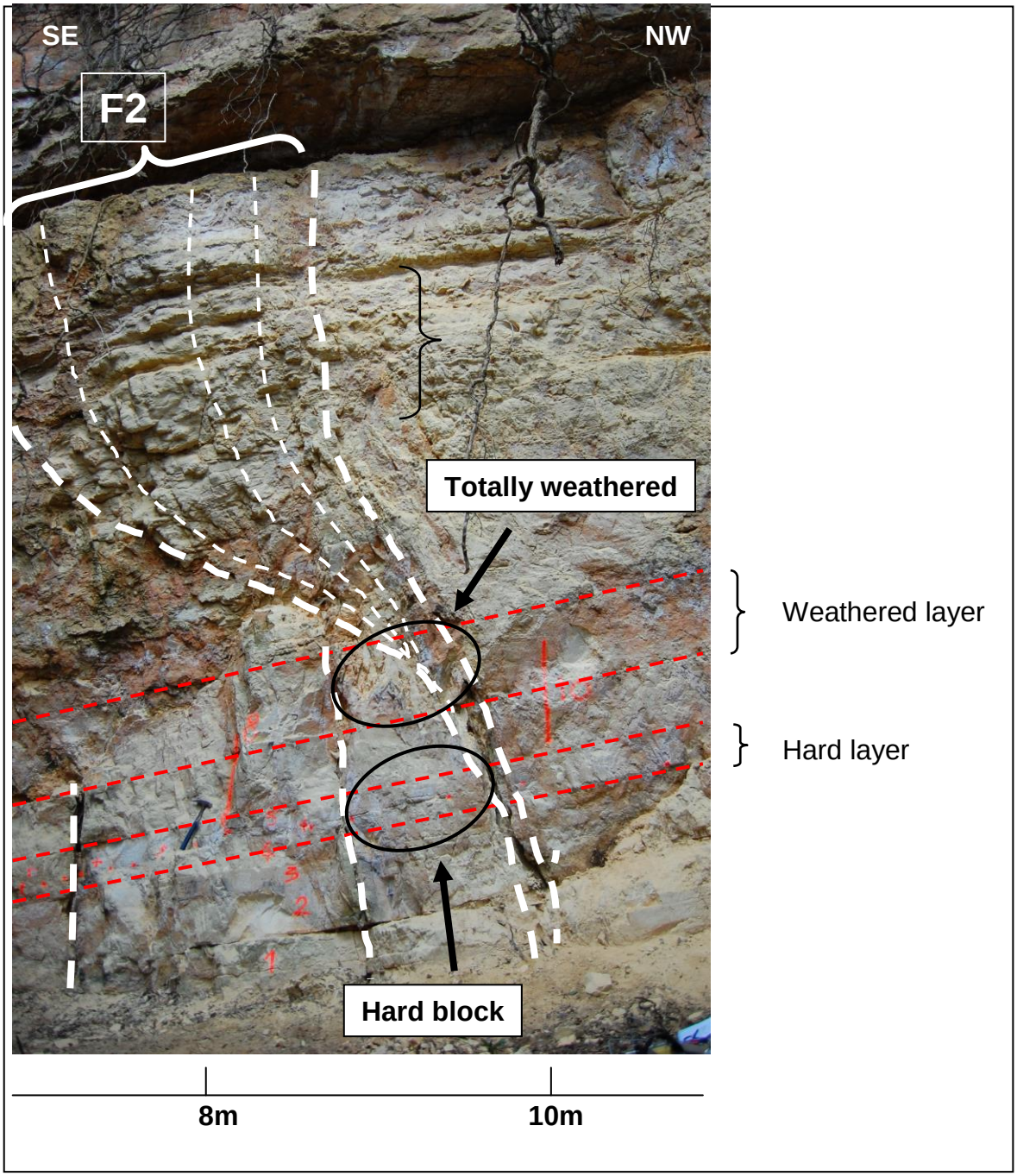

Figure 20 : Fracture family F2 on the cliff face

4.3.4. Conclusion

This result differs totally from that found by Tansi et al.(2000) and Greco et al. (2005). It is absolutely not possible to find a power law which relates the AJS with the distance from the fault. The rock of this cliff face is highly damaged by mechanical and chemical weathering which augments in proximity of the big fracture families and can clearly be seen by a sharp drop of the AJS but no correlation is found in relation of the distance from the major fault. It could be very interesting to perform this test along a horizontal line on the whole versant or even further, out of the zone of the gravitational slope movement, to make a comparison between the damaged and the undamaged zones. Unfortunately there is no continuous outcrop on the versant and the outcrops that are available are often on totally different heights of the

formation. Some are manmade as in proximity of the Foulon channel or besides the roads and have therefore suffered stresses of anthropic origin.

4.4 *Schmidt hammer rebound value: SH*

"Rock strength is commonly assessed directly by engineering design tests. However, testing of mechanical properties is time consuming, expensive and restricted to those rocks that can be machined into regular test samples. Therefore, indirect tests are often used to estimate this property. Most of these tests are simpler, require less preparation, and can be adapted to field testing. The Schmidt hammer is one of the widely used portable instruments for estimating rock strength indirectly. In the civil engineering and mining industries, it is used for non-destructive testing of the quality of concretes and rocks, both in the laboratory and on exposures in situ." (Goktan and al. 2005) Schmidt Hammer rebound value reflects an interrelated combination of rock properties such as the strength of the cementation between grains, hardness and reflect the real inherent inhomogeneity of rock masses.
"The Schmidt Hammer was developed in 1948 for non-destructive testing of concrete hardness, and was later used to estimate rock strength. It consists of a spring-loaded mass that is released against a plunger when the hammer is pressed onto a hard surface. The plunger impacts the surface and the mass recoils; the rebound value of the mass is measured either by a sliding pointer or electronically. Hammer rebound readings are considered consistent and reproducible." (Katz and al., 2000)

4.4.1. Bibliography:

As resumed by Goktan and al. (2005) and Kahraman (2001) Schmidt Hammer is generally used for prediction of UCS and other physic mechanical properties, but many authors have reported other specific applications: Among these are:

- the assessment of rock discontinuities
- joint wall strength
- state of weathering
- mine roof control
- road header and tunnel boring machine performance
- drilling machine penetration rate
- prediction of rock uniaxial compressive strength
- rock rippability
- rock deformation coefficient
- rock abrasivity
- abrasion resistance of rock aggregates
- as a classification parameter for rock excavation
- hardness characterization of granite flooring tiles
- and estimation of large-scale in situ strength in a gallery

"Mechanical properties such as hardness and strength are not intrinsic material properties. The type of the testing instrument and the adopted test procedure will affect the obtained hardness and strength values. Therefore, when defining a mechanical property it is extremely important to specify the test procedure adopted. Various techniques of recording Schmidt rebound hardness data have been proposed in the literature. As can be followed from Table 1, Schmidt hammer test procedures that have been put forward so far are based on either "single impacts" or "continuous

impacts" at a point. While the International Society for Rock Mechanics and a majority of other authors have adopted the test procedures that are based on single impacts, a number of authors have adopted the test procedures that are based on continuous impacts at a point suggesting that they are more consistent and repeatable than single impact tests. One almost common approach that is followed in the testing procedures is the rejection of a certain portion of the observations, before a mean value is calculated (Table 1). Such observations, known as the outliers, are the suspected observations that appear to be inconsistent with the remainder of the observations, and may be too small or too high compared to the bulk of the data." (Goktan and al., 2005)

Author	Test Procedure
Deere DU, Miller RP [2]	Record three readings along the length of NX-size core for each 45° rotation. Average a total of 24 readings, disregarding the erroneous readings.
Young RP, Fowell RJ [17]	Divide rock mass surface into grids and average the single impacts from each grid.
ISRM [37]	Record 20 rebound values from single impacts separated by at least a plunger diameter, and average the upper 10 values.
Goktan RM, Ayday C [38]	Record 20 rebound values from single impacts separated by at least a plunger diameter. Reject outlier values by using Chauvenet's criterion, and average the remaining readings.
Soiltest [42]	Record 15 rebound values from single impacts and average the highest 10. The maximum deviation from the mean should be less than 2.5.
Matthews JA, Shakesby RA [16]	15 measurements on any sample. The mean of the rebound values are calculated and the five values deviating most from the mean are discarded.
Kazi A, Al-Mansour ZR [33]	Record at least 35 rebound readings, drop the 10 lowest readings and average the remaining 25.
Katz O. et al. [13]	Perform 32–40 individual impacts and average the upper 50%.
Poole RW, Farmer IW [39]	Select the peak rebound value from five continuous impacts at a point. Average the peaks of the three sets of tests conducted at three separated points.
Hucka V [40]	Select the peak rebound value from 10 continuous impacts at a point. Average the peaks of the three sets of tests conducted at three separated points.
GBG [41]	Record 12 readings taken in a diamond pattern at the test point. Discard the lowest and highest values to obtain a mean rebound number.
USBR [43]	Ten readings at various locations on each surface. Discount the five lowest readings, and average the highest five.
Sumner P and Nel W [46]	Take 15 readings at different points and discard five great outliers to obtain a mean value from the remaining 10 values.

Table 1 : Some recommended Schmidt Hammer test procedures and discard of outliers (Goktan and al. 2005)

4.4.2. Test protocol

The different grade of weathering which influences the mechanical and structural properties of the rock is studied along the cliff face. Schmidt hammer test in order to investigate the link between the apparent joint separation and the mechanical strength of rock in function of the distance from the fault has been performed. Starting from the fault the tests have been made on a total length of 20 m on two different layers: a very weathered layer and a very hard one

The rebound value (SHRV) was measured on the same layers with a Schmidt hammer: Original Schmidt, N type (Figure 21)(Characteristics in Annex)

Figure 21 : Schmidt Hammer « Original Schmidt, N Type » (left), operator using the Schmidt Hammer on the cliff face (right)

As suggested by Katz and al. (2000) the test-surfaces are polished with an electrical grinder before performing the test: The grinding cleans the test surface from the outermost weathered layer reducing the standard deviation from the mean value because surface irregularities often crush before the plunger tip reaches the main surface, resulting in a loss of impact energy and a non representative value.

On the very weathered layer two series of test have been performed:

During the first test series the whole layer of superficial calcite has been taken of, in fact a whole chip of rock has been taken away from the surface, in order to perform the test on a rock portion that has not been exposed to the atmosphere so as to perform the test on an inner rock core. During the second test series on the weathered layer and the test series on the hard layer the rock has only been ground superficially with the electrical grinder without taking away a whole rock portion, clearing only off the irregularities, asperities and the calcite on the very surface.

At each test point 15–30 continuous impacts were made and the rebound values were adjusted according to the hammer attitude with respect to the horizontal. The performed test procedure is based on continuous impacts at a point which is more consistent and repeatable than single impacts. As recommended by Katz and al. (2000) the individual impacts were conducted with the minimal separation of the plunger diameter between impact locations. This separation ensures that the impact hits undamaged rock. The different number of continuous impacts is dependent on the available test surface. It was not always easy to find a test surface big enough to carry out the whole number of tests. This test surface has to be perfectly vertical (as the chosen normalisation of the SH is to the horizontal in our test procedure) and sufficiently hard in order to avoid cracking or visible damage on the rock. Where possible, several test series of 15 or 30 continuous impacts have been performed.

4.4.3. Statistical reduction of Data

Statistical test results suggest that incorporation of all recorded rebound values at a point, rather than selecting only the peak values, gives a better representation of overall rock

hardness and hence a better performance prediction, provided the outliers are statistically discarded (Goktan, 2005)
One method that has gained wide acceptance is Chauvenet's criterion; this technique defines an acceptable scatter, in a statistical sense, around the mean value from a given sample of n measurements. The criterion states that all data points should be retained that fall within a band around the mean that corresponds to a probability of $p = 1 - \frac{1}{2n}$. In other words, data points can be considered for rejection only if the probability of obtaining their deviation from the mean is less than $\frac{1}{2n}$. (**Figure 22**)

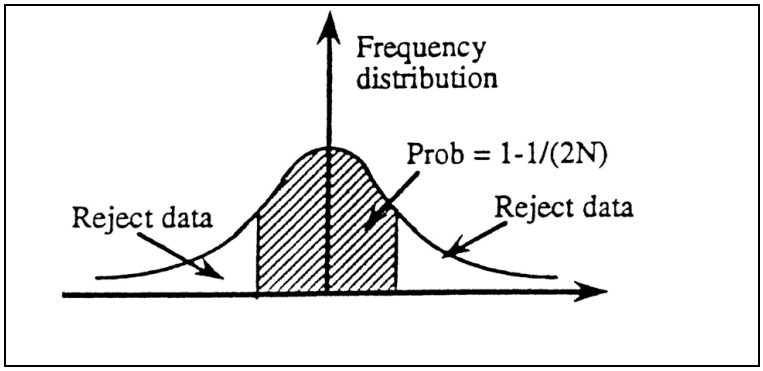

Figure 22 : Chauvenet's criterion (Bayless D.J.)

4.4.4. Analysis

As for the AJS the mean value out of three adjacent values has been calculated and plotted. (Figure 23) The reason for analysing a mean value instead of each single measurement is the same for which 15 or 30 continuous impacts are performed on each measured point: the extreme variability of these values. Furthermore the aim of this test is to show the course of how the mechanical parameters change in space; therefore analysing mean values out of three measured points avoids a lot of noise in the data.

The results of the first test series on the weathered layer regrettably produced results that would mislead the analysis: It was not always easy to take away a whole part of rock from the surface and it was necessary to use a chisel and a hammer. In this process the underlying rock has visibly been damaged and many micro fractures were induced. Therefore the SHRV were very low (~15) and sometimes it was so low that the test machine did not even register the result. Using this data would distort the results of the analysis since the tests were carried out on recast and not on untouched rock material. Therefore only the results of the tests that were carried out on the polished, superficial rock are plotted in Figure 23 and discussed in the following paragraph:

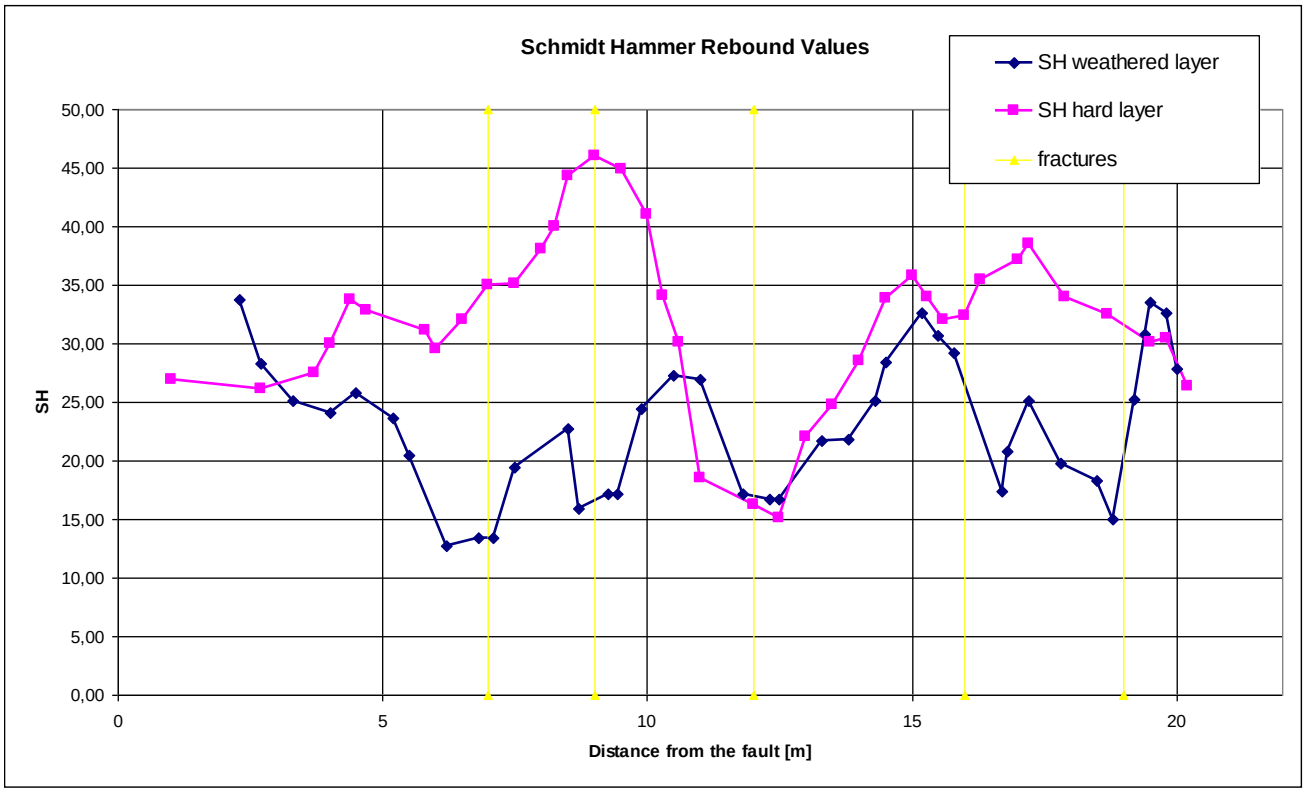

Figure 23 : Schmidt Hammer Rebound Values in function of the distance from the fault

As for the AJS here as well it becomes evident how the properties of the two layers are absolutely not the same. The global mean SHRV is 32 on the hard layer and on the weathered layer almost only two thirds of it (SHRV=22,6)
On the first 4m starting from the fault an interpretation is difficult due to the heavy calcification. The SHRV of the weathered layer reflect the fracturing of the rock. The 5 fracture families F1-F5 are clearly recognizable through a drop of the SHRV of about 10 units in comparison to the surrounding measurements. The lowest measurable value is 15. Under 15 the Schmidt Hammer does not measure the rebound value. There where the rock is totally decomposed the value 0 was attributed.
Obviously the values of the hard layer are higher. As for the AJS, F2 does not influence the measurement at about 9m where the hard layer is cut in blocks by the fractures but is not further altered. (Figure 20)

4.4.5. Conclusions

No linear correlation has been found between SHRV and the distance from the fault but a very clear relation between SHRV and the fracturing of the rock. The SHRV sharply diminishes in the fractured zones on the weathered layer, which represents better the altered structure of the whole cliff face. Fracturing favours weathering by allowing an increased fluid circulation and both cause the disintegration of the rock and weaken the rock strength which is clearly demonstrated above. In § 5.2.2 and §5.2.3 the SHRV is correlated with the AJS and the UCS respectively as can be fully found in literature. (Respectively: Greco et al. 2005 and Kahraman 2001, Katz and al. 2000, Aydin et al, 2005).

4.5 *Triaxial Compression Tests (TCT)*

Shear strength parameters are basic input parameters of all kind of approaches in landslide problems. We want to compare these mechanical parameters with weathering parameters in order to characterize weathering process and the interaction with landslide generation.
With the cohesion and friction values obtained in these tests an easy slope stability calculus has been performed in order to see how the factor of safety changes.

4.5.1. Theory:

The TCT is used to measure the shear strength of a soil under controlled drainage conditions. A cylindrical specimen of soil is encased in a confining fluid pressure and then loaded axially to failure. The test is called "triaxial" because the three principal stresses are assumed to be known and are controlled.
This test equipment is conventionally used because it offers advantages like: drainage can be well controlled, no rotation of the principal stresses likes in the direct shear test and the failure plane can occur anywhere.

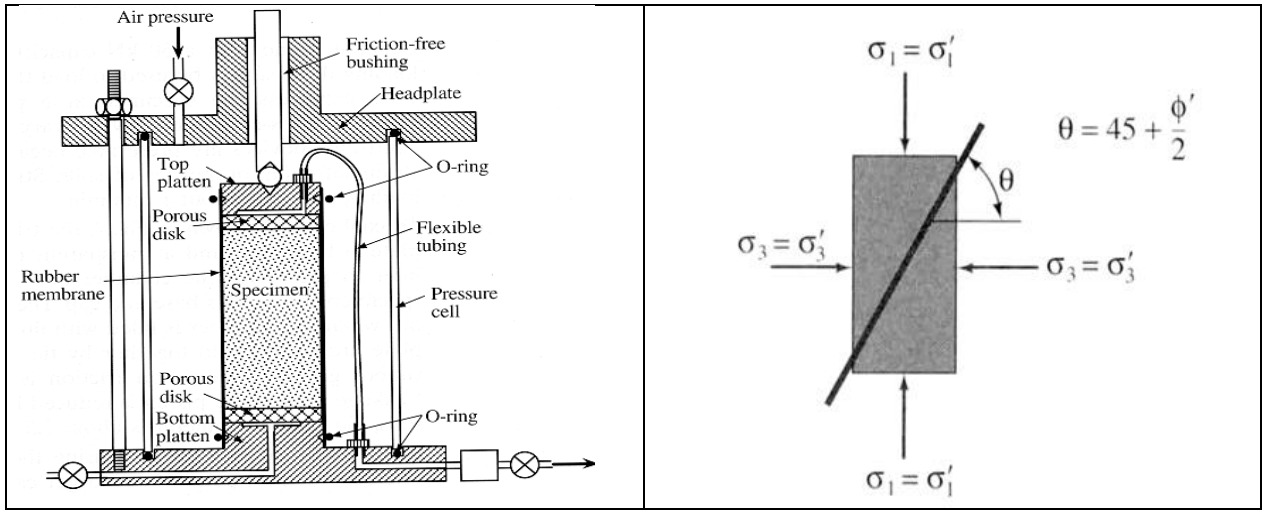

Figure 24 : Simple demonstration of triaxial compression test, (left) and stresses applied during experiment, (after: Geotechnical Engineering Laboratory, CE 3121, Texas tech. University) (right)

During shear, the major principal stress, σ_1, is equal to the applied axial stress ($\Delta\sigma = P/A$) plus the chamber (confining) pressure, σ_3. In Mohr diagrams, these stresses are represented as shown in Figure 25. The applied axial stress, $\sigma_1 - \sigma_3$ is called the "principal stress difference" or the "deviator stress". The intermediate principal stress, σ_2 and the minor principal stress, σ_3 are identical in this test, and are equal to the confining or chamber pressure.
Soil specimens are loaded to failure under 3 different confining pressures. Failure will be defined as the peak or maximum value of the reached deviator stress (ASTM D2850). Using Mohr diagrams of these experiments, the shear strength components of the sample can be estimated (Figure 26).

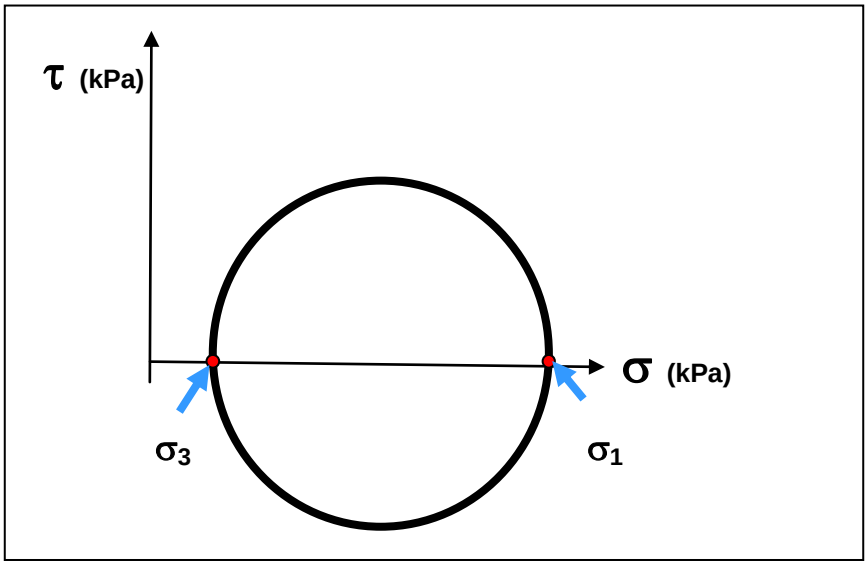

Figure 25 : Generation of Mohr diagram related with triaxial compression test (after: Geotechnical Engineering Laboratory, CE 3121, Texas tech. University)

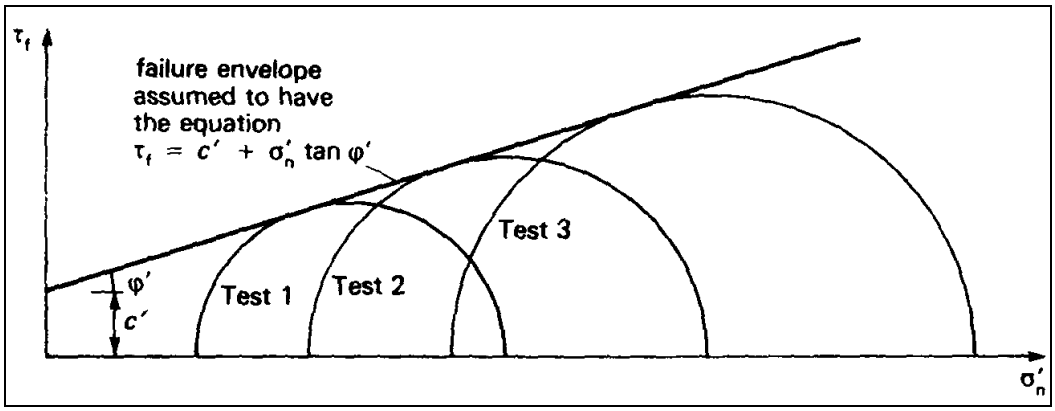

Figure 26 : Calculation of c' and φ' by using triaxial test results (after: Geotechnical Engineering Laboratory, CE 3121, Texas tech. University)

Drained conditions occur when the rate at which loads are applied are slow compared to the rates at which soil material can drain (k – dependent). Sands drain fast; therefore under most loading conditions drained conditions exist in sands.

The shear strength parameters φ' and c' are the mechanical state expression of a granular and cataclastic material. These mechanical parameters can be explained by the shape and the particle size distribution. As studied by Lebourg (2000) the mechanical parameters of loose material are strongly influenced by external processes as tangential displacement, weathering and leaching (Figure 27)

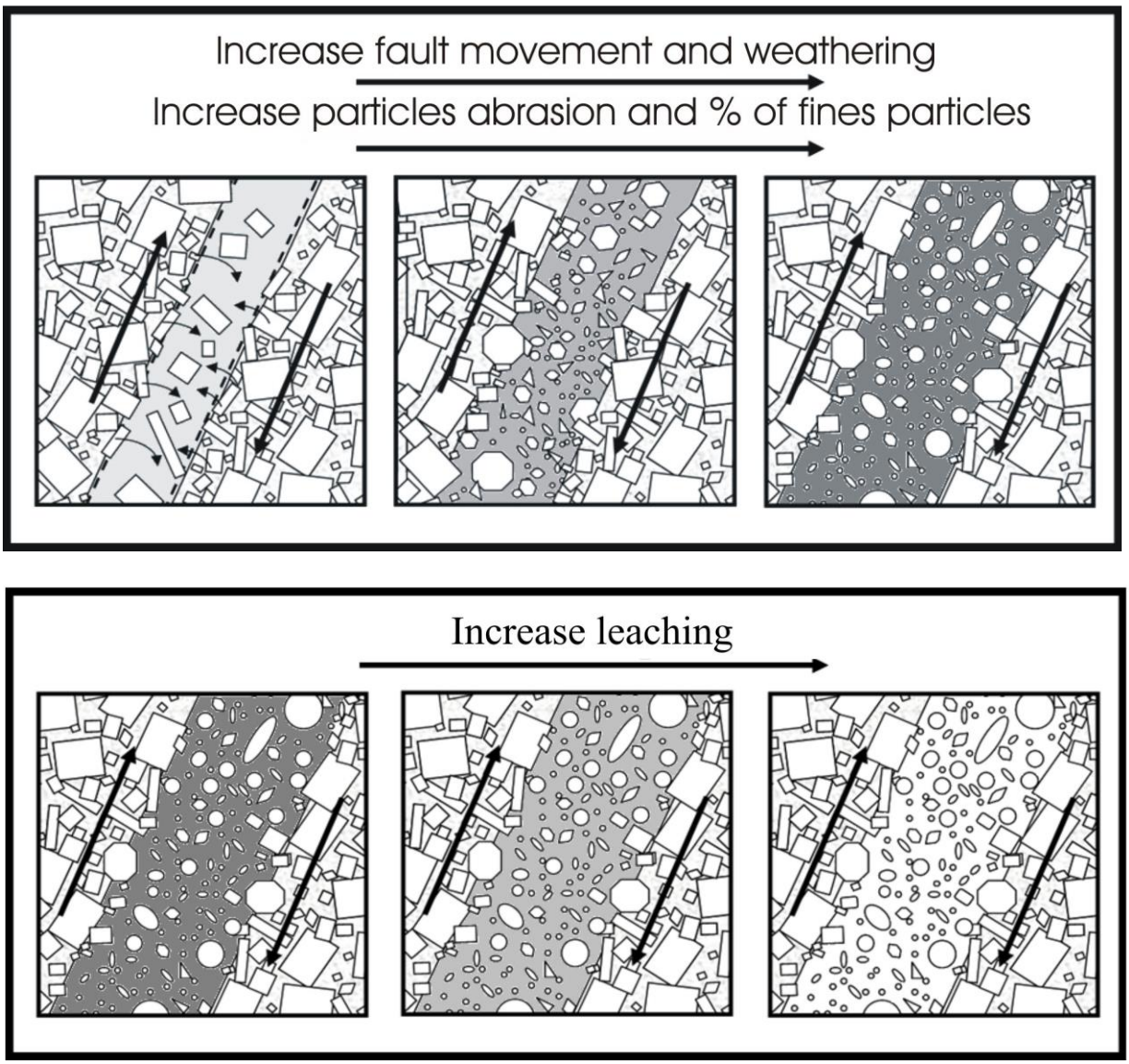

Figure 27: Effect of fault movement and weathering on rock, (top), effect of leaching on rock (bottom) (Lebourg, 2000 ???)

- The tangential displacement and the weathering are the processes which increase particle crushing and so decrease grading and particle diameter which results in a decrease of φ' and increase of c'
- The leaching is the phenomenon which increases φ' and decreases c' due to a loss of mineral and organic solutes trough percolation.

4.5.2. Test protocol

For these experiments, we have used triaxial compression test machine (Heavy Duty Banded Triaxial Cells, Wykeham Farrance) (Figure 28).

Figure 28 : Triaxial compression test equipment

The TCT were performed on samples taken in the open fractures that are present all over the cliff face and are mostly filled with fine material which has its origins from the alteration of the original dolomite rock (Figure 29). Where no fracture was present the material has directly been dug out of the cliff face.

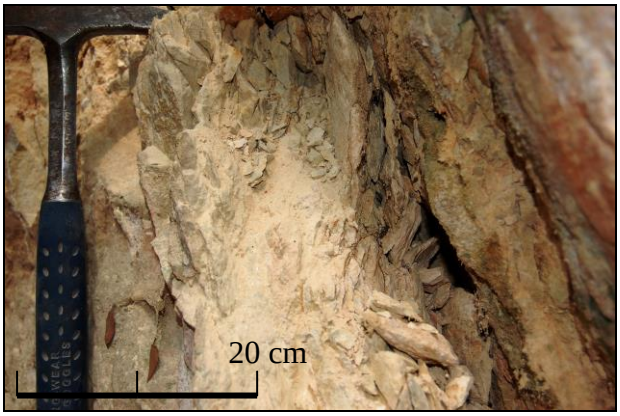

Figure 29 : Fine material generated by alteration of dolomite rock. It fills the fractures and constitutes the most weathered parts of the cliff face

Because of the granular nature of the samples and the different opening grade of the fractures it was impossible to take undisturbed samples.
The different sampling protocol divides the samples in 2 groups:

- 5 samples taken in fractures (96,9º N 86,7), which have been more exposed to erosion than the others : 6m, 8m, 11m, 18m, 19,3m
- 4 samples dug directly out of the cliff face : in the fault, 1,5m, 10m, 14m

The sample of loose material is compacted in the laboratory. Only the part with a grain size lower than 4 mm is taken. The bigger parts are rock fragments of variable size but all bigger than some cm and cannot be identified as the sampled soil.
The specimen (Figure 30) (Diameter 50mm, height around 100mm) is enclosed vertically by a thin rubber membrane, on both ends by rigid surfaces (platens) and by a porous membrane on the bottom.

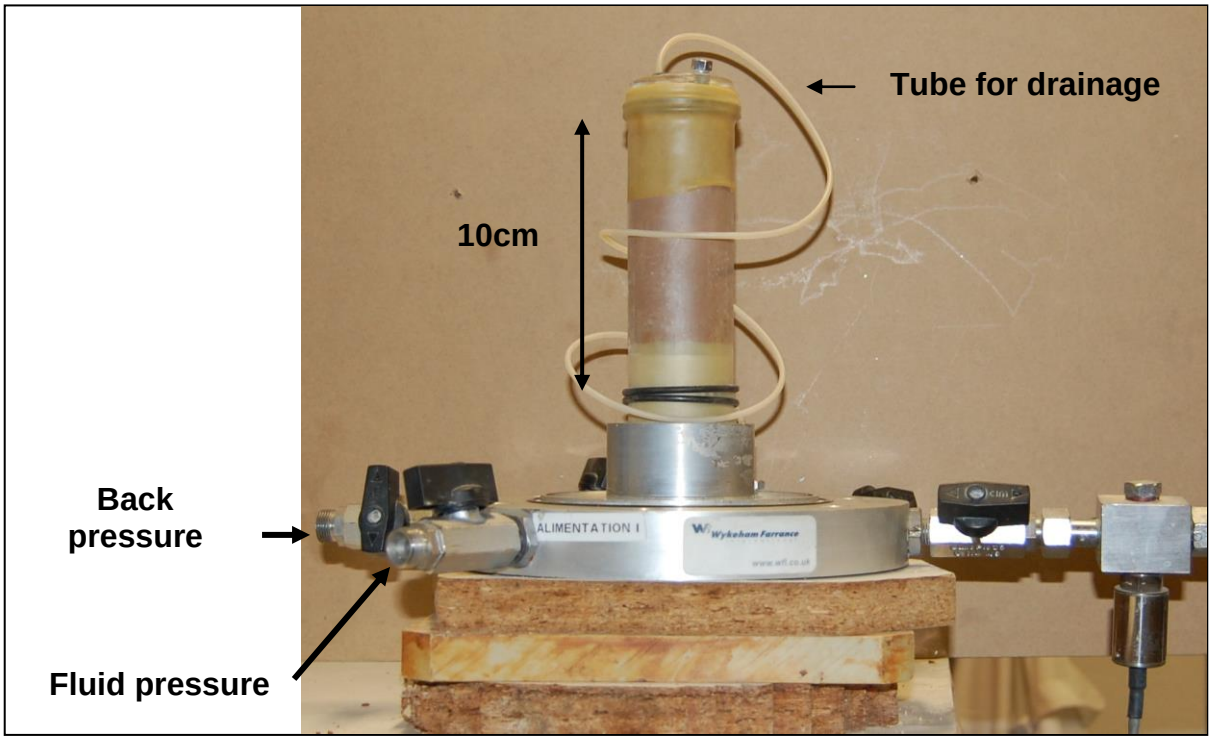

Figure 30 : Specimen for triaxial compression, h=10cm, Ø=5cm

Then it is placed in a pressure chamber and a confining pressure σ_3 is applied. Three tests are carried out on each sample with consolidation and drainage:σ_3 = 100kPa, 200kPa and 300kPa.. For the standard triaxial compression test the axial stress (σ_1) is applied by the testing apparatus with a constant loading velocity of 3mm per second reaching a maximum deformation of 30%.In most cases the specimen broke long before reaching the 30% of deformation. In some cases these parameters are not sufficient to destroy the specimen during the standard triaxial test, higher pressures up to 500 kPa and loading velocities of 5 mm/s are used. Thought of the loose granular and poorly cohesive nature of the material the tests were performed in drained conditions: the stress is therefore directly applied to the solid skeleton and interstitial overpressures are negligible, thus this adjustment of the test procedure does not influence the test results. The mechanical parameters of cohesion (c' in kPa) and internal friction (φ' in degrees) are calculated using the method of the least rectangles and according to the formula of Mohr-Coulomb: $\tau_{max} = c' + \sigma' \tan\varphi$ where τ_{max} is the maximal shearing stress and σ' is the normal effective stress.

4.5.3. Analysis of the results:

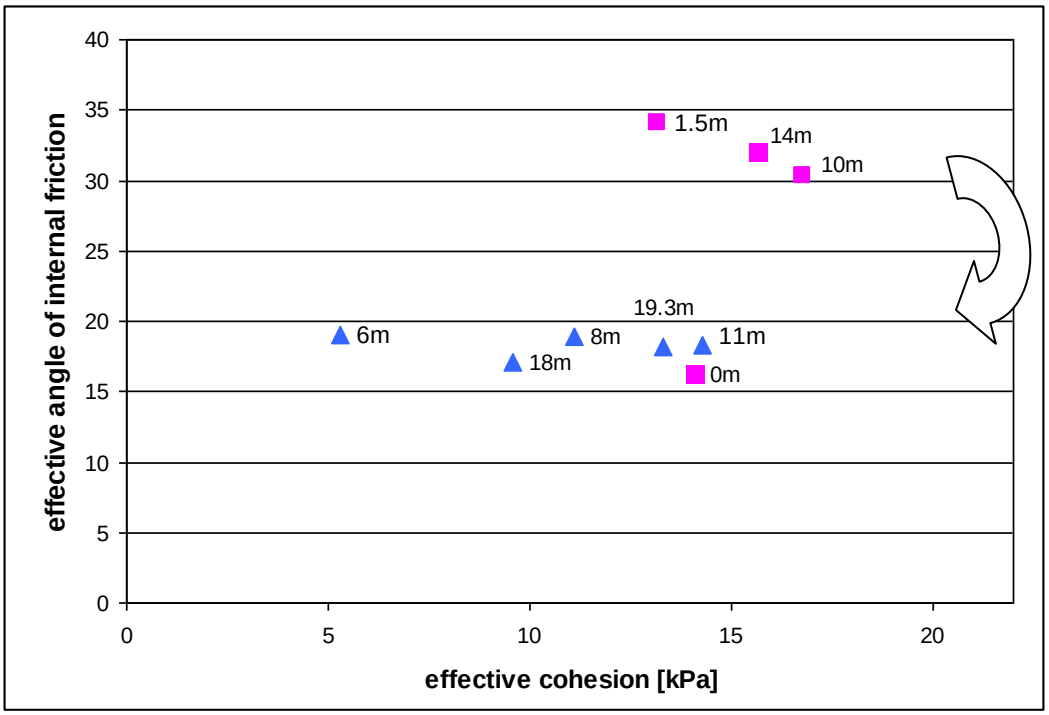

Development of a week zone of the cliff face into an open fracture.

Figure 31 : Development of the mechanical parameters (Effective internal angle of friction in function of the effective Cohesion) in time, affected by weathering.

The effective angle of internal friction is plotted against the effective cohesion in Figure 31. The squares (pink) represent those samples that were dug out of the cliff face, the triangles (blue) those sampled as loose material in the fractures. They can well be divided in two groups.
The samples dug out of the cliff face have an effective internal angle of friction, φ' which varies between 32º and 34 º, and an effective cohesion between 13 and 17kPa, except the sample taken on the fault wall. The mechanical parameters of this sample match with those of the samples taken in the fractures: φ' varies between 16,7 º and 19 º, and c' varies between 5,3 and 14,3 kPa. The exception of the sample "0 m" can easily be explained: this material has not been sampled on the cliff face but on the fault wall (which can be seen as an enormous open fracture) at about 15m from the cliff face where the extremely high weathering reduces the rock to soil. (It is reminded that the cliff face is perpendicular to the fault wall which is exposed on the left side of the cliff face). (Figure 9) Therefore this sample will be considered in the evaluation as one taken in a fracture.

In a first time of the evolution the variation of the mechanical parameters can be attributed to tangential displacement and weathering: The development of a week zone of the cliff face into an open fracture. In this development the mean value of φ' drops from 32,1 º to 18 º which is exactly a loss of 44% of friction! The mean value of c' decreases 26% of its original mean value: from 15,2 to 11,3 kPa.

The analysis of the variation of c' and φ' in relation to the distance from the fault does not have a significant result. Not enough samples are available and the distinction in the two groups deprives the number of comparable samples furthermore.

4.5.4. Conclusions

The values of c' and φ' are key properties in geotechnical analysis for stability calculations in gravitational risk prevention and the study of their temporal evolution is of primary importance. In this analysis it has been found that the cohesion drops 26% of its original value and the internal angle of effective friction is almost halved: it has a loss of 44% in the evolution from very altered rock to open fractures. In stability models this important loss of shear strength absolutely has to be taken in account as shown in paragraph 5.4.

4.6 *Uniaxial Compression Tests (UCS)*

4.6.1. Theory:

Two aspects of rocks must be recognized when formulating any testing program: one is the nature of the rock substance or combination of minerals, that comprise the basic material, the other aspect is the nature of the rock mass or formation, which includes not only the rock substance but all of the structural features such as joints, faults, bedding, warping and other discontinuities. Paradoxically whereas for most problems the purpose of laboratory testing is to find out the strength characteristics of the rock mass, the majority of testing techniques concern the rock substance.
The purpose of the uniaxial compression test is to determine the compressive strength of the ground for engineering purposes. It has been assumed that failure in compression could than be predicted by comparing the calculated stresses around the opening with the strength that has been tested. This procedure has been based on the assumption that the strength of laboratory samples would be representative of the rock mass but it is being increasingly recognized that structural geological factors normally make this an invalid assumption. (CONTROLLA) Compression testing can be used to classify rocks for both strength and deformation properties as well as to provide a rough index of drilling and grinding properties. In this study the USC is analysed in order to determine the rock strength quantitatively for showing the extreme alteration of this dolomite in confronting its resistance values with those normally indicated in tables for a sane dolomite or limestone. Some of these values have been resumed in (Table 2) Therefore the dilemma if it really represents the whole rock mass will not play an important role for this purpose of this study. Additionally the found strength values will be used to determine their correlation with the SHRV, non destructive, easier, cheaper and less time consuming test. Where a good correlation between UCS and SHRV consists, this last one can be used to estimate the USC.

Uniaxial compressive strength (Mpa)	**Low**	**Normal**	**High**	**Mean**	**Reference**
Limestone	5-50	50-150	150-215	88	Ippolito, (1975)
Dolomite	38			108	
Limestone, Solenhofen				225	Wiebols et al, (1968) in Jaeger, (1969)
Limestone	35	105		70	CONTROLLA

Table 2 : UCS Values of Limestone and Dolomite

4.6.2. Test protocol:

"The uniaxial compression test, in which right circular cylinders or prisms of rock are compressed parallel to their longitudinal axis, is the oldest and simplest test, and continues to be one of the most convenient and useful ways for determining the properties of rock. In the past tests were usually made on cubes as it is still the case with tests on concrete or with cylinders having a length equal to their diameter, which is still the practice with coal. The behaviour of rock specimens which are short in relation to their diameter is affected strongly by contact with the platens between which they are compressed. Even when the surfaces of the specimen and the platens are flat and parallel, the rigidity of the platens restricts the lateral expansion of the ends of the specimen. The recent tendency is to use relatively longer cylinders with a ratio between length, L and diameter, D, which ranges from 2 to 3." (Jaeger et al. 1969) Short specimen might not show the preferred plain of failure whereas long specimen may fail by elastic instability. (LIBRO, CONTROLLA) The strength decreases with increasing length in relation to the diameter.

The uniaxial compression tests of this study were performed on cylindrical drill cores with a ratio L/D=2 (H=100mm, D=50mm) which is the minimum of the values recommended in literature. The tests were performed using an IGM Press with a 300kN captor (Figure 32). The samples were loaded vertically in axial strain control at a rate of 0,2 MPa/s.

Figure 32 : UCS test with IGM Press with a 300kN captor. Specimen h=10cm, Ø=5cm

4.6.3. Analysis:

Due to the extremely high alteration of the rock not many specimens could be prepared for the UCS test. Only 6 tests could be carried out. The UCS of the altered dolomite ranges from 12 to 31 Mpa (Figure 33). The high alteration grade of this dolomite becomes clear when its UCS values are confronted to those of fresh dolomite or limestone.
The mean values for Limestone are 70 and 88 MPa respectively after CONTROL, and Ippolito (1975). Wiebols et al. found even a mean value of 225 MPa for the Limestone of

Solenhofen. Regarding the Dolomite, Ippolito found of 108 Mpa as a mean value, and for low quality Dolomite he found 38MPa. (Table 2) The UCS values found on the Hettangien cliff face range from 12 to 31 MPa. That means that the highest UCS value measured on specimen from the studied area is almost 20% lower than the lowest value and 70% lower than the mean value found in the resuming and representative tables of Ippolito (1975). This proves the extremely high alteration grade of this Dolomite. In addition it can also be said that the length/diameter ratio of the used specimen was L/D=2, which in literature is the minimum accepted value. Since it is generally admitted that strength increases with decreasing length, these short specimen should provide relatively strong values of UCS but due to their extreme alteration also with this minimum L/D ratio the resulting strength values are extremely weak.

Unfortunately the UCS values have been determined only for the first 10m of the cliff face. Even so it is clearly visible how the shear strength decreases at 6m from the fault. This is probably due to the high alteration of the rock caused by the fracture family F1. The fracture family F2 (at 9m) does not affect the rock of the hard layer where F2 is expressed as one open fracture in the solid, not very altered rock. The same result was found for the SHRV and the AJS. The diminution of UCS towards 10m might be influenced by F3 (11-13m) which diminishes the rock strength of all layers and is the broadest damage zones, also if the AJS and the SHRV of the hard layer actually presents a peak at about 10m.

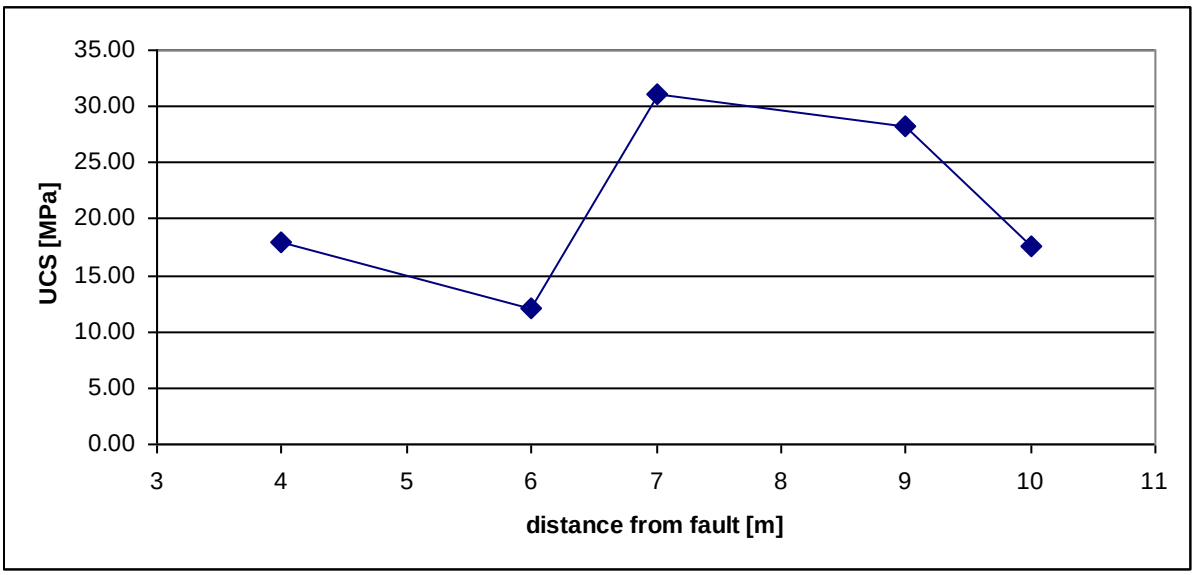

Figure 33 : UCS of the drill cores B in function of the distance from the fault

4.7 *Drill cores:*

4.7.1. Analysis of drilling session A

The first sampling session is performed on a hard layer, just underneath and with the same characteristics of the hard layer on which all the other tests are performed. (Figure 34) The distance between the drill cores is in-between 0,7 – 2,7 m and a total number of 13 core runs are sampled.
The diamond-tipped core drill used is a "Golz gmbH typ FB 100" with a core run of 40cm.

Figure 34 : Drilling on the cliff face

Much of the extracted material cannot be collected since the strongly weathered material disintegrates during the sampling and is washed away by the injected water. In some cases the last part of the core run is lost in the bore hole because they do not break and remain attached to the rock. For this reason the RQD was not performed.

Nr: A	Distance from fault(m)	Thickness of calcite (mm)	Longest fragment (cm)	Dry bulk density [g/cm^3]	Effective porosity [%]
1	fault	45	piece 2,5 x 3,5	2,08	9,26
2	0.5	15-27	4,5	2,15	11,63
3	2	2	3	2,20	14,65
4	4.3	1-5	31	2,51	10,84
5	5.8	1-3	piece 2x5	2,33	11,00
6	7.5	0,5	7	2,22	23,76
7	8.2	0	13	2,19	19,53
8	8.3	Missing outer part	14	2,06	20,71
9	10	0	20	2,50	9,12
10	12.7	0	5-10	2,07	23,87
11	14.2	0	piece 2x7	2,16	20,99
12	16.2	<0,5	3-8	2,11	22,24
13	18.7	<0,5	10	2,39	8,97

Table 3 : Characteristics of Drill cores A

4.7.1.1 Visual analysis:

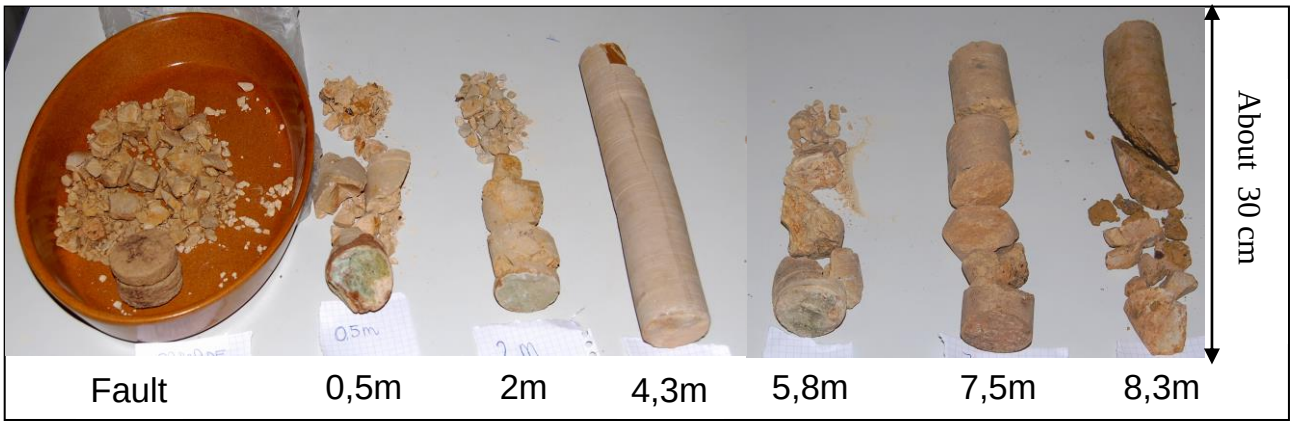

Figure 35 : Drill cores A 1-7

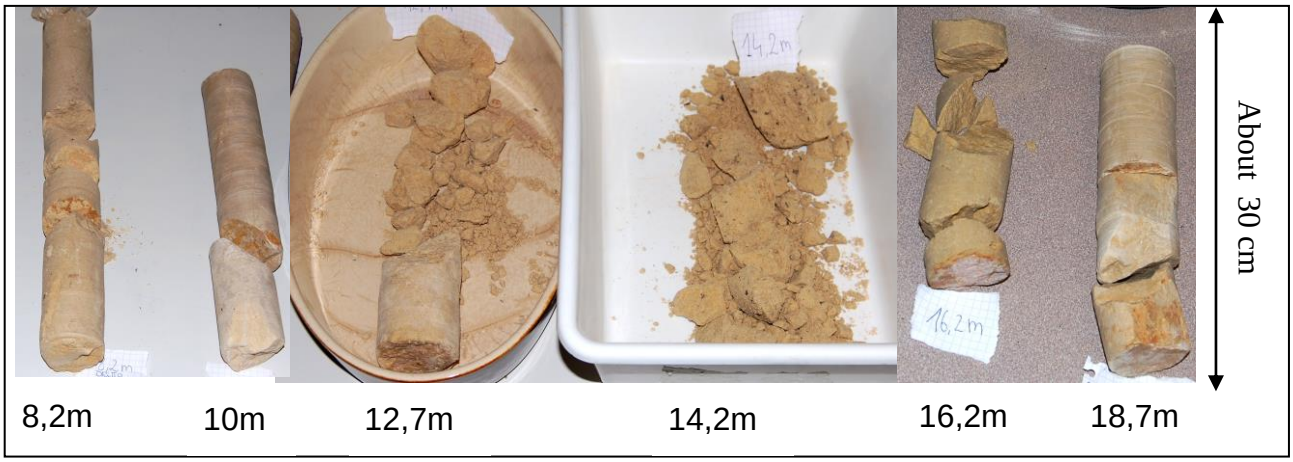

Figure 36 : Drill cores A: 8 – 13

Drill cores Nº1 to Nº3, extracted starting from the fault to a distance of 2m from the fault contain "Bimrocks" as firstly described by Medley et al.(1994). "Bimrocks" is a contraction of the term "block-in-matrix rocks" and defined a bimrock as " a mixture of rocks, composed of geotechnically significant blocks within a bonded matrix of finer"." The expression "geotechnically significant" means that there is a mechanical contrast between blocks and matrix." (Kahraman et al., 2006)
This finer matrix has totally been destructed during the sampling and has so been washed away by the drilling water. The remaining debris have a size mostly in between 4 and 16 mm.

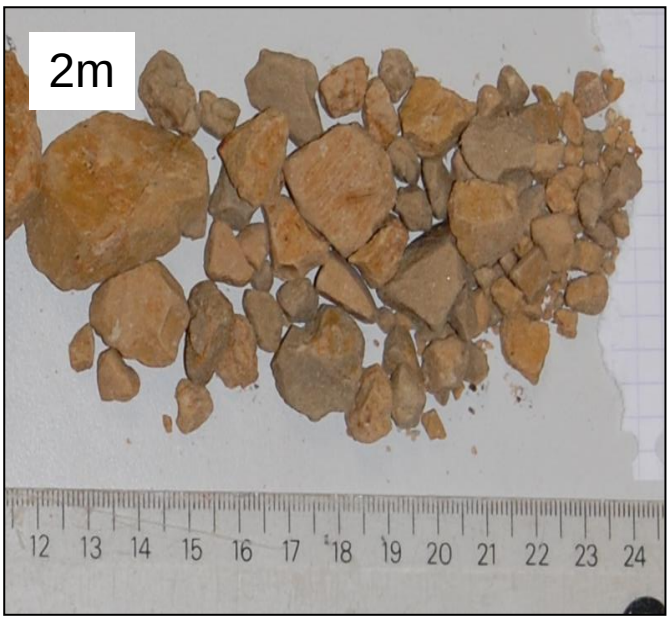

Figure 37 : Bimrocks sampled at 2m from the fault: the only remaining material out of a drill core of 40cm of length and 5cm of diameter.

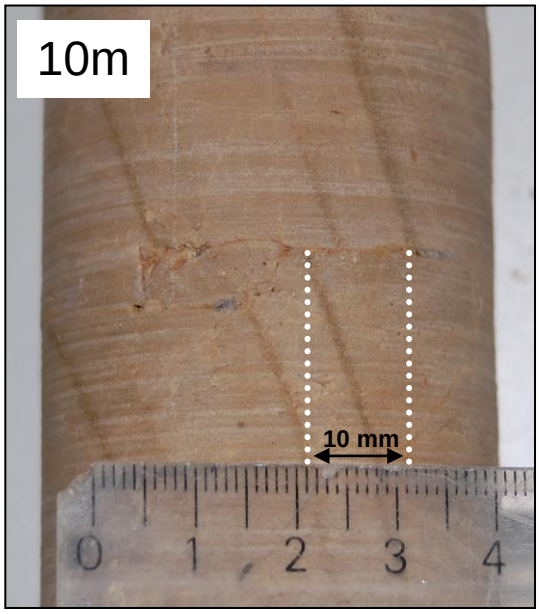

Figure 38 : Drill core Nº9A which presents a shift of 10mm along a fracture that has subsequently been recalcified

The drill core Nº4 sampled at 4,3m from the fault is the longest. Small veins of calcite, up to 1mm of thickness, can be observed in the core. It shows as well a micro-fracturing filled with calcite. Some of these fractures have permitted a shift of some mm of the rock before being re-calcified. The same can be observed on drill core Nº9 (10m from fault). Here the shift is of 10mm. (Figure 38)

Drill core Nº5 sampled at 5,8m from the fault is totally destructed. Most of the core run has degraded to soil which has been washed away by the drilling water and not much material is left. The debris contain pieces of calcite, up to 3cm, and thicker veins of calcite (2mm) than the other drill cores.

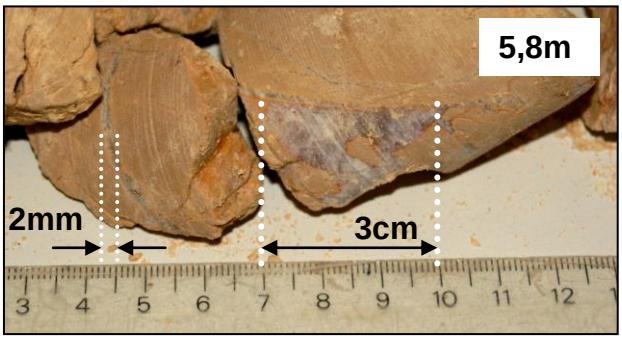

Figure 39 : Drill core Nº5A with the highest content of calcite: veins up to 2mm of thickness and pieces up to 3cm of length.

From drill core Nº5 to Nº9, which means from 5,8m to 10m a progressive improvement of the rock quality can easily be observed. The rock is less fractured and less material has been washed away by the drilling water.

Core run Nº10, drilled at 12,7m in the very fractured zone F3 right beneath the open fracture and core run Nº11, drilled at 14,7m , before the fractured zone F4 can be crumbled by hand and become sand.

Core run Nº12 and Nº13, 16,2m and 18,7m respectively, present no particular properties. Nº13 presents a high micro-fracturing, without a preferential direction. The micro-fractures are filled with calcite.

The visual analysis of the rock quality in terms of fracturation of the cores as described above matches perfectly with the AJS of the hard layer. The fracturation direction which has the major influence on the fracturation of the drill cores is the N95º, perpendicular to the drilling direction. Even though the RQD, which in this case measures this N95º fracturation has not been performed, after this visual analysis it can be said that it matches with the AJS, which measures the fracturation N175º.

- Layer of calcite on the surface:

In the fault the layer of calcite is 45mm thick, at 0,5m there are 15-27mm and at 2 m from the fault the thickness is only of 2mm and it decreases down to a fraction of a mm from a distance of 8m from the fault onwards. This testifies that the rock at a distance farther than 8m is only partially submitted and affected by superficial fluid circulation which takes mainly place inside and near the fault, proving the draining character of the fault for superficial and epidermic ?? fluid circulation.

- Calcite crystals in the cores:

The content of calcite crystals in the drill cores increases from drill core Nº1 to Nº5, which means from the fault to a distance of 5,8m. Drill core Nº5 has the biggest amount of calcite crystals.
It contains pieces up to 3x2 cm and the calcitic veins are 2mm thick, 1mm more than the calcite veins in the other drill cores.
Drill cores Nº8 Nº10 and Nº13 respectively near F2, in F3 and in F5, also present some small vein of calcite with a thickness up to a mm, filling the microfractures, but which do not arouse further interest.
The presence of this calcite has its origins in fluid circulation inside the fractured rock. In the dolomite rock the water solubilises the CaCo3 which is deposed in the fractures where it re-crystallizes. The biggest amount of calcite is found in drill core Nº5, which has been sampled near the first fracture-zone F1. As it is the fractured band which is the nearest to the fault and the cataclastic zone of the cliff face it is obvious that a high fluid circulation takes place inside these fractures, which explains the high amount of calcite that fills almost completely the pores and the fractures of this core. The draining character of the fault and of its nearby fractures is therefore proved again.

4.7.1.2 Bulk density and effective porosity:

- Measuring protocol:

The samples were first dried in the oven at 120°C for 24 hours and then weight. Afterwards they were soaked in water and placed in an under pressure cellule for 3 days, at 100mBar, until no more air bubbles came out. The less porous specimen were left for 6 days, to be sure that all connected pores were filled with water. The weight of the saturated specimen was carefully taken. The rock material that has been destroyed was filtered and weight as well. The specimen volume was determined by calliper readings, and the bulk density values were obtained from the ratio of the specimen dry weight to the specimens volume. The effective porosity was calculated as follows: $(V_{pores} / V_{tot})*100$, where the V_{pores} was obtained by the difference of mass of the dry and the saturated specimen: $V_{pores} = M_{sat}-M_{dry}$

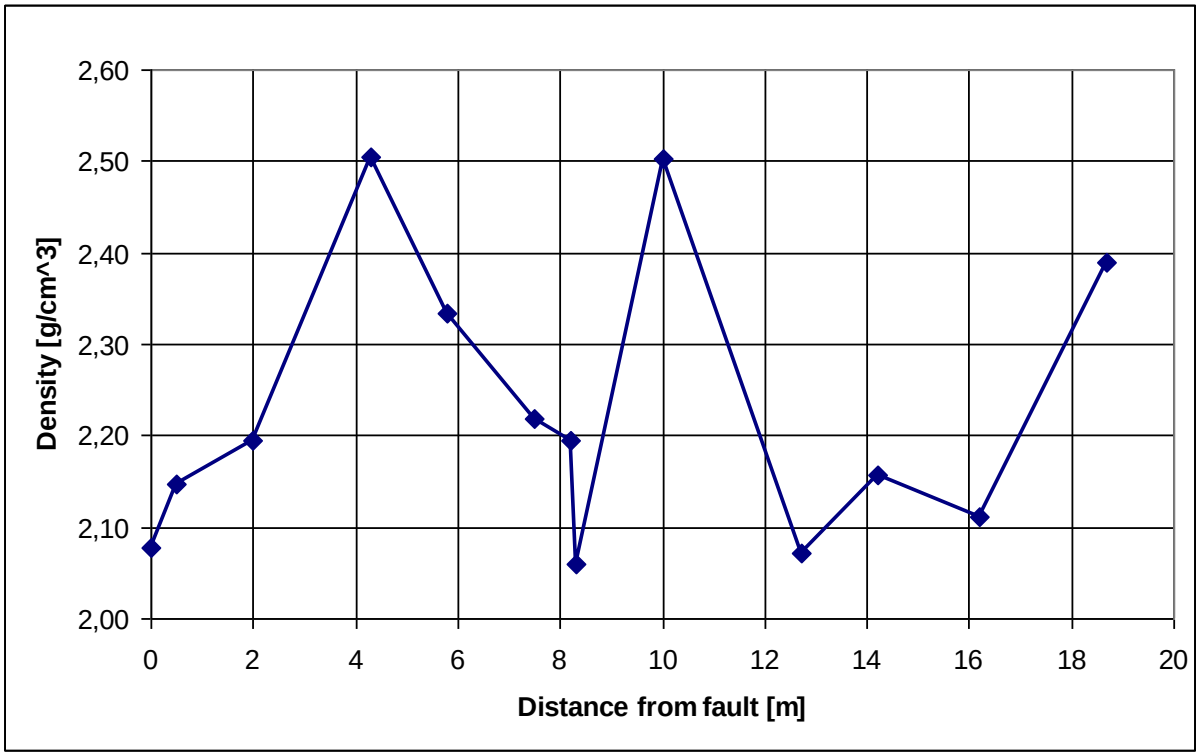

Figure 40 : Drill Cores A: Density in function of the distance from the fault

The trend on the density variations of the drill cores matches very well with the trends of the variation of AJS. In 5.1.2.1 the correlation factor of these two values is r=0,4 which is somehow a correlation also if not too strong. This means that the trends are not perfectly proportional. Nevertheless an accordance of the two trends can be observed. In the first fractured band F1 the density decreases from 2,51 g/cm^3 at 4,3m to 2,06 g/cm^3 at 8m from the fault, and re-increases up to 2,5 g/cm^3 at 10m. It decreases again to a value of about 2,10 g/cm^3 from 12 to 16 m, which means broadly in the second big fractured zone F2. After 16 m the density re-increases. The only value that one would expect to be very different is that of drill core Nº5, at 5,8m. From the visual description this sample appears totally destructed and porous, but the porosity and fractures are filled with big crystals of calcite which have a density of 2,7 g/cm^3, which explains the strangely high density.
It can be concluded that fluid circulation, which takes mainly place in the fractured bands has a strong dissolution power and alters the rock severely.

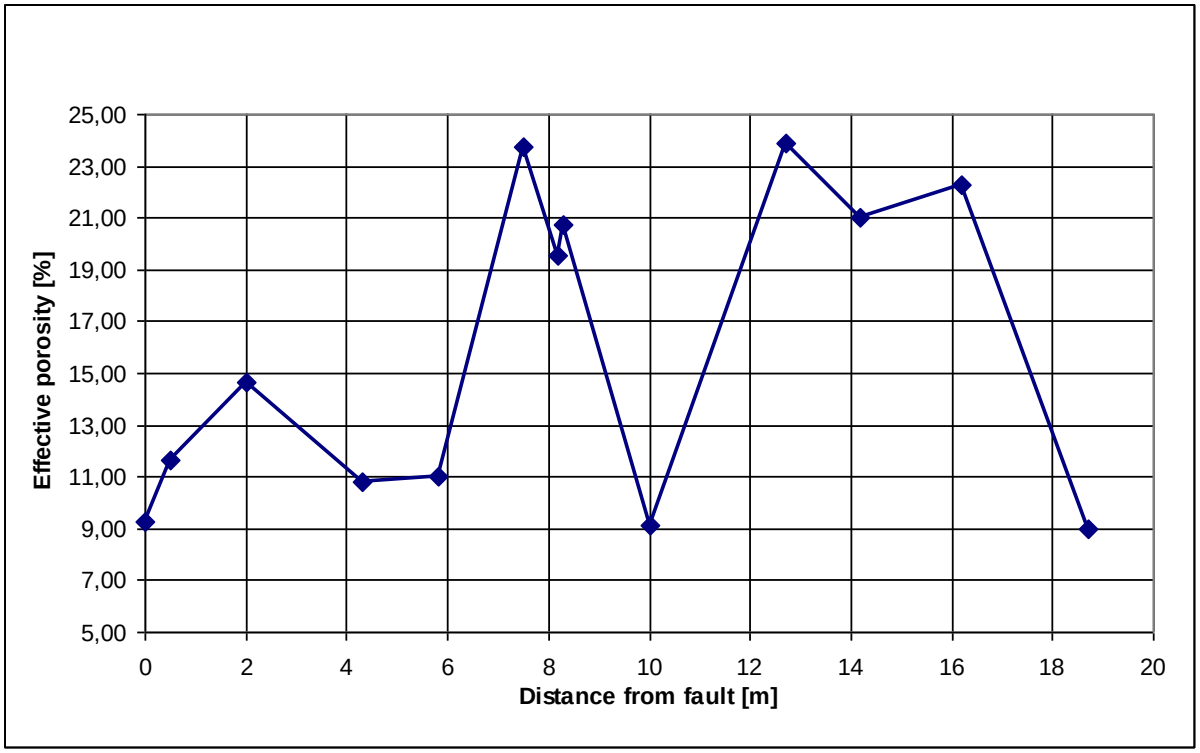

Figure 41 : Drill cores A: Effective porosity in function of the distance from the fault

Obviously the Effective porosity is in contrast to the Bulk density. This is confirmed also by the Principal Component Analysis carried out in §5.1 where these two parameters show a negative correlation (r=-0,71) The same results as for the density can be interpreted from the effective porosity: in the fractured bands, the effective porosity is between 19 and 24% whereas the rest of the specimens have an effective porosity contained in between 9 and 15 %. As for the density, specimen N°5 presents a lower value than expected, caused by the high amount of calcite crystals that fill the pores and fractures.

4.7.2. Analysis of drilling session B

4.7.2.1 Description

The second sampling session is performed on the hard layer, exactly at those points where the Schmidt Hammer test was performed, in order to make a comparison between the characteristics of the drill cores (RQD, Bulk density, Effective Porosity, UCS) and the SHRV analysed in Chapter 5.
A total number of 9 core runs are sampled (Figure 42). The test results are resumed in Table 4.

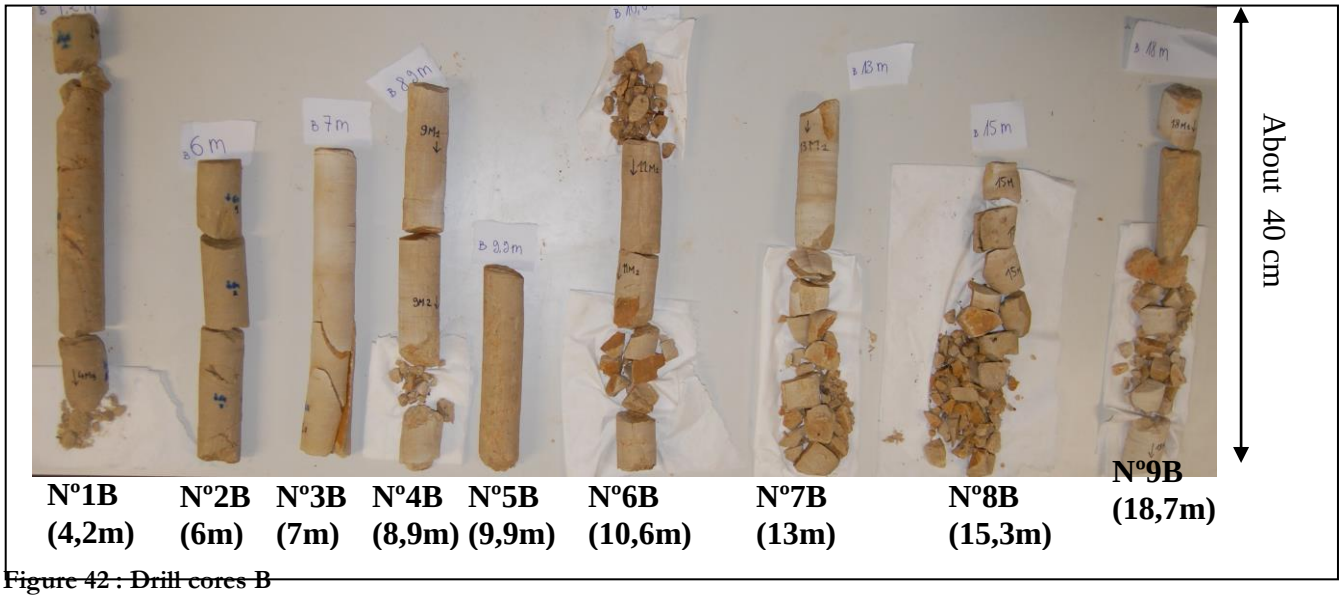

Figure 42 : Drill cores B

Drill core Nº1B and Nº5B and Nº9B are sampled respectively at 4,2m, 9,9m and 18,7m from the fault. They are the most brittle of all drill cores and crumble almost by hands. Nº1B has lots of re-calcified fractures and presents one 2mm thick vein of calcite whereas Nº5B is one undivided piece without fractures and contains pieces of calcite which follow no specific direction, they just fill some of the bigger pores. Nº9B has one piece (its longest piece) which corresponds to these characteristics, other pieces that are much harder, but smaller and pieces of calcite are visible in the joints.

Core run Nº2B sampled at 6m from the fault is less brittle but presents many re-calcified fractures and lots of little veins of calcite.

Core run Nº3B seems to be harder than the others. It presents re-calcified fractures which are tightly and neatly cemented and less open than the fractures in the other cores. Nevertheless the core run broke along these fractures while handling in the laboratory.

Core run Nº4B presents a particularity: Part of the drill core is very porous and the other part not at all. It presents many re-calcified fractures. Nº6B, sampled at 13m from the fault is compact and not brittle with some re-calcified fracture. Nº7B and Nº8B, sampled respectively at 13m and 15,3m have totally broken up in many pieces.

This visual analysis does not reflect as well as analysis on drill cores A the global behaviour of the cliff face. Despite this the status of most of the samples could somehow be explained. To resume with a little more order what has been analysed above it can be said that:
The brittle behaviour of Nº1B is totally in contrast with the hard integer sample of drilling session A. This is a zone which is covered by calcite so no fracturation can be seen on the cliff face. Nevertheless from SHRV, UCS and the ERT it ensues that this zone is of low resistance. In Nº2 a lot of calcite is found which is formed by the fluid circulation in F1. Nº3 is more intact and comes in fact from an intact zone between F1 and F2. Nº4 has re-calcified fractures probably from F2. The brittle behaviour of Nº5 is not explainable with what has been observed and said until now. Nº6 was sampled in the hardest zone of the cliff face and is very compact. Nº7 is totally fragmented and was sampled in F3. Nº7 is fragmented and no explanation was found for it. Nº9 is brittle and was sampled in F5.

Nr: B	Distance from fault(m)	SHRV	UCS [MPa]	RQD [%]	Rock mass quality	Total weight extracted (g)
1	4,2	32.53	17.95	84,63	Good	1646,9
2	6	27,44	12.02	67,07	Fair	1404,0
3	7	36.54	31.07	87,32	Good	1535,8
4	8,9	42.17	28.27	56,83	Fair	1665,4
5	9,9	34.82	17.57	61,46	Fair	986,7
6	10,6	28,71		58,05	Fair	1574,7
7	13	23,71		44,39	Poor	1376,4
8	15,3	35,65		0,00	Poor	1370,7
9	18,7	25,41		37,56	Poor	1507,2

Table 4 : Characteristics of the Drill cores B

4.7.2.2 Rock Quality Designation (*RQD*)

In order to quantify the evolution of the fracturing density (N95º) along the cliff face the Rock Quality Designation (RQD) has been performed on the core runs. This method has been developed by Deere et al.(1967) with the purpose to give a quantitative estimation of the fracturing which influences the behaviour of rock masses. The RQD is based on measuring core recovery percentage which incorporates only pieces that are greater than 100 mm in length.

RQD is defined as the quotient:

$$RQD = \frac{(\text{Sum of length of core sticks longer than } 10\,\text{cm})}{\text{Total length of core run}} * 100$$

In accordance with the obtained results the rock can be classified following Table 5. Consequently a high RQD value points out a massive rock and on the contrary a low RQD value stands for a fractured rock.

RQD	Rock mass quality
< 25%	Very poor
25 - 50 %	Poor
50 - 75 %	fair
75 - 90 %	Good
90 - 100 %	Excellent

Table 5 : Rock Quality Designation

The core runs have been bored perpendicularly into the cliff face: the direction of fracturing which most affects the RQD is therefore the 96,9º N 86,7º. The result has been plotted in Figure 43. Core run Nº8B at 15m has been left out of this analysis because this core run has accidentally been completely fractured during the boring process due to some problems of the drilling machine.

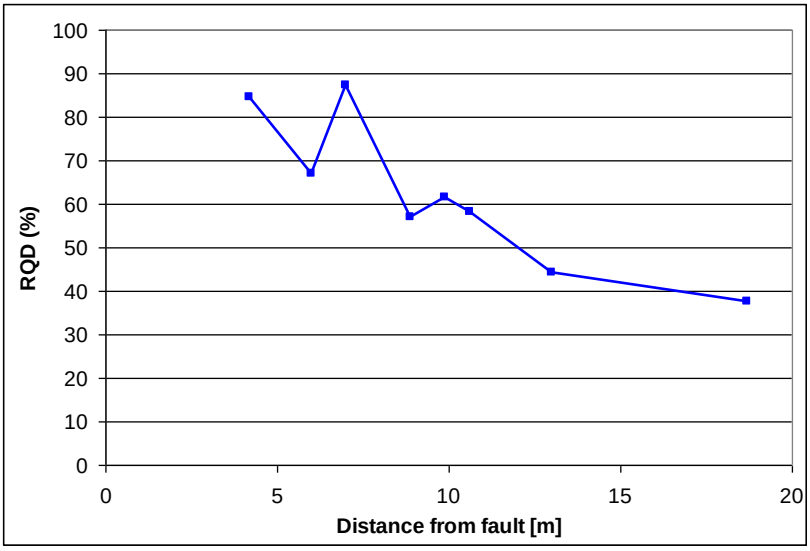

Figure 43 : RQD of core runs B

In accordance with the values of Table 5 the status of the rock is defined as "good" at 4m and 7m from the fault, as "fair" at 6m and from 8m to 12m from the fault and as "poor" from 12m on. The result is basically the opposite of what is expected: near to the fault the Rock Mass Quality is classed as "good" and becomes "poor" from 12m on. At this point it has to be pointed out that the drill cores are only 40cm long: That means that this trend represents only the outer 40 cm of the cliff face and might not be representative of the whole rock mass, or the samples might have broken in the drilling process.
In making a comparison with the trend of the apparent joint separation which describes the fracturing 175,7º E 81,9º (Figure 19) it can be observed that the fracturing has a similar trend as the fracture family 175,7º E 81,9º. At 6 and 9m from the fault the fracture families F1 and F2 cause a drop of AJS, similarly the conjugated fractures N°95 cause a drop of RQD at 6 and 9m from the fault. Another similarity is the flattening of the curb from 12m on, the RQD as the AJS becomes more homogenous and the peaks and minima are less acute.

It can be concluded that near the fault the variability of the index values is greater, and from about 10m from the fault on their variability decreases. In this first ten meters the rock has suffered the evolution and the gravitational movement of the fault, it is more fractured and weathered in some parts, and very compacted and resistant in other parts.

4.8 *Thin slices*

The study of rocks in thin section is a routine technique involving cutting thin slices of rock to allow study of the component crystals, which dates back to the beginnings of modern geology at about 1850.

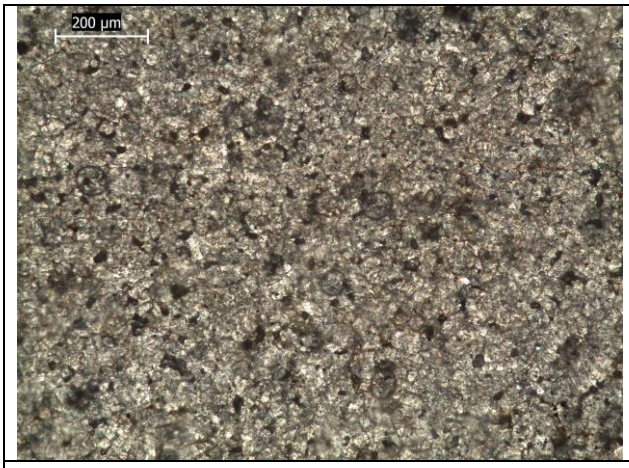	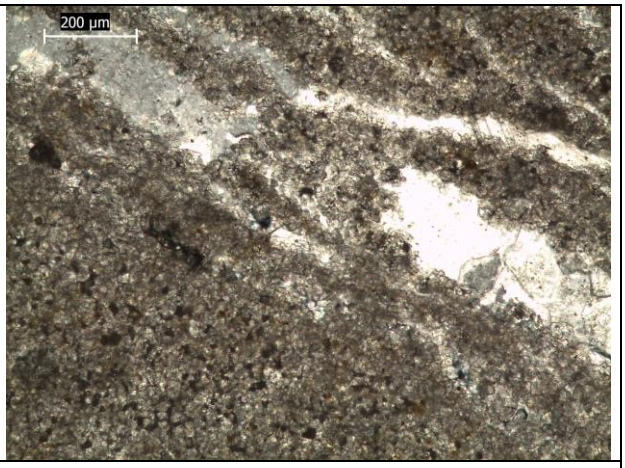
Slice Nr4A: 4,3m from fault Porosity~5%	Slice Nr5A: 5,8m from fault 5%
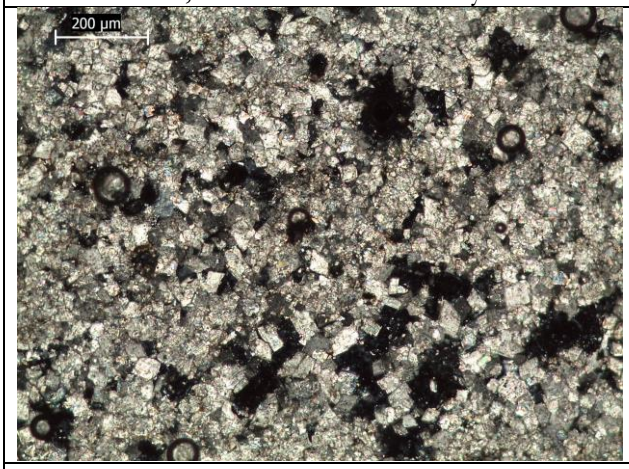	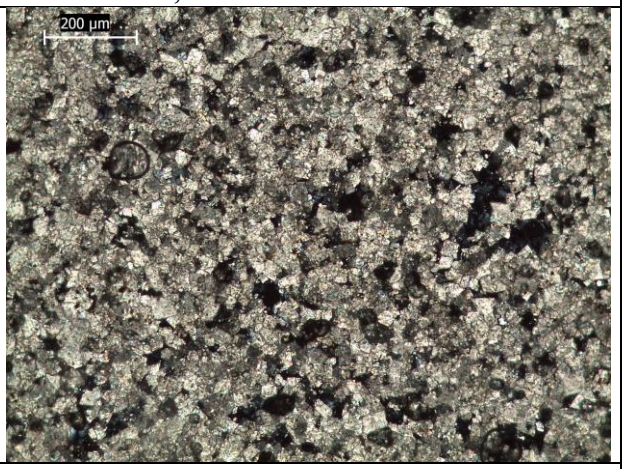
Slice Nr6A: 7,5m from fault. Porosity~20%	Slice Nr7A: 8,3m from fault. Porosity~10%
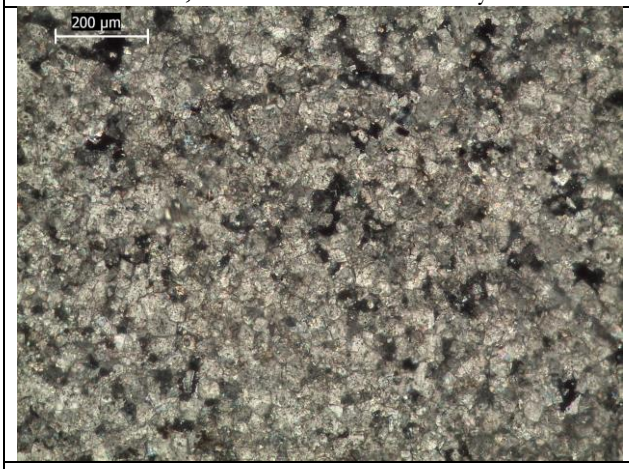	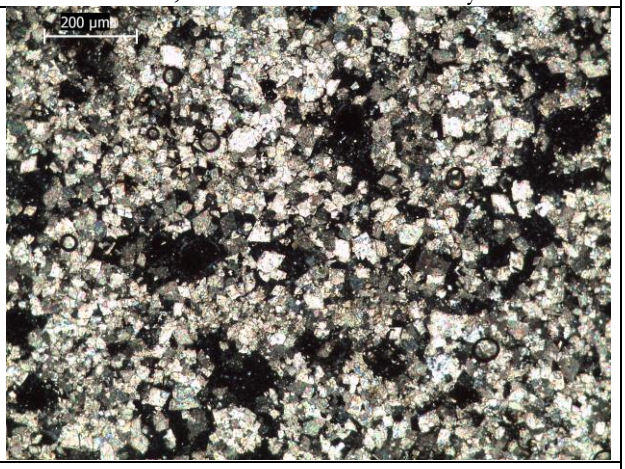
Slice Nr9A: 10m from fault Porosity~5%	Slice Nr10aA:12,7m Porosity: ~20%

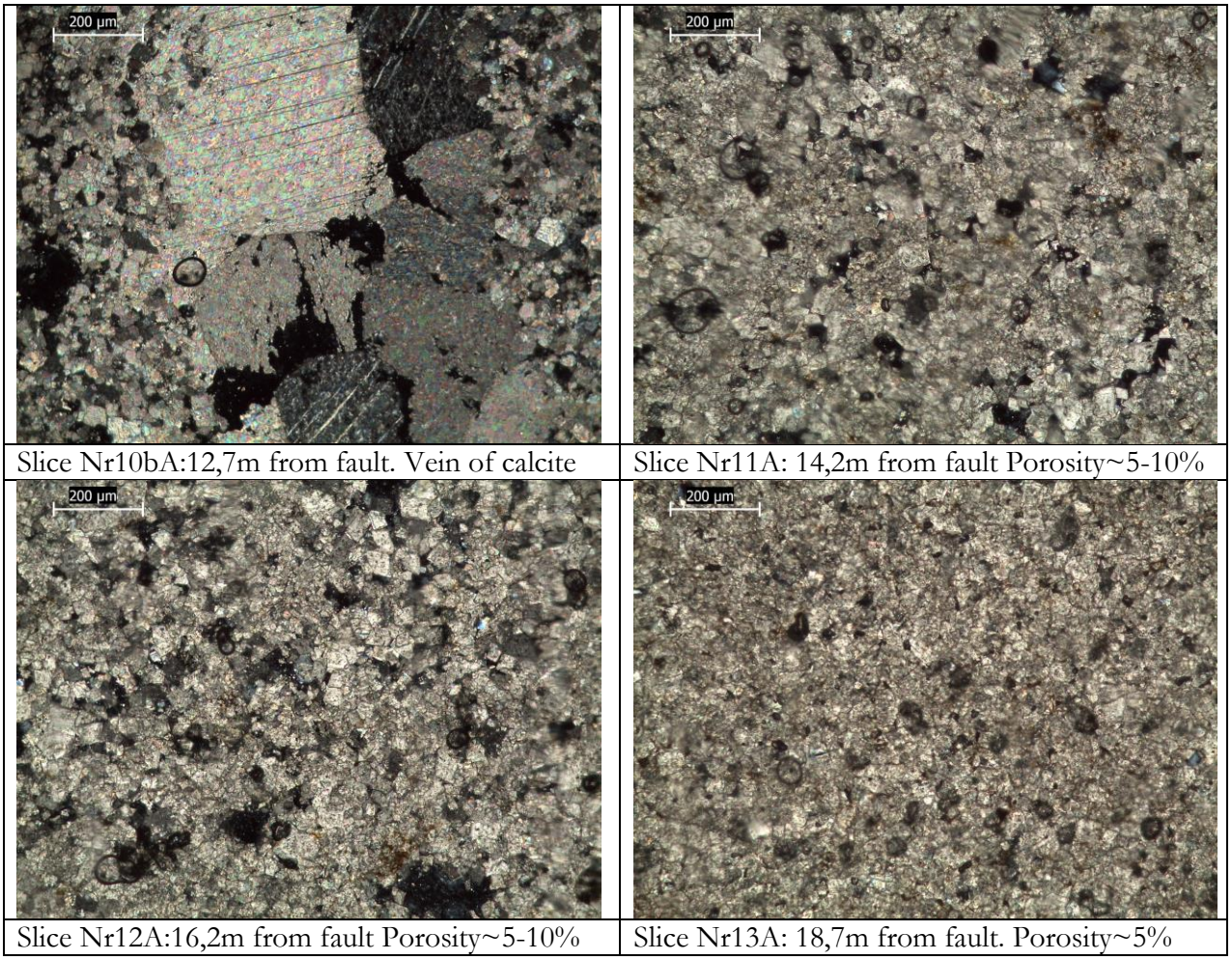

Slice Nr10bA:12,7m from fault. Vein of calcite | Slice Nr11A: 14,2m from fault Porosity~5-10%

Slice Nr12A:16,2m from fault Porosity~5-10% | Slice Nr13A: 18,7m from fault. Porosity~5%

Figure 44 : Photos of the thin slices Nº4A-13A of drilling session A in polarized light (same enlargement) and evaluation of porosity.

Sample	Microscopic description
n°4A	Dolomitic micro sparite, absence of bioclasts, ~5% porosity, rounded regular shaped pores with Ø of 10-20 µm, Ø grains ~ 10 -20µm
n°5A	Dolomitic micro sparite, absence of bioclasts, ~20% interstitial porosity, rounded less regular pores with Ø of 10-50 µm, Ø grains 10 -20µm. Presence of calcite veins Ø~20-200µm
n°6A	Dolomitic sparite, absence of bioclasts, porosity of ~20%, rounded and stretched pore shape with Ø of 50 - 150 µm, Ø of grains 20-50µm
n°7A	Dolomitic sparite, absence of bioclasts, porosity of ~10%, rounded and stretched pore shape with Ø of 50 - 100 µm, Ø of grains 20-50µm.
n°9A	Dolomitic sparite, absence of bioclasts, porosity of ~10%, more rounded and pore shape (some stretched) with Ø of 20-50 µm, Ø of grains ~20-50µm.
n°10aA	Dolomitic sparite, absence of bioclasts, porosity of ~20%, rounded and stretched pore shape with Ø of 20-200 µm, Ø of grains ~20-50µm
n°10bA	Vein of calcite with crystals of Ø 200-500µm
n°11A	Dolomitic sparite, absence of bioclasts, porosity of 5-10%, pore shape with Ø of 20 - 50 µm, Ø of grains 20-50µm
n°12A	Dolomitic sparite, absence of bioclasts, porosity of 5-10%, pore shape with Ø of 20 - 150 µm, Ø of grains 10-50µm

n°13A	Dolomitic micro sparite, absence of bioclasts, ~5% porosity, rounded regular shaped pores with Ø of 10-50 µm, Ø grains ~ 10 -30µm

Table 6 : Microscopic description of thin slices 4A-13A cut from the drill cores of the drilling session A

The thin slices were cut out of the drill cores of the drilling session A. The macroscopic description of the drill cores can be found in §4.7.1. The pictures of the lames Nº1A, 2A and 3A are not published because they are not considered as representative samples: Those lames are made from the bimrocks found on the first meters of the fault and as bimrocks their provenience is unknown.

It is observed that the samples Nº4A, 5A and 13A have a different facies than the others. The grains are finer (10-20/30µm) and the porosity is lower (5%) and more regularly shaped as in the other samples. In fact the drill cores Nº4A and 5A were taken a little bit lower in the stratigraphy (20cm) and probably another layer with a different digenesis was touched. Sample Nº13A was taken in the same layer as the rest of the drill cores, its microscopic characteristics are in fact not as fine as those of Sample Nº4A and 5A but a midway between those and the others. No logical explanation has been found for this variance.

In observing the slices crossed by veins of calcite an important correlation can be remarked: those lames are the Nº5 and Nº10 sampled respectively at 5,8 and 12,7 m from the fault, that means in the zone of fracture families F1 et F3 which are in fact the two most important and pronounced fracture families which affect most the physical and mechanical characteristics of the rock. This means that there is a good correlation between the macro and micro-fracturing.

The analysis of these thin slices becomes interesting when compared with the slices of other samples collected on a vider zone of the versant. This analysis is described in §5.3.

4.9 *Conclusion:*

In this chapter the data of field observations together with index- and engineering design tests, carried out in situ on the dolomite cliff face and in the laboratory on samples of its rock, have been analysed in terms of weathering and in relation with their distance to the fault. The results are briefly resumed in the following paragraphs:

- A first interpretation of the ERT (§ 4.2) reveals the fracturation and decompression of this zone, made visible on the ERT thanks to a resistivity decrease caused by chemical and mechanical weathering or more exactly by weathering factors as mayor fluid circulation in the fracture network, induced shear stresses by the faults movements, pressure reduction by unloading and rock cracking by plant roots. However it is not possible to correlate this jointing and weathering with the distance from the fault.

- The evaluation of the AJS (§ 4.3) confirms the presence of the major fracture families and reveals the totally different characteristics of the hard and the weathered layer in some areas. Here as well no correlation with the distance from the fault can be found.

- Almost the same results can be found for the SHRV. (§ 4.4) This value sharply diminishes in the fractured zones where the weathering is at a more advanced state. In the same way the SHRV is globally a lot lower on the weathered layer than on the hard one.(Respectively SHRV=22,6 vs SHRV=32) Here too, no linear correlation has been found between SHRV and the distance from the fault.

- Regarding the TCT the most important result is the extreme reduction of shear strength resistance with weathering: The internal angle of effective friction is meanly reduced of 44% of its original value by weathering. In § 5.4 the results of this test are used for a stability calculation and their evolution in time is analysed.

- The UCS test (§ 4.6) has been carried out on specimen sampled only on the first 10m of the cliff face. The found values range from 12 to 31 MPa, against the 108 MPa of a sound Dolomite (Ippolito et al. 1975). This demonstrates the extremely high grade of alteration of this rock. These values will be used for a correlation study between the UCS and the SHRV in § 5.2.3.

- According to the visual analysis of the drill cores and its thin slices it can be said that superficial, sub-epidermic and ipodermic [IS THAT RIGHT ???] fluid circulation takes mainly place near the fault. This can be seen by the cover of calcite on the outer rock and the pieces and veins of calcite inside the fractures and microfractures of the drill cores. This demonstrates the draining character of the fault. Furthermore it can be observed that the trend of the AJS, that means of the fracturation N175º matches with the trend on the RQD, which represents the fracturation N95º. This grades the rock in some very damaged zones, affected by two conjugated fracture families, and sane zones less affected by fracturation. Moreover the analysed values present higher peaks and lower minima on the first 10m starting from the cliff face and a flattening or homogenisation of its values from 10m on.

After having evaluated these tests a preliminary answer to the first two guideline questions posed in §3.2 can be given:

- Is this extreme weathering caused or at least favoured by the closeness of the fault?
- Which are the mechanical properties of the rock and how are they affected by weathering or rather by the closeness of the fault?

To find an answer to these questions the tests have been conducted on a total horizontal length of 20m, starting from the fault. After 20m is it not possible anymore to follow the same stratigrafic layer because the topography has a higher gradient than the immersion of the stratigraphy (Figure 9). However, the execution of the tests for 20m was thought to be enough and that after 20m the variation of the rock properties caused by the closeness of the fault as Imposa et al. (2004) stated would be negligible.
In the aftermath of all these analysis it becomes clear that these tests have to be carried out on a wider zone of an outcrop, when possible. The first 20m that have been analysed are completely weathered by the fluid circulation and the mechanical movements of the fault and it is almost impossible to see a global difference between near (some meters) and far (max20 meters) from the fault because the characteristics are so heterogeneous that a global trend disappears in the “noise”. To remedy this problem the mean value out of three has been analysed, at least in the tests where lot of data was available, (SHRV, AJS) but the variability is still too strong. What has though been observed in some tests is a sort of flattening (but not a global rising) of the maxima and minima of the AJS, RQD and SHRV from about 12 on. The throw and the heave of the fault (vertical and horizontal displacement respectively) have crumbled and fractured some parts and have really hardened other parts. The maxima and minima are accentuated on the first dozen of meters from the fault.
The calcite content of drill cores and superficial coverage of the outcrop which both are higher near the fault indicate that fluid circulation is conveyed in the fault zone. This draining

character of the fault causes a more pronounced weathering close to the fault, especially in the fractures.
All in all a positive answer can be given to the first question: Yes, the vicinity of the fault favours weathering of the rock mass but it is not possible to give a quantitative answer, in terms of the distance from the fault at which the rock is affected by this increased weathering.

The problem of the decline of the mechanical properties of the rock in terms of strength caused by weathering in time will be discussed in Chapter 5, but a preliminary answer can already be given to the second question at this point of the work:
The strength of this rock has been evaluated by means of the TCT, UCT and the index test of the Schmidt Hammer. Globally the mechanical resistance of this outcrop is very low: 12 to 31 MPa, against the 108 MPa of a sound Dolomite (Ippolito, 1975). This proves the extremely high alteration of the whole outcrop. But on the spots of the outcrop where weathering is most active, that means the zones affected by the fracture families and the open fractures, a further abjection of rock resistance has been found: the internal angle of effective friction decreases 44% from the "fresh-weathered" rock of the cliff face to the soil that fills the fractures, and even 50% to the material sampled on the fault wall.

The answer of these questions leads to another question that will be discussed in chapter 5:
How do these differential mechanical properties influence the gravitational movement and the slope stability ?

Chapter 5 : Discussion

In this chapter the results obtained with the tests described in Chapter 4 will be discussed, correlated with each other and the obtained parameters will be applied in rock strength and a stability analysis at the scale of the Marbrière versant. For a better overview the 10 analysed parameters are briefly resumed in Table 7.

Measured on : where :	**Rock**				**Soil**		**Complex**
Field	SHRV	AJS	RQD				Electric Resistivity
Laboratory	UCS	Density	Porosity	Image analysis	C'	φ'	

Table 7 : Resume of the different tests that have been carried out on the cliff face.

At first a Principal Component Analysis will be carried out to find the correlations between the different measured parameters. This advanced multivariable method of data analysis makes it possible to extract relevant information from confusing data sets of high dimension, to find patterns in the data and to point out their similarities and differences.

Based on these results the focus will be pointed singularly on the parameters and their correlation with some of the other parameters.

Due to the results of the other tests the electric resistivity tomography will be re-analysed and most of the suppositions made in the first analysis will be confirmed.

The correlation of the AJS and the SHRV will be discussed. Literature review shows that it is possible to correlate these two parameters with a formula. The same has been tried in this study but the rock conditions are too heterogeneous and depend from too many factors and no correlation formula was found for these dolomites of the Hettangien.
The correlation of the UCS and the SHRV has been more successful. Many authors have proposed various formulas which correlate the UCS of rocks with the SHRV determined with this simple non destructive and time saving tool. Two correlation formulas are proposed in this work.

In §5.3 thanks to the analysis of the thin slices a lateral variation of facies has been found within the Hettangien dolomites. These syndiagenetic facies differences imply horizontal variations of the mechanical properties of the rock along the versant. It is found out that in proximity of the fault the SHRV and therefore of the UCS decrease sharply due to the strong weathering that affects the fault zone.

Finally a slope stability analysis by means of the rigid-plastic method of Fellenius is performed in §5.4. It results that the mechanical parameters of this versant are strongly worsened in time by weathering which roughly halves the safety factor.

5.1 *PCA: Principal Component Analysis*

5.1.1. Theory

Principal component analysis (PCA) is a standard tool in modern data analysis. It is a simple, non-parametric method for extracting relevant information from confusing data sets. " It is a way of identifying patterns in data, and expressing the data in such a way as to highlight their similarities and differences. Since patterns can be hard to find in data of high dimension, where the luxury of graphical representation is not available, PCA is a powerful tool for analysing data. The other main advantage of PCA is that once you have found these patterns in the data, and you compress the data, i.e. by reducing the number of dimensions, without much loss of information " (http://www.cs.otago.ac.nz)
In this study PCA is used to quantify the correlation between the different parameters (UCS, SHRV, AJS, RQD, bulk density, effective porosity, c', φ') (variables) that have been studied on the two layers, at different distances (individuals) from the fault. The set of these p variables which characterize the meters of distance from the fault, can be represented in a p-dimensional space. The structure of this data-cloud shows essentially the distances between the points, the relative distance of the points in respect to each other and to the axes and the position of the centre of gravity of the set of individuals.
Principal Component Analysis allows the representation of the set of variables in a new space, in which the axes pass in the gravity centre of the cloud of data and where the principal components represent the highest absorbed variance. This representation allows to "see" the dispersion of the cloud. (Riss and Grolier, 1997)
This for it is necessary to define and to calculate:

- M_{ID}: The matrix of the initial data composed by n lines (meters of distance from the fault), and by p columns (variables)

- M_{RCD}: The matrix of the reduced centred data of n lines and p columns which general term is: $\frac{xij - \overline{xj}}{sj}$ where xij is the general term in the matrix M_{ID} and $\overline{xj}$ and sj respectively the mean and the standard deviation of each variable.

- M_c: The correlation matrix given by the matricial product of the transposition of M_{RCD} by itself , divided by N, the number of individuals.

In this way the matrix of the eigenvectors and eigenvalues can be obtained after the diagonalisation of M_c. (Lebourg ,2000, Riss and Grolier,1997, Dagnelie, 1982)

Now it is possible to represent the variables on a new plan by means of the correlation circle. The coordinates of the variables are obtained by the product of the eigenvector matrix by the square root of the eigenvalues. This plan is hold by two axes that absorb a part of the total variance absorbed by all the new axes (F_n) together. The best correlation is obtained on the plan hold by those axes that absorb the biggest part of the total variance. Consequently the most used couples of axes are F_1 F_2, F_1 F_3, F_2 F_3, according to the percentage of absorbed variance. The variance absorbed by the general axes (i,j) is given by the relation: $\frac{\lambda i + \lambda j}{\sum_p \lambda_p}$, where λ corresponds to the eigenvalue.

5.1.2. Analysis

The matrix of the initial data, M_{ID}, upon which the correlation matrix as well as the components of the new axes are calculated is given by:

- Schmidt Hammer Rebound Value (SHRV) of the hard and the weathered layer
- Apparent Joint Separation (AJS) of the hard and of the weathered layer
- Uniaxial compressive strength (UCS)
- Effective cohesion (c')
- Effective angle of internal friction (φ')
- Density (dens)
- Effective porosity
- Rock Quality Designation (RQD) of the drill cores extracted in drilling session B
- Resistivity values of the ERT (Res)

These variables are expressed in function of the distance from the fault. The meters of distance from the fault represent 20 different individuals.
A first PCA has been performed on all the variables of the weathered and of the hard layer together. This analysis does not have an acceptable result; The cumulated absorbed variance of the axes F_1 and F_2 is only 54% and the highest correlation coefficient between two variables is r = 0,58 for the RQD (of the drill cores B) and the AJS of the weathered layer, that means between the two fracturing directions, 96.9º N 86.7º and 175º E 80º.
Therefore it has been decided to perform the ACP separately on the two studied layers because their properties are too different in some places.(ex: at about 8 – 9 m from the fault the weathered layer is totally degraded to soil and has a mean SHRV of 15, whereas the compact block of the hard layer has a SHRV of about 45) as to be treated as the same individuals.

On the hard layer an analysis of correlation between SHRV, AJS, UCS, Density, Effective porosity and RQD has been carried out, whereas on the weathered layer SHRV, AJS, c', φ' and the electric resistivity have been correlated.

5.1.2.1 The Hard Layer

The variables of the hard layer that have been correlated are the SHRV and the AJS taken directly in situ on the hard layer and the UCS, effective porosity, density and RQD performed in the laboratory on the drill cores of the hard layer.

	SH	AJS	UCS	Density	Porosity	RQD
SH	1.00	0.29	0.81	0.21	-0.12	0.03
AJS		1.00	0.06	0.39	-0.39	0.49
UCS			1.00	-0.03	0.19	0.01
Density				1.00	-0.79	0.47
Porosity					1.00	-0.34
RQD						1.00

Table 8 : Correlation matrix (M_c) for the variables of the Hard Layer

The correlation coefficient between the variable *SH* and *UCS* is the highest (*r=0,81* Table 8). This coefficient shows a relatively good relationship between the results obtained with the Schmidt Hammer and the Uniaxial compressive strength of the material tested in the laboratory. This is a very satisfactory result which might be of great academic interest. On the basis of this relation it is possible to propose a function of UCS and SHRV. This will be discussed in § 5.2.3. The strongest negative correlation is between the bulk density and the effective porosity with r = -0,79 . This is not surprising at all since a porous material is evidently less dense than a less porous material. The other correlation coefficients are not strong enough to allow any dependence hypothesis. A surprising result is the bad correlation of the SHRV with the AJS.(r =0.29%). As well the density and porosity are badly correlated with the SHRV. (r = 0.21% and r = -0.12% respectively) This means that there are many other factors that strongly influence the SHRV and that the influence of the fracturing, micro fracturing, density and porosity are not so strong on this variable.

(SO WHAT IS IT THAT INFLUENCES THE SHRV?????)

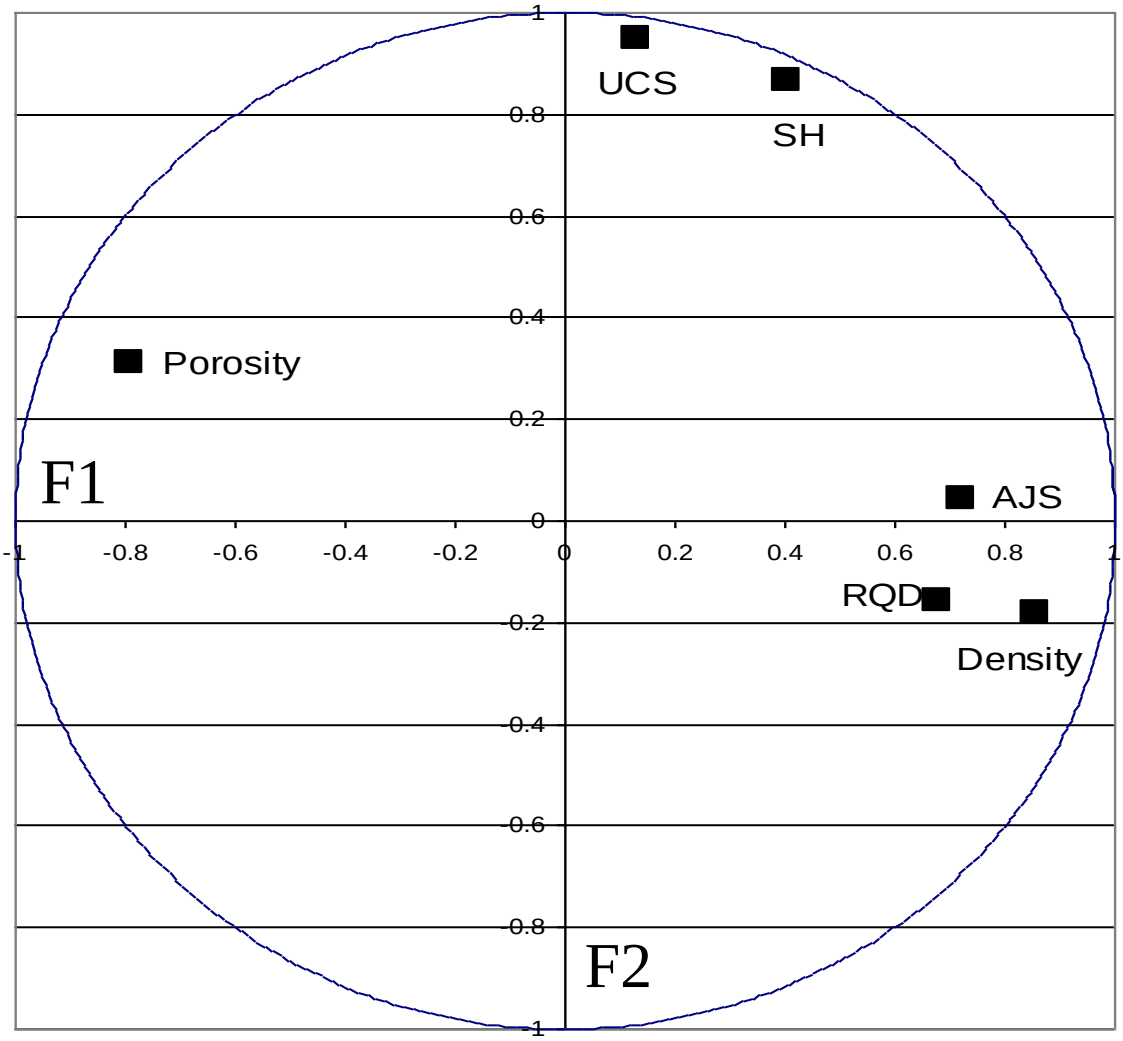

	SH	AJS	UCS	Density	Porosity	RQD
F1	0.40	0.72	0.13	0.86	-0.79	0.68
F2	0.87	0.04	0.95	-0.18	0.31	-0.16
F3	-0.16	0.44	0.01	-0.33	0.44	0.56

Figure 45: Factor loadings plot, 71% of the total variance is hold by the first two components. Table of the correlation of the old variables with the new ones: F1, F2, F3 data for each variable of the hared layer

Figure 45 shows the variable projection in the space F_1, F_2, representing 71% of the total variance. The variables that contribute to the creation of the space F_1, F_2 are those close to the circle. This variable projection in the F_1, F_2 space allows us to visualize the concentration and distances between variables.

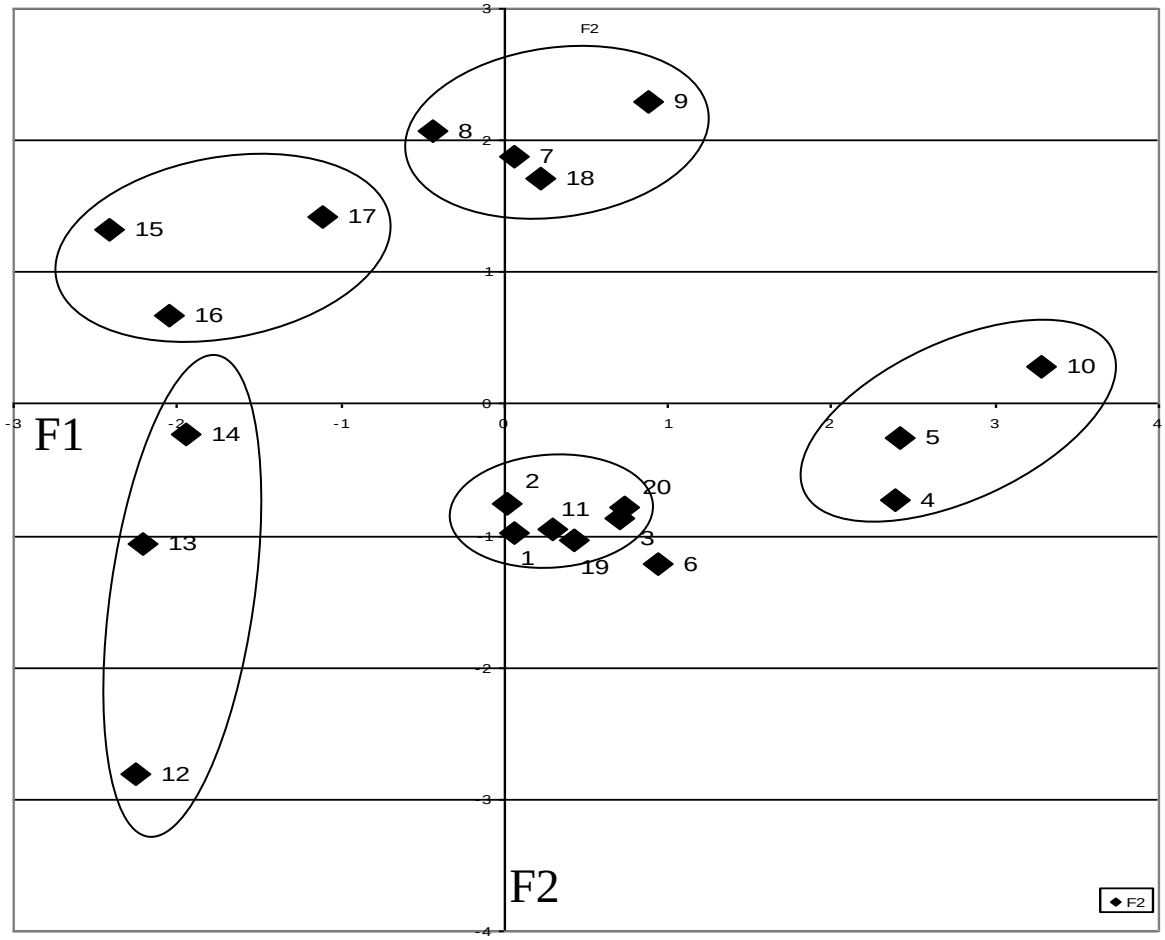

Figure 46 : Individuals of the hard layer plotted on the new coordinate axes F_1 and F_2 holding 71% of the absorbed total variance.

Figure 46 shows the individuals in the main plane F_1,F_2 . With this representation the similarities and differences of the rock in relation to the distance from the fault are shown.

The values at 1,2,3,6,11,19 and 20m from the fault, that means the border values of our study are near the origin of this graph. In fact for many variables the border data was not available and mean values have been taken in order to complete the database. The fact that also the measurements at 11m belong to this group is because it is located in the transition of a very strong and an extremely weathered zone. Individuals 4m, 5m and 10 lay on the opposite site of the F_1 axis than individuals 12 and 13. In fact at 4-5m and especially at 10m the rock properties are globally the strongest and at 12-13m globally the lowest, this last one caused by fracture family F3.

(WHAT CAN I SAY ABOUT THE GROUPS 7,8,9,18 AND 15,16,17????)Tu peux aussi annoncer que l'évolution des points de prélèvement sont fonction de la participation à la construction de l'axe F1 et F2 par les variables explicatives....(on en rediscutera en septembre) AGHHHH

5.1.2.2 The weathered layer

[IN THE PCA OF THE WEATHERED LAYER THERE IS NOT ONE GOOD RESULT...NOTHING MATCHES.I THINK THAT I WILL NOT PUT IT IN THE RAPPORT, THE CORRELATIONS FOUND ON THE HARD LAYER ARE ENAUG...OR NOT????IN ADDITION I AM COMPARING VALUES MEASURED ON THE ROCK: SH AND AJS WITH VARIABLES MEASURED ON SOIL C AND φ WITH A VARIABLE MEASURED ON THE WHOLE COMPLEX: THE RESISTIVITY. I THINK THAT THIS DOESN'T MAKE ANY SENSE!!!! WHAD DO YOU SAY CHEF??????]

The variables of the weathered layer that have been correlated are the SHRV and the AJS and the electrical resistivity (Res) taken directly in situ on the weathered layer and the results of the triaxial tests c' and φ' performed in the laboratory on the sampled soil, which comes from the extreme altered material of the weathered layer.

	SH	AJS	c'	φ'	Res
SH	1.00	0.40	0.36	-0.49	0.11
AJS		1.00	-0.31	-0.14	0.05
c'			1.00	-0.25	0.35
fi'				1.00	0.12
Res					1.00

Table 9 : Correlation matrix (M_c) for the variables of the Weathered Layer

None of the correlation coefficients between the variables is higher than r=0,40% or lower than r= -0,49%. This bad correlation of the variables shows the multitude of factors that determine the strength of the cliff face. SHRV and apparent joint separation have a correlation coefficient of r=0,40, that means that the resistance of the rock determined with this instrument depends somehow on the fracturing of the rock but as well on many other factors. A great influence of this parameter is certainly the micro-fracturation (Katz et al. 2000) which is not visible on the rock and therefore not taken into account in the evaluation of the AJS. Density will as well influence this parameter also if in a limited way as shown in the PCA for the hard layer. The other correlations are not strong enough and no interpretation has been found for their correlation. All in all it can be said that this very weathered layer has so many different factors that influence its poor rock quality that no real correlation can be found.

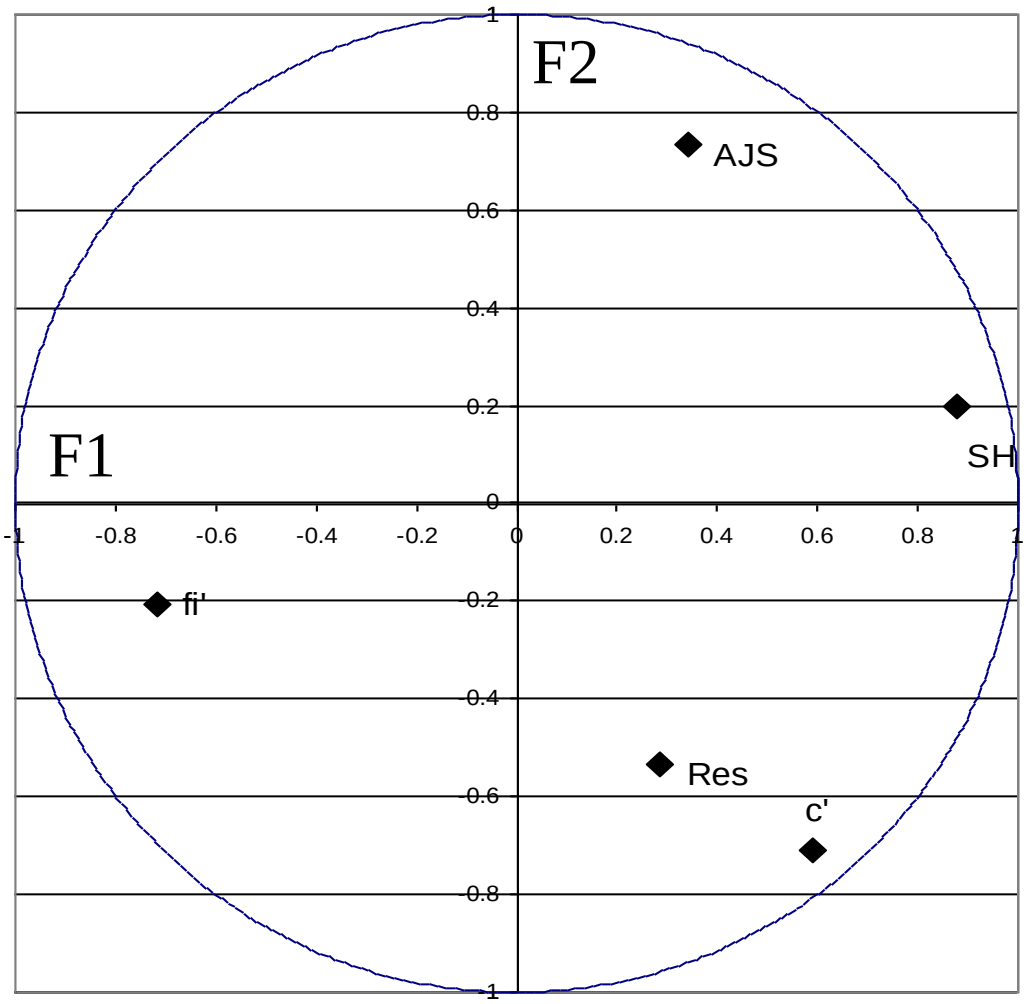

	SH	AJS	c'	fi'	Res
F1	0.88	0.34	0.59	-0.72	0.28
F2	0.20	0.74	-0.71	-0.21	-0.53
F3	0.05	0.52	-0.14	0.48	0.73

Figure 47: Factor loadings plot, 65% of the total variance is hold by the first two components. Table of the correlation of the old variables with the new ones: F1, F2, F3 data for each variable of the weathered layer

Figure 47 shows the variable projection in the space F_1, F_2, representing 65% of the total variance. The F_1 axis is constituted for 0,88% by the SHRV and the electric resistivity represents the F_2 axis for 74%. ..... AND THEN ??????

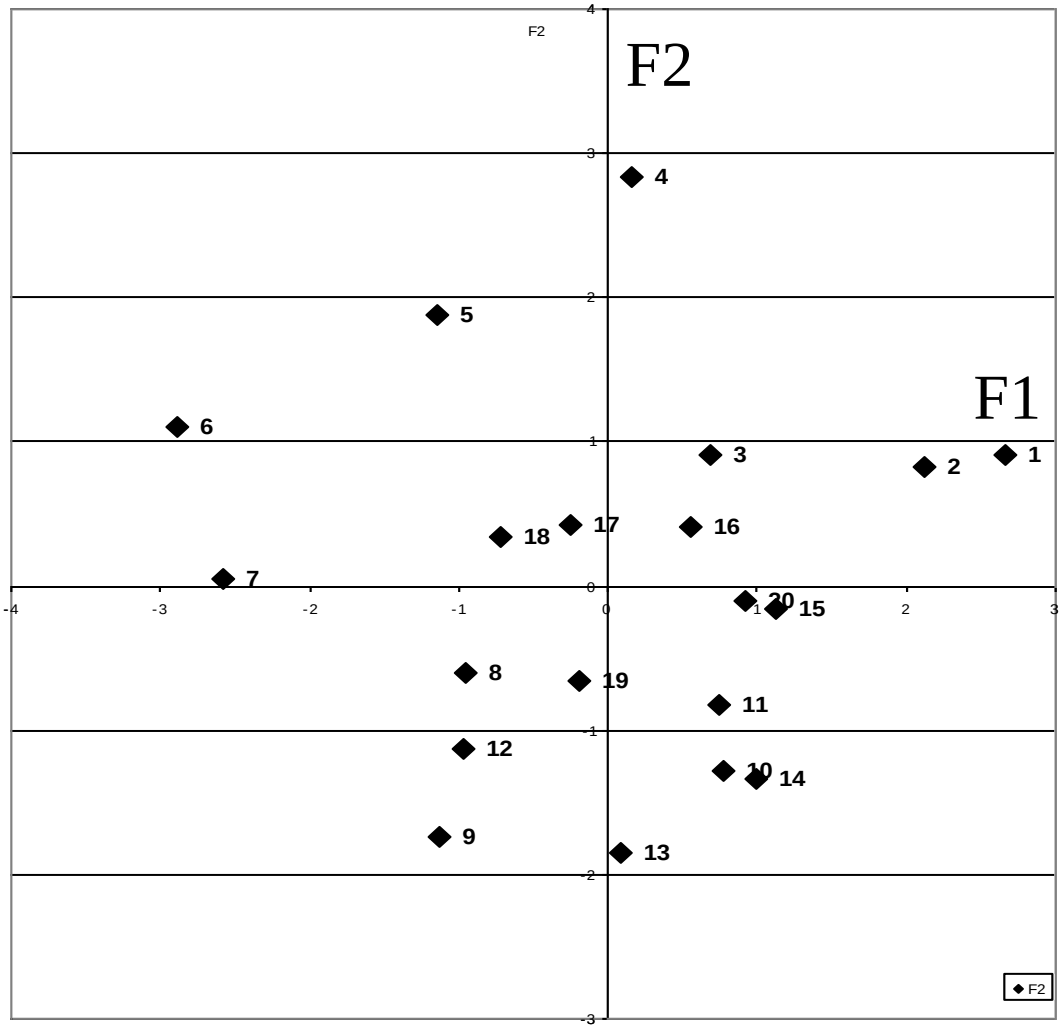

Figure 48 : Individuals of the weathered layer plotted on the new coordinate axes F_1 and F_2 holding 58% of the absorbed total variance.

AND HERE NOTHING MATCHES..... ☹
CETTE PARTIE JE NE PENSE PAS DE LA METTRE….OU EST CE QUE ON PEUT EN INTERPRETER QUELQUE CHOSE ???????????

5.1.3. Conclusion

5.2 *Relationships between the different tests*

5.2.1. Electric tomography

In the light of the results of all the tests that have been executed on the cliff face which have been analysed in Chapter 4, the electric resistivity tomography (Figure 17) can be analysed a little bit more precisely. In spite of the high Rms of 74,3% it can now be said that the result is not bad at all.

5.2.1.1 Analysis:

For the great band which is parallel to the surface of the cliff face (W-E) of very low resistivity (ρ1<60 Ωm) the interpretation presented in §4.2.2 is maintained: It is probably due to the W-E fracturing and represents a decompression of the massif. Fluid circulation is therefore favoured in this fractured, decompressed zone, which results in a drop of resistivity.
The interpretation of the superficial blocks of ρ3>400 Ωm cut by zones of ρ2 = 150–400Ωm can be confirmed. These zones of lower resistivity ρ2 are the expression of the fracturing Nº175. Especially the drop of resistivity at 5,5 to 6,5m, 7,5 to 8m, from 11 to 13m, at 17 and from 19 to 20m, are respectively caused by the big fracture families F1 to F5. The drop of resistivity at 4m might as well be caused by a fracture which is not visible on the cliff face but probably hidden by the thick layer of calcite. The same results were given by the SHRV and the AJS, especially of the weathered layer in which the fractures are much more expressed. In F1 and F3 the high degree of fracturing and the associated fluid circulation is confirmed by the calcite veins that are present all over the drill core and are visible in the thin slices as presented in §4.8
The more resistive point (ρ up to 230Ωm in the band of ρ1<60 Ωm) at about 9-10 m from the fault and 1,5 – 3,5 m in the interior of the massive is confirmed to be a more compact and resistant part of the rock or a harder block between two fractured and altered zones. The same peak of the rock quality at this particular point is confirmed as well by the SHRV of the hard layer and the AJS of both the hard and the weathered layer. (Figure 19, Figure 23)

5.2.1.2 Conclusion:

The electric resistivity tomography has proved to be a good analytical tool also if used in extremely unfavourable conditions as with horizontally planted electrodes, in a very dry season, just in order to see the fractures and discontinuities in one and the same lithologie. It confirms the results found with the Schmidt Hammer and the calculation of the Apparent Joint Separation. Fractures, even if dry, are clearly visible on the profile thanks to low resistivity and a more compact and resistant area thanks to higher resistivity. It could be interesting to repeat the ERT in the humid season after heavy rain falls. Water will easily penetrate into fractures and weathered porous material also in the depth of the versant and it might be possible to analyze deeper, more profound zones of the massif.

5.2.2. Apparent Joint Separation (AJS) and Schmidt Hammer Rebound Value (SHRV)

5.2.2.1 Bibliography

In the study of Greco et al. (2005) the relationship between the jointing of rock masses and master faults is investigated, since it is generally assumed that high jointing frequency favours fluid circulation and therefore increases weathering affecting the rock resistance. The SH test was performed on Sedimentary rocks, Plutonic rocks, Augen gneiss and Metamorphic rocks in order to investigate the link between the apparent separation of jointing and the mechanical strength of rock. It was found that the relationship between the SHRV and AJS is problematic and difficult to model but nevertheless it was shown that this relation is similar to that which describes the dependence of AJS on the distance from the major fault.
For the sedimentary deposits a law is proposed to correlate SHRV with AJS:

$$SHRV = 7{,}936 + 1{,}429\ (AJS)^{0,5}$$

5.2.2.2 Analysis:

In this study no formula could be found to correlate the SHRV with the AJS. In the PCA the correlation coefficient is r=0,40 for the weathered layer and only r=0,29 for the hard one. Nevertheless a good relation between the two parameters can be seen if the two variables are plotted together in function of the distance from the fault, for both the weathered and the hard layer. These variables and their dependence from the major fracture families F1-F5 has been discussed in § 4.3 and §4.4. In order to show their similar trend the AJS has been multiplied by 500 and they have been plotted together. Both variables broadly decrease in proximity to the major fracture family but no precise relation between the two can be found.

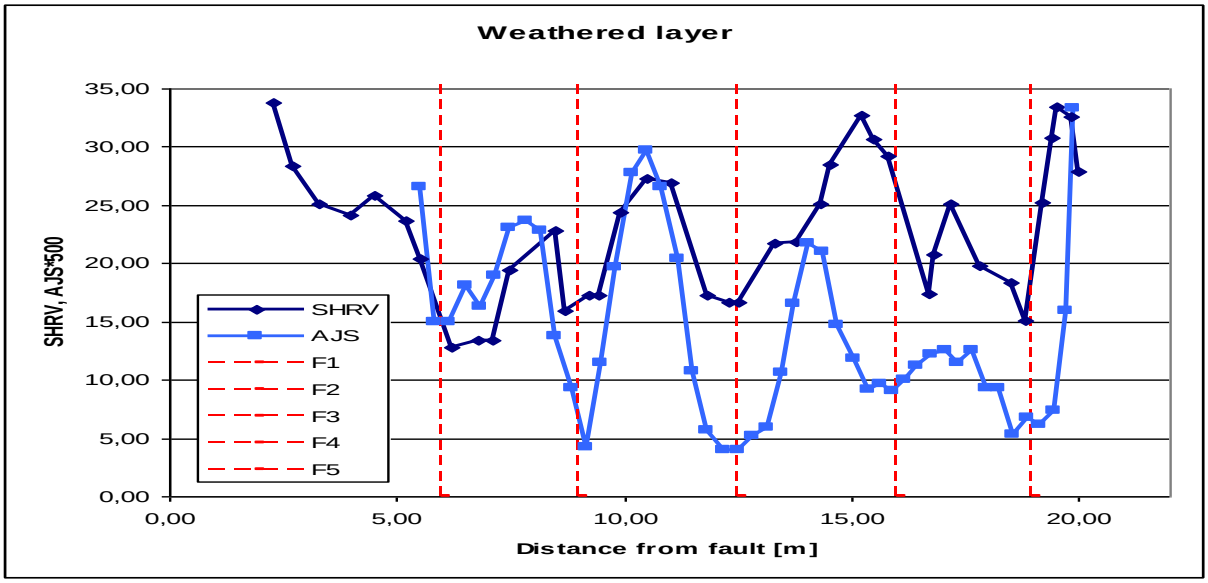

Figure 49 : SHRV and AJS in function of the distance from the fault on the weathered layer

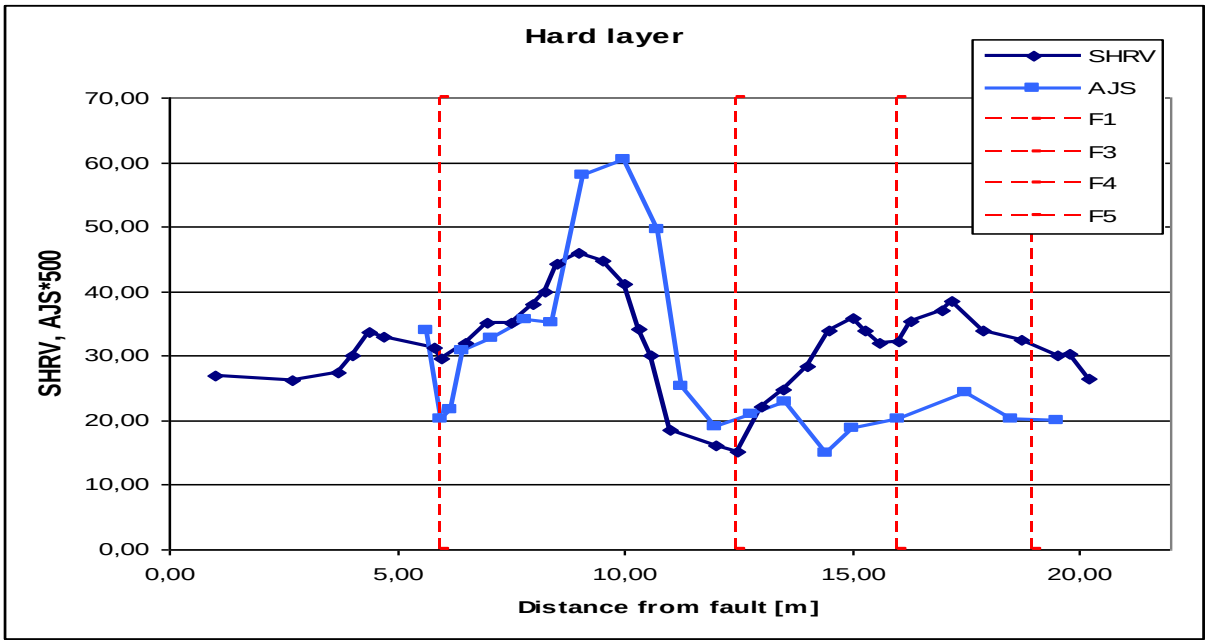

Figure 50 : SHRV and AJS in function of the distance from the fault on the hard layer

5.2.2.3 Conclusion:

This study of the correlation between the AJS and the SHRV demonstrates that the rock strength depends from several factors and not only from the density of jointing which favours weathering and decreases rock strength. Fracturing and micro-fracturing plays clearly a very important role in the drop of the mechanical parameters measured on the cliff face but too many heterogeneities (as different diagenic mineralogy, porosity, density) are present to find a mathematical law which describes rock strength in relation to the sole jointing density.

5.2.3. Uniaxial Compressive Strength (UCS) and Schmidt Hammer Rebound Value (SHRV)

5.2.3.1 Bibliography:

UCS is widely used in rock engineering to determine the mechanical strength of rock. This method is simple but it is extremely time consuming (drilling of core, preparation of specimen, the test itself). Therefore many authors have proposed various simple methods for assessing the UCS of rocks. (Kahraman 2001, Katz and al. 2000, Aydin et al, 2005) Indirect tests like Schmidt hammer test, point load index and sound velocity test are generally well correlated with the UCS. Various formulas which correlate the UCS with these simple non destructive means have been found, as resumed in the work of Kahraman (2001). Some of these formulas are reported in Table 10. It is concluded that they can be used to predict the compressive strength of rocks but that the prediction equation derived by different researchers are dependent on rock types and test conditions. Aydin et al (2005) as well studied the correlation of SHRV with UCS and Young modulus and resume the empirical correlation formulas. Many of these formulas include also the dry density as a secondary variable in order to improve the correlations but Aydin warns that the use of additional variables such as density, porosity and ultrasonic velocity should be avoided in establishing empirical correlations for practical use unless their roles are complementary and significant and can clearly be explained. Aydin et al. (2005) states that UCS of crystalline igneous rocks at any degree of weathering can be predicted from one of the following generalized expressions;

$UCS=a*e^{(b*SHRV)}$,

$UCS=a*SHRV^{b}$

where a and b are constants based on the rock type. In this study a correlation between the UCS and the SHRV which matches with these formulas has been found.

5.2.3.2 Analysis

In order to find an easy mean to determine the UCS it has been plotted against the SHRV to find a correlation (Figure 51)
Despite the small amount of available data one of the two empirical correlations that were found to correlate UCS with the SHRV is very similar to those found by other authors as resumed in (Table 10) also if the coefficient of correlation found in this study is lower than those found by other authors.

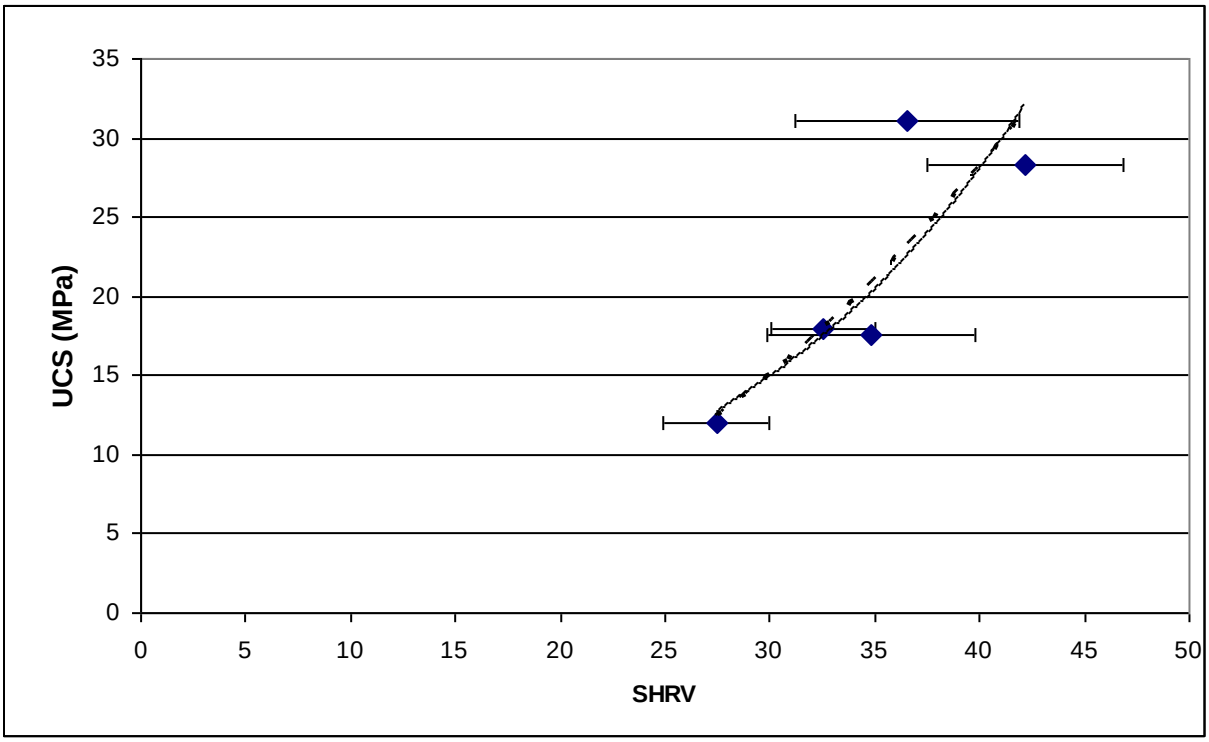

Power law ---------- **$UCS = 2{,}2899 * e^{0{,}0627*(SHRV)}$** $R^2 = 0{,}76$

Exponential law - - - - - - **$UCS = 0.0091*(SHRV)^{2.1778}$** $R^2 = 0{,}79$

Figure 51 : Empirical relations between Schmidt hammer rebound values and the Uniaxial compressive strength. The plotted lines are the best fit correlations: an exponential law (dotted regression curve) and a power law (continuous regression curve). Horizontal error bars indicate standard deviations of the hammer values.

Formula found	**Coefficient of correlation R^2**	**Rock type**	**Author**
$UCS=2{,}208*e^{0{,}067*(SHRV)}$	0,96	7 different lithologies	Katz et al.(2000)
$UCS=2{,}27*e^{0{,}06*(SHRV)}$	0,91		Yilmaz et al.(2002)
$UCS=2{,}99*e^{0{,}06*(SHRV)}$	0,91	Prasinite	Xu et al. (1990)
$UCS=2{,}98*e^{0{,}063*(SHRV)}$	0,94	Serpentinite	Xu et al. (1990)
$UCS = 2{,}2899*e^{0{,}0627*(SHRV)}$	**0,76**	**Dolomite**	**this study**
$UCS = 0.0001*(SHRV)^{3.27}$	0,84	Marl	Gokceoglu (1996)
$UCS = 0.00016*(SHRV)^{3,47}$		Granite	Dearman and Irfan (1978)
$UCS = 0.000004*(SHRV)^{4,29}$	0,89	Carbonates Sandstone, Basalt	Yasar and Erdogan (2004)
$UCS = 0.0091*(SHRV)^{2.1778}$	**0.79**	**Dolomite**	**this study**

Table 10 : Relations between UCS and SHRV resumed by Aydin et al. (2005) and those of this study. (UCS in Mpa)

5.2.3.3 Conclusion:

As a conclusion a further investigation of the correlation between SHRV and UCS on the Hettangien series in the sector of the Marbrière versant is proposed in order to confirm the found formula. It is reminded that this correlation has been made with only 6 UCS values and has therefore to be controlled on a larger number of samples. In the case of a verification of the found formula, this easy, cheap, not time consuming and non destructive tool can be very helpful to determine the mechanical strength of the studied rock. On this versant it is especially useful to have an easy tool to control the mechanical parameters of the weathered rock because it will remain under constant control for the study and the prevention of landslides

5.3 *The lateral variation of facies in the Hettangien*

The Hettangien is the second level of the inferior Jurassic (Lias). In the bibliography it is described as an alternation of ash-grey Dolomite in thick banks and well stratified and separated by green or yellow Marls in the upper part of the formation. One of the guideline questions of this study was how much influence does the proximity of the fault have with the increasing weathering and the sharp drop of the mechanical properties on this lithologie. With this analysis it is attempted to find an answer to this question.
A lateral variation of facies in this stratigraphic level can be noticed in field observation (more brittle and soil like aspect). This variation of facies has a significant correlation with the mechanical properties of the rock.. In order to quantify this lateral variation a series of specimen has been sampled at middle height of the formation (which is about 40m thick). Specimen n°1 been taken at the level of the Boulevard Georges Clemenceau , and the n°2, 3, 4, have been taken successively starting from the South-western boundary of the Marbrière versant (boulevard Bellevue) to the base of the plateau of Haut Malbosc which is the sector that is affected by the active gravitational deformations. (Figure 52)

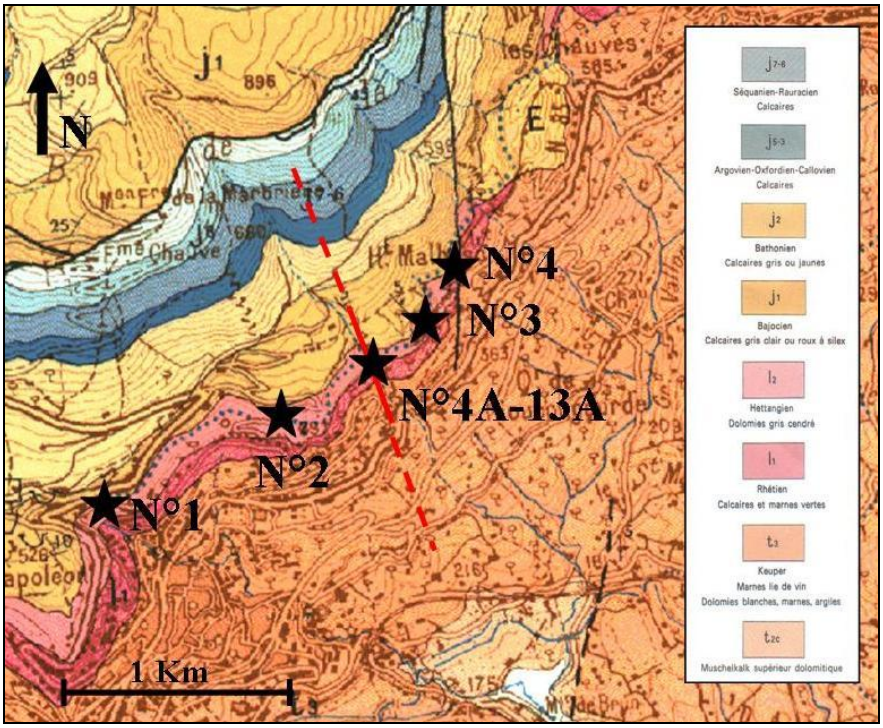

Figure 52 : Sampling location for the realisation of thin slices on the geologic carte of Cannes Grasse, BRGM

5.3.1. Analysis of the thin slices:

With the objective to understand the origins of these variations of local alteration (tectonic and recent fluid circulation, or diagenic origin) thin slices have been made for each sample and analyzed with the microscope in polarized light (Figure 53), Their macro and microscopic description follows in Table 11.

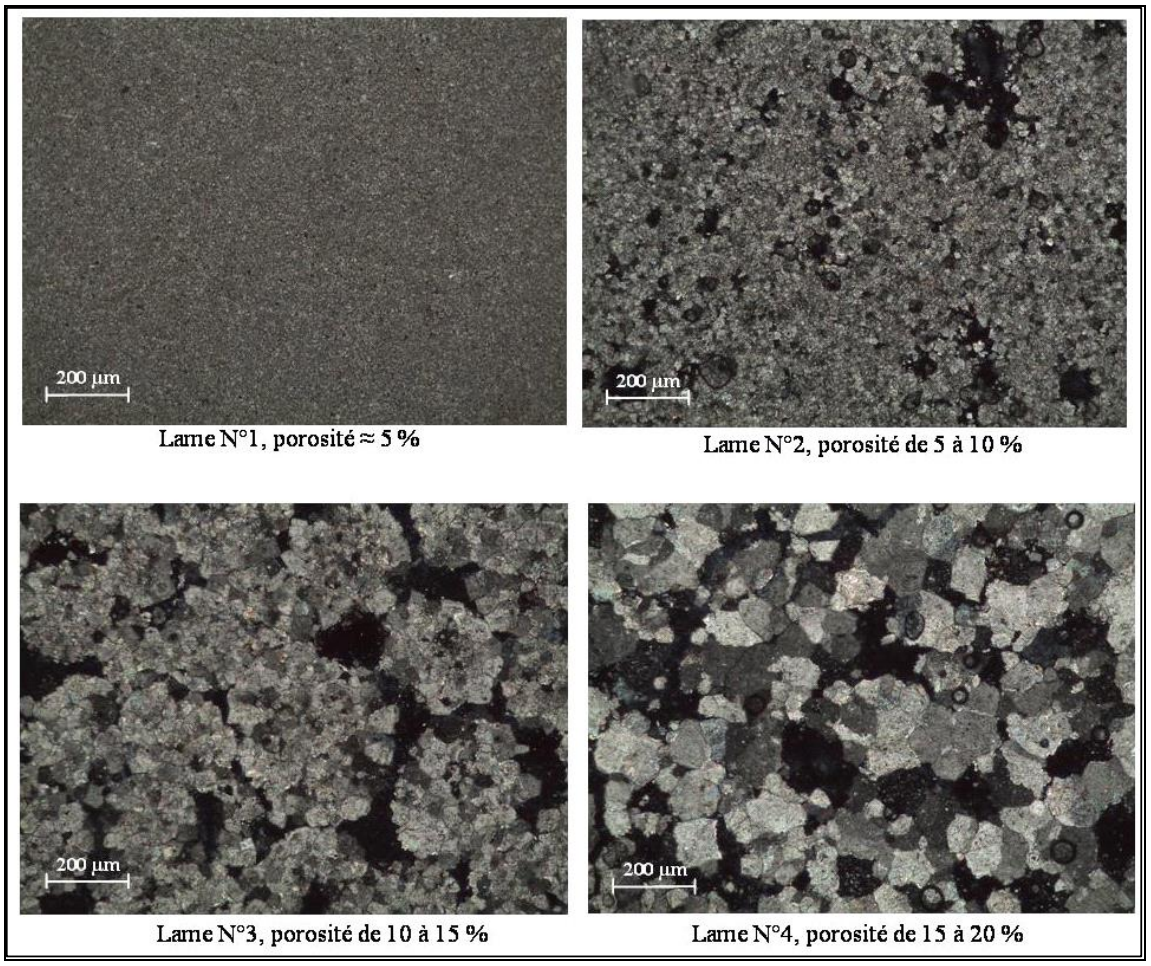

Figure 53 : Photos of the thin slices in polarized light for the samples N*º 1 - 4* (same enlargement) and evaluation of porosity.

Sample	Macroscopic description	Microscopic description
n°1	Very fine grained dolomitic limestone disposed in thick banks with steady thickness, lithographic, very massif, yellow patina ,intercalations of fine greenish levels of marls.	Very fine, homogeneous Micrite, absence of bioclasts, ~5% porosity, rounded regular shaped pores with Ø of 10-15 µm, Ø grains < 10 µm
n°2	Dolomitic limestone with sandstone like aspect, disposed in thick banks with steady thickness, locally lightly dusty, very massif, light yellow patina, intercalations of fine yellowish levels of marls.	Dolomitic micro sparite, absence of bioclasts, porosity of 10 – 15%, pore shape more irregular with Ø of 30 – 100 µm, Ø of grains ~ 20µm
n°3	Dolomite with sandstone like aspect, disposed in banks with variable thickness, presence of cross beds and lenses, lamination , visibly porous, light yellow patina, fine yellowish intercalations	Dolomitic sparite, absence of bioclasts, porosity of 10 – 15%, irregular pore shape with Ø of 10 - 15 µm, Ø of grains ~ 50µm, geode like figures
n°4	Totally dusty dolomite with sandstone like	Coarse dolomitic sparite, absence of

	aspect, stratification not very visible, presence of cross beds and lenses, lamination , visibly porous, whitish patina	bioclasts, porosity of 15 – 20%, irregular pore shape with Ø of 50 - 200 µm, Ø of grains ~ 150µm. Geode like figures, zoning of dolomitic crystals, figures of successive crystallization.

Table 11 : Macro and microscopic description of the samples N°1 – 4 , illustrating the lateral variation of facies.

After these observations the primary or diagenetic origin of these variations of the alteration and dolomitisation are confirmed. Effectively it is not possible to observe preferential orientations in the organization of the minerals on any of the thin slices. Therefore a tectonic origin of these variations is excluded and the actual continental environment doesn't seem to allow such a dolomitisation (cold fluid circulation with low magnesium rates)

It is a matter of differential circulation of warm fluids that are oversaturated in magnesium and in salt, which provoke the dissolution of calcite and the successive re-crystallization of dolomite, at the time of the burying of the material in the paleo environment. These phases of successive dissolution/crystallisation cause the modification of the texture. In this way the diameter of the grains and of the pores can increase up to a factor 20 and the form of the pores becomes more irregular. (Figure 53) These variations of the dolomitisation state induce up to date variations of the mechanical parameters of the rock. In fact an important grain size implies a decrease of the contact between the grains and consequently a diminution of friction. In the same way a coarser porosity (irregular, stretched pores) implies a diminution of the cohesion and allows an easier localisation of the deformation.

To confirm and qualify these variations of the mechanical properties in the frame of the differential dolomitisation of the rock, a series of Schmidt Hammer tests have been realised directly on the sampled outcrops (N°1,2,3,4) (Figure 54)

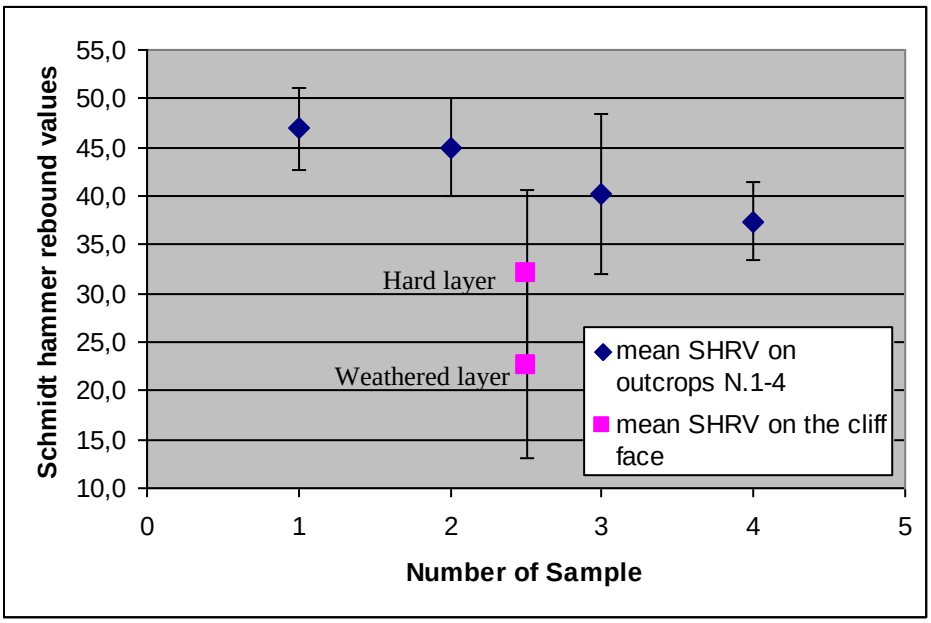

Figure 54: Mean SHRV for each sampled outcrop N°1-4 and for the hard and weathered layer on the cliff face

Figure 54 (mean SHRV on outcrops Nº1-4) shows a significant, general decrease of the SHRV from the sample Nº1 to Nº4. This trend correlates very well with the identified mineralogical evolution also if the number of data is small (Figure 53)

Both geographically (Figure 52) and mineralogically (Table 6, Figure 44,Figure 53,Table 11) the cliff face is situated between the sampled outcrops Nº 2 and Nº3. In fact, despite the lithological differences that are present also on the cliff face among the different layers (Microsparite of samples Nº4A,5A,13A and sparite of samples Nº6A-12A) the grain size of most of the slices of the cliff face is Ø=20-50µm which is in-between the grain size of slice Nº2 (Ø=20µm) and slice Nº3 (Ø=50µm).

The parameter that does not fit in this trend is the SHRV measured on the cliff face. (Figure 54) In taking the mean values of all the SH tests executed on the cliff face (differentiating only the weathered layer from the hard layer because of their extremely different mechanical properties) it becomes clear that they are much lower than the SHRV of the outcropping rock of samples Nº2-3.

Using the formula that was found for the correlation between the SHRV and the UCS on the Hettangien material a rapid confrontation can be made between the UCS values of the samples N1-4 and the mean values of the cliff face:

Sample	Nº1	Nº2	Nº3	Nº4	Hard layer	Weathered Layer
UCS(MPa)	43,32	38,37	28,49	23,809	17,09	9,44

The UCS value of the weathered layer is only 22% of the value of sample Nº1, but it has to be admitted that sample Nº1 has a different lithologie. So, if the UCS of the same lithologies are confronted near and far from the cliff face (the cliff face lies lithologically and geographically between sample Nº2 and Nº3 which have a mean value of UCS of 33,4 MPa) the UCS of the weathered layer is only 36% of the UCS of the rock with the same lithology far from the cliff face. This drop of 64% of UCS within the same facies and the same lithology is merely caused by the extremely high weathering of the cliff face.

5.3.2. Conclusion:

This analysis demonstrates that it is the proximity of the fault which extremely increases the weathering (physical and chemical) which provokes the drop of the SHRV and therefore of the UCS. A lateral syndiagenetic variation of the mineralogy has been found in the Hettangien facies, and the rock becomes more friable and brittle from sample Nº1 to Nº4, that means from the stable to the unstable zone. Since the Hettangien is located in the lower part of the versant and is therefore the base of the deformation, together with the Rhetien, (Figure 7) it is important to observe how its mechanical behaviour changes horizontally throughout the versant, decreasing in the unstable zone and presenting a sharp drop especially in the proximity of the principal fault that plays a major role in the development of this instability. A further investigation is therefore proposed throughout the Hettangien series and especially in proximity to the other faults that cut this versant.

5.4 *Slope stability Analysis*

5.4.1. Theory:

Slope stability analysis involves a comparison of the gravity induced stresses in a slope to the available soil strength. Available static equilibrium methods solve for one or more of the three equations of equilibrium: horizontal force, vertical force, and moment. The availability and speed of personal computers have made the use of methods of analysis that satisfy all equations of equilibrium feasible for practicing engineers. Proper analysis of the static stability of a slope requires representations of the slope configuration, external loading conditions, distribution of earth materials, subsurface water-conditions, material densities, and material strengths. To analyse the stability of slopes the traditional methods of slices with circular (Fellenius, 1927; Bishop, 1955) and non-circular (Morgenstern and Price, 1965; Sarma, 1973, Matos et al, 1986) surfaces of sliding have been broadly used. These methods of limit equilibrium are of the type "rigid-plastic methods", and assume that the soil body above the slip surface is subdivided into slices. The dividing planes between slices are always vertical and of a width dx**,** which is small enough to allow the simplification that the base of each slice is straight. Forces acting on individual slices are displayed in Figure 55.

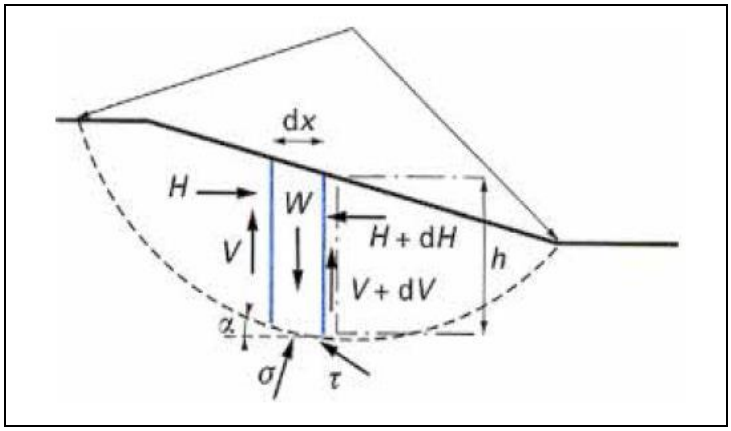

Figure 55 : Static scheme of slices

Here, W= γ h dx is the weight of the slice. V and H are the shear and normal forces (including the hydraulic pressures) acting between individual slices, τ and σ are the resulting shear and normal stresses on base of individual segments of the slip surface. The equilibrium of the slice n is found by projecting the forces on the horizontal and vertical axes:

$$dH_n - \sigma_n \tan \alpha_n \, dx + \tau_n \, dx = 0$$

$$dV_n - \gamma h_n \, dx + \sigma_n \, dx + \tau_n \tan \alpha_n \, dx = 0$$

Considering the Mohr Coulomb criterion ($\tau_{max} = c' + \sigma' \tan \varphi'$) and taking all the slices of the same thickness it results:

$$F = \frac{\sum [c + (\sigma_n - u_n)\tan\varphi] \frac{1}{\cos\alpha_n}}{\sum \gamma h_n \sin\alpha_n}$$

where u_n is the hydraulic pressure on the base of the slice n, supposed as known. The second member contains the unknown variables σ_n ; the relations of equilibrium of the slices are used to evaluate the unknown variables.
Individual methods of slices differ in their assumptions of satisfying the force equations of equilibrium and the moment equation of equilibrium with respect to the centre O. Fellenius (1927) makes the simplificatory hypothesis that $dH_n = dV_n = 0$ which gives immediately:
$\sigma_n = \gamma h_n \cos^2 \alpha_n$ and the security factor becomes:

$$F_{\text{Fellenius}} = \frac{\sum [c + (\gamma h_n \cos^2\alpha_n - u_n)\tan\varphi] \frac{1}{\cos\alpha_n}}{\sum \gamma h_n \sin\alpha_n}$$

5.4.2. Analysis:

The infinite slope analysis method, discussed above, when combined with properly determined shear strength parameters represents an analysis that should accurately represent the worst conditions for this type of failure. (Guidelines for Analyzing and Mitigating Landslide Hazards in California, Southern California Earthquake Centre, 2008)
The analysis by means of rigid-plastic methods with the traditional method of Fellenius, has been carried out on a rock mass (Figure 56 , Figure 57) that is partially cut apart from the versant by one the crevasses present a few m under the Foulon channel (N40º) which controls the slope movement from behind as shown in Figure 13.
The use of this method which generally concerns the stability of soil material and not of rock material is justified by the fact that this rock is that much weathered that is has actually a soil like behaviour. It is remembered that in order to collect the mechanical parameters of the "fresh rock" some samples were dug out of the cliff face using a geological pick. Once the very superficial layer of calcite was removed in many places it was possible to easily crumble the material by hands without any effort or strength.

Figure 56 : One of the crevasses (N40º) on the Marbrière versant a few m under the Foulon channel.

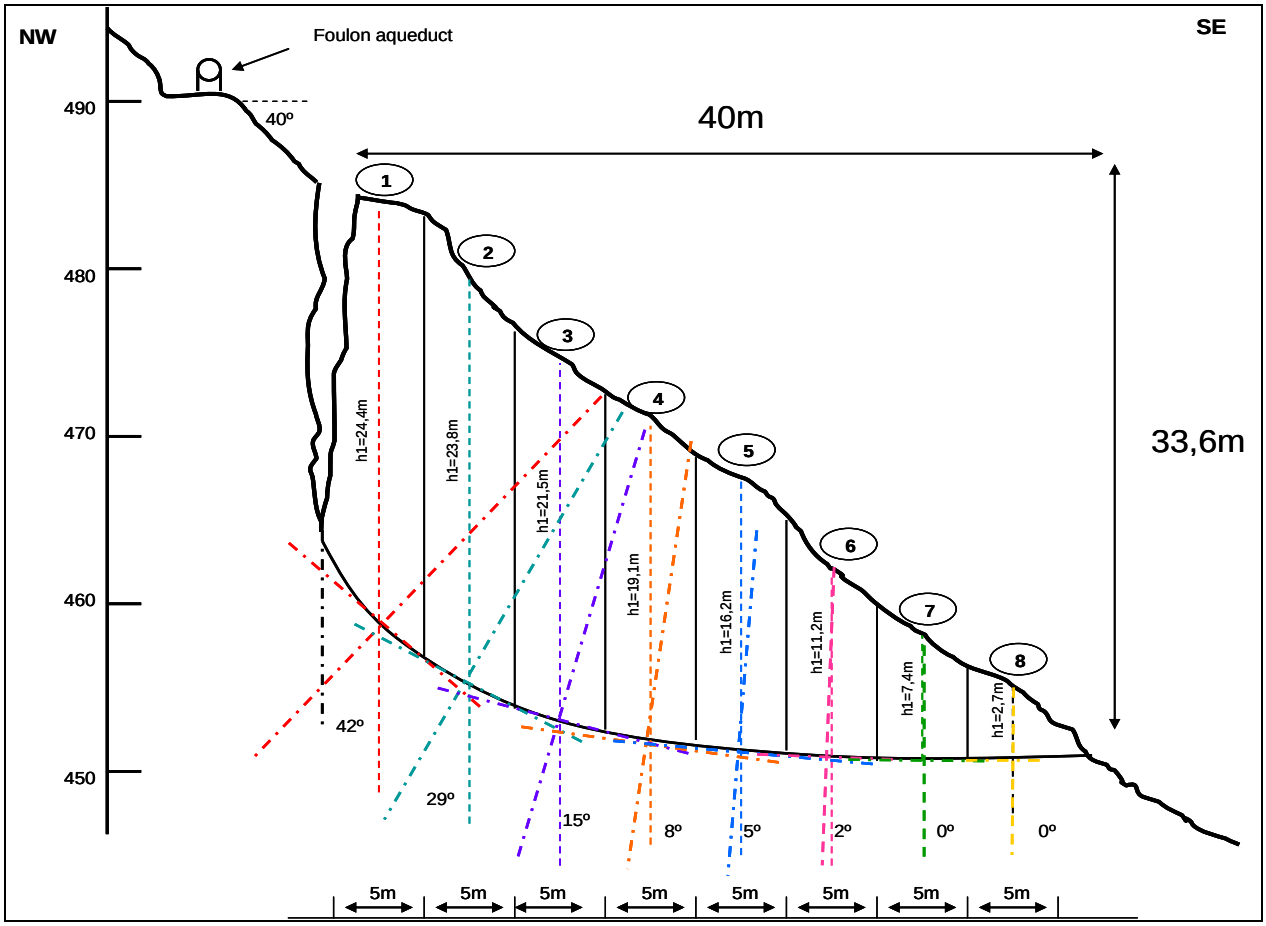

Figure 57 : Topography for stability analysis

The topography of the versant and its division in slices is represented in Figure 57. The characteristics of the soil are the following: The density includes the different degrees of water saturation:

$$\gamma = (\gamma s\ (1- (n/100))) + ((Sr/100)(n/100)\ \gamma w)\ ,$$

With:

- Density of the solid rock: γs=27,3 kN/ m^3 (is the mean value of the measured rock densities),
- Porosity: n=16% (is the mean value of the measured porosities)

Which measurement is discussed in Chapter: 4.7.1.2

- Internal angle of effective friction φ' varies from 10º to 40º,
- Effective cohesion c' varies from 5 to 20 kPa

C' and φ' were determined with the triaxial test discussed in Chapter: 4.5. The values of the c' and φ' which safety factors are discussed in the following paragraph are representative of 3 different weathering grades of the rock.

	c' (kPa)	φ' º
Fresh rock	13,20	34,10
	16,80	30,30
	15,70	32,00
Mean value	**15,23**	**32,13**
Fracture filling material	5,30	19,00
	11,10	18,90
	14,30	18,30
	9,60	17,10
	13,30	18,20
Mean value	**11,28**	**17,95**
Fault rock	**14,10**	**16,20**

Table 12 : Effective cohesion and internal angle of effective friction

The material named: "fresh rock" is the material which represent those samples that were dug out of the cliff face. The "fracture filling material" is the soil that was sampled in the more or less open fractures (N95º) present on the cliff face and "fault rock" represents the sample that was taken on the fault wall at 15m from the cliff face. Their mechanical properties are remembered in Table 12. The properties of the fracture filling material and the fault rock are very similar but nevertheless they have not been mixed in a single mean value because the fault rock has absolutely the lowest φ' of all samples. Also if the sampling and the analysis on the samples have been made in the same time period, these 3 groups represent 3 different stages of alteration in time of the same rock material which is exposed to weathering. The "fresh rock" is the less altered one. This does not mean that it is intact with good mechanical properties, since it has been exposed to weathering (underground fluid circulation, climatic variations...) but it will certainly be less weathered than the rock of the other two groups. Physical stresses and chemical reactions that have opened fractures in the rock altering strongly the material and then, once the fractures were open the fracture filling material has additionally been exposed the atmosphere (superficial fluid circulation, erosion...). In the same way also the fault rock has suffered all the physical stresses associated to the history of

the fault, as friction, loading and uploading, increased fluid circulation and all chemical reactions dolomite undergoes when exposed to fluid circulation. Therefore these 3 groups can be considered as the same rock material that has suffered increased weathering in time.

Five different situations have been analyzed: The piezometric level has been varied from 0% to 100% of the versant in steps of 25%. The iterations have been made with a program on Excel. The complete tables of the results are reported in the Annex. Obviously the most stable situation occurs when the versant is completely over the hydraulic head of groundwater. The safety factor of the versant decreases with increasing saturation of the slope.

	φ'	C'	**Scenario 1 Saturation = 0%**	**Scenario 2 Saturation = 25%**	**Scenario 3 Saturation =50%**	**Scenario 4 Saturation = 75%**	**Scenario 5 Saturation = 100%**
"fresh rock"	32,00	15,0	2,06	1,81	1,57	1,35	1,12
Fracture filling material (high c')	18,00	15,0	1,14	1,01	0,89	0,77	0,65
Fracture filling material (low c')	18,00	10,0	1,09	0,96	0,84	0,72	0,60
fault rock	16,00	15,0	1,02	0,91	0,80	0,69	0,59

Table 13 : Safety factor of slope stability for 5 different scenarios in 3 different time stages of weathering.

The processes leading to failure in rock slopes are still difficult to understand. The change of the safety factor with time is dependent on both fatigue and weathering of the rock mass. (Jaboyedoff et al, 2004)
The safety factor of the "fresh rock" decreases from 2,06 to 1,12 from the dry to the completely saturated scenario. The safety factor of the fracture filling material and of the fault rock is greater than 1 only in the first scenario, which means that from a saturation ratio of 25% upwards the versant is unstable if the sliding surfaces are pre-existent. In the 5 scenarios the safety factor is roughly halved from the fresh rock to the fault rock.
The most likely scenario is the one with a saturation ratio of 50%. This does not mean that half of the versant lies under the water table but thanks to capillary forces the pore pressure is that of a saturated material. The behaviour of this versant is assimilable to that of a karstic system. At a distance of about 30m from the cliff face on the fault wall a fracture drains constantly water out of the versant; even in summertime the flow is about 0,05 l/s. (No value is available for the wintertime.) Scenario Nr 3 has therefore been chosen as the most representative one. In this configuration only the fresh rock has a security factor bigger than 1. The fracture filling material with high and low c' and evidently the fault rock have security factors in-between 0,9 and 0,8 , but in fact this is not surprising. The material was sampled in open fractures, as described in the sampling protocol in §4.5.2. Now, if the mechanical properties, that means the values of c' and φ', to make stability calculations are taken from these materials it is as if the hypothetical sliding surface were already totally open, that means the versant finds himself already in a postruptural state, and the safety factor has to be minor than 1.

However, the interesting value is the safety factor of the "fresh rock", since the versant is fortunately still in a preruptural state, and this value is F=1,57, that means not only mayor than one, but even mayor than 1,5 which is considered as the limit acceptable value in most engineering handbooks.

5.4.3. Conclusion:

This study of the evolution of the safety factor in time, demonstrates how weathering affects slope stability. The Mechanical parameters of the soil like rock are strongly worsened by weathering (drop of 44% of φ' and 26% of c') which roughly halves the safety factor in all 5 scenarios. The most realistic situation is scenario Nr 3 with a saturation of the versant of 50%. The safety factor of the "fresh rock" which is already much altered is 1,57, that means greater but too close to 1,5, normally considered as the smallest acceptable value in civil engineering. In fact this versant is in a precarial state of equilibrium. The preparing factors for slope instability listed in §1.1.2 and §1.1.4.2 have undermined the safety of this versant and go perpetually on in their work of alteration. It cannot be excluded that the next triggering event (§1.1.3 and §1.1.4.2) as for example seismic solicitations or simply the next mayor climatic event as an abundant rainfall will not set of a greater and faster movement of the versant. In fact the Marbrière versant has been put under instrumental control of inclinometers and distanciometers which will be installed in August of this year.

Chapter 6 :Conclusion

After the analysis and discussion of the results of the different tests that have been carried out in situ and in the laboratory on the dolomite rock of the Marbrière versant it is now possible to answer the questions that have been posed in § 3.2.

Question d: "are there any simple means to characterize the mechanical properties of the rock?" has been discussed in § 5.2.3.

The answer is positive. A correlation between the SHRV and the UCS of rock has been found. UCS determines the mechanical strength of rock quantitatively and is internationally accepted as an engineering design test, whereas the SHRV is only an index test which describes qualitatively the rock strength but is very subjective and depends very much on the test conditions as the hammer type that is used, the position in which it is hold, the polishing of the rock before the test, etc. Nevertheless this test is not time consuming, cheap and very easy to perform whereas the determination of the UCS of rock is more expensive due to the sophisticated machinery (drilling machine, transport of drill cores and UCS machine) and the high amount of consumed time. Therefore many researchers have proposed correlation formulas of these two tests which are specific for the studied lithology. In this study two formulas has been found for the dolomite of the Hettangien series in the sector of the Marbrière versant.:

Exponential law : $\mathbf{UCS = 0.0091*(SHRV)^{2.1778}}$ $R^2=0,79$

Power law : $\mathbf{UCS = 2,2899*e^{0,0627*(SHRV)}}$ $R^2=0,76$

It is though reminded that this correlation has been found with only 6 UCS values and has to be controlled on a larger number of samples. A further investigation of this correlation is proposed for the dolomite of the Marbrière since it will remain under constant instrumental and anthropic control for the study and the prevention of landslides. With this easy, cheap, not time consuming and non destructive tool trends of the variation of mechanical strength can be investigated almost effortless and therefore an investigation can be made with small spacing. Then, there where such an evaluation shows interesting results a more accurate investigation by means of the uniaxial compressive strength test on drill cores can be made. In this way a lot of time, work and money are saved because the time consuming and expensive drilling and uniaxial testing are performed only on samples of aimed key locations of particular interest.

Question a: "Is this extremely high grade of weathering caused by the proximity of the fault?" has partially been answered in the conclusion of § 4.9.

It has been seen in field observation and by the analysis of drill cores and thin slices that the fault has a draining character, and the increased fluid circulation in the faults proximity clearly favours weathering. Additionally the throw of the fault, which has been demonstrated to be about 20m, has clearly damaged the rock. After the first 3m of bimrocks on the cliff face great fracture families have been observed. Certainly the fracturation favours fluid circulation which in turn widens the fractures and this vicious circle accelerates weathering in the fault zone. On the first dozen of m from the fault the maxima and minima of AJS, RQD and SHRV are sharper than from 12m onwards. Nevertheless it is observed that the first 20m of outcrop from the fault on are completely weathered and that a wider zone has to be analysed in order to really see the influence of the fault on the alteration of rock. In fact some values have been studied all along the Hettangien series of the Marbrière versant: The SHRV and the mineralogy of the studied rock.

At this point also **question b: "Which are the mechanical properties of this material and how much are they affected by the weathering process or rather by the closeness of the fault ?"** has to be posed since the answers of question a and b overlap.

The mechanical properties of the dolomite of the Hettangien series are strongly affected by weathering in **time**, and by the closeness of the fault, which causes an increased weathering, in **space**.

The alteration of this rock in **space** has been investigated by means of the Schmidt Hammer, its correlation with the UCS, and an image analysis of the thin slices of rock samples discussed in § 5.3:
The Hettangien series presents throughout the versant a diagenetic modification of the texture (diameter of the grains and of the pores and their irregularity) and dolomitisation which induce variations of the mechanical parameters of the rock: a diminution of friction and a diminution of cohesion caused respectively by a coarser porosity (irregular, stretched pores) and by decrease of the contact between the grains. Because of this syndiagenetic alteration a general almost linear decrease of the SHRV has been found on the Marbrière versant from the West to the East. The SHRV measured near the studied fault are much lower and do not fit in this linear trend even though it fits in this trend both geographically (Figure 52) and mineralogically (Table 6, Figure 44, Figure 53, Table 11) Using the formula which correlates the SHRV with the UCS of rock it comes out that the UCS of the weathered layer of the cliff face suffers a drop of 64% of the UCS of the rock with the same lithology not affected from

the fault. A further investigation is therefore proposed throughout the Hettangien series and especially in proximity to the other faults that cut this versant.

The alteration of this dolomite in **time** has been investigated by means of the TCT as has been discussed in § 4.5:
On the cliff face the rock is that much weathered that it is reduced to soil; soil samples have been taken out of the cliff face, of the fault wall and picked up in the open fractures and c' and φ' have been measured in the laboratory. It has been determined that the internal angle of effective friction is meanly reduced from 32,1º to 18º. That means that it loses 44% of effective friction in its evolution in time from the "fresh rock" of the cliff face to the fracture filling soil. The alteration of the material of the fault wall is even worse and it suffers a loss of 50% of its original φ'. The variation of the effective cohesion is less evident since c' covers a wider set of values. Nevertheless its mean value decreases 26% of its original mean value: from 15,2 to 11,3 kPa. This extreme drop of the mechanical strength can be attributed to the tangential displacement of the rock and to weathering which downgrades week zones of the cliff face into open fractures.

The answer of these questions leads to the next and last one:
Question c: How much influence has the change of the mechanical properties on slope stability? This problem has been analysed in § 5.4
After an analysis by means of a rigid-plastic method of Fellenius using the determined shear strength parameters it can be stated that the safety factor of the versant obviously decreases with increasing saturation of the slope. The fracture filling material and all the more the fault rock have security factors $F \geq 1$ only in a completely dry state. In fact an $F<1$ from a saturation grade of 25% upwards confirms the open state of the fractures which represent hypothetical sliding surfaces and simulate the situation of post rupture. However, the interesting value is the safety factor of the "fresh rock", since the versant is fortunately still in a preruptural state. The most likely scenario considers a saturation of 50% of the versant and in this configuration the "fresh rock" (and only the fresh rock) presents a stable situation ($F=1,57$) which is though very close to what is considered to be the limit value of stability in civil engineering. Therefore the answer of question c is in fact that the extreme weathering causes in this study case the degradation of the mechanical parameters from a stable ($F>1,5$) to an unstable ($F<1$) situation.

All in all it can be concluded that weathering composed by physical stresses associated to the history of the fault, as friction, its throw of 20m, loading and uploading, and all chemical reactions dolomite undergoes when exposed to fluid circulation which is conveyed in the fault zone because of its draining character altering strongly the material and its mechanical stress resistance undermining the stability of the versant which could fail after the next triggering event. It is therefore proposed to continue and complete the investigations described in this work:

- The SH Test should be performed all along the versant in the Hettangien series, especially in proximity of other faults and its correlation with the UCS which is of academic research interest besides its practical utility in this work should be .
- To gather more detailed information about the fault, its adjacent damage zone and its drainage function it has already been programmed to execute ERT vertically over the fault and horizontally on the cliff face in the humid season after important precipitations.
- In August 2009 the versant will be equipped with approximately 30 measuring instruments: 3–4 inclinometers and 20-25 extensometers will be placed on key sectors of the versant which present the most evident signs of gravitational movements. A

GSM base with a solar panel will as well help to capture the movements of this versant. Furthermore the Foulon channel will be equipped with microsismic sensors in order to provide a fast alarm, closure and evacuation system.

Bibliographie:

Aydin A, Basu A. ,2005
The Schmidt hammer in rock material characterization.
Eng Geol 2005; 81:1–14.

Bayless D.J.
" Chauvenet's Criterion " Website of the Ohio University,
http://www.ent.ohiou.edu/~bayless/seniorlab/chauvenet.pdf

Borelli, L., Greco, R. Gullà, G., 2006
Weathering grade of rock masses as a predisposing factor to slope instabilities: Reconaissance and control procedures
Geomorphology 87 (2007) 158–175

Calcaterra, D., Parise, M., 2005
Landslide types and their relationships with weathering in a Calabrian basin, southern Italy.
Bull Eng Geol Environ (2005) 64: 193-207

Cargill JS, Shakoor A. 1990
Evaluation of empirical methods for measuring the uniaxial strength of rock.
Int J Rock Mech Min Sci Geomech Abstr 1990; 27:495–503.

CONTROL (gotta surch for it at home…)

Durgin, P.B. 1977
Landslides and the weathering of granitic rocks
Geological Society of America, Rev. Eng. Geol. 3 (1977), pp. 127–131

El Bedoui, 2009
Rupture progressive des versants rocheux: Etudes des secteurs de la Haute-Tinée (Alpes du Sud – France et du Golfe de Corinthe (Grece), These, 2009

Geotechnical Engineering Laboratory, CE 3121, Texas tech. University,
After: Soil Mechanics – Laboratory Manual, B.M. DAS (Chapter 16 & 18) Soil Properties, Testing, Measurement, and Evaluation, C. Liu, J. Evett

Goktan RM, Gunes N. 2005
A comparative study of Schmidt hammer testing procedures with reference to cutting machine performance prediction.
Int J Rock Mech Min Sci 2005; 42:466–72.

Greco R., Sorriso-Valvo M., 2005
Relationships between joint apparent separation, Schmidt hammer rebound value, and distance to faults, in rocky outcrops, Calabria, Southern Italy
Engineering Geology 78 (2005) 309–320

Hill, S.E., Rosenbaum, M.S., 1998
Assessing the significant factors in a rock weathering systhem
Quarterly Journal of Engineering Geology and Hydrogeology; 1998; v. 31; issue.2; p. 85-94

http://www.cs.otago.ac.nz/cosc453/student_tutorials/principal_components.pdf p.12

Ippolito, F., Nicotera, P., Lucini, P., Civita, M., De Riso, R.,
Geologia tecnica, ISEDI , 1975

Jaeger, J.C., Cook, N.G.W.,
Fundaments of rock mechanics,
Science Paperbacks, 1969

Jaboeydoff, M. Baillifard, F., Bardou, E., Girod, F., 2004
The effect of weathering on Alpine rock instability
Quarterly journal of engineering geology and hydrogeology, vol. 37, n° 2 pp. 95-103

Jomard Hervé, Analyse multi-échelles des deformations gravitaires du Massif de l'Argentera Mercantour, These, Université de Nice Sophia Antipolis, 2006

Kahraman S., 2001
Evaluation of simple methods for assessing the uniaxial compressive strength of Rock, 2001.
International journal of Rock Mechanics and Mining Sciences, Volume 38, Issue 7, Pages 981-994

Kahraman, S., Alber, M., 2006
Estimating unconfined compressive strength and elastic modulus of a fault breccia mixture of weak blocks and strong matrix
International Journal of Rock Mechanics & Mining Sciences 43 (2006) 1277–1287

Katz, O., Reches, Z., Roegiers, J.-C., 2000.
Evaluation of mechanical rock properties using a Schmidt Hammer.
Int. J. Rock Mech. Min. Sci. 37, 723–728.

Le Pera, E., Sorriso- Valvo, M., 2000
Weathering and morphogenesis in a mediterranen climate, Calabria , Italy
Geomorphology, Volume 34, Number 3, September 2000 , pp. 251-270

Medley EW, 1994
The engineering characterization of mélanges and similar block-in-matrix rocks (bimrocks)

PhD, dissertation, University of California at Berkeley , CA. Ann Arbor,MI:UMI; 1994

Pellegrino, A. Prestininzi, A., 2006
Impact of weathering on the geomechanical properties of rock along thermal-metamorfic contact belts and morpho-evolutionary processes: The deep-seated gravitational slope deformastions of Mt Granieri-Salincriti (Calabria- Italy)
International Journal of Rock Mechanics and Mining Sciences
Volume 46, Issue 5, July 2009, Pages 929-939

Shengwena, Q. Zhong Qib ,Y. Faquana, W. Zhonghuaa, C. 2009
Deep weathering of a group of thick argillaceous limestone rocks near Three Gorges Reservoir, Central China (2009)
International Journal of Rock Mechanics and Mining Sciences
Volume 46, Issue 5, July 2009, Pages 929-939

Southern California Earthquake Center, 2008
Recommended Procedures for Implementation of DMG Special Publication 117
Guidelines for Analyzing and Mitigating Landslide Hazards in California
Committee organized through the ASCE Los Angeles Section Geotechnical Group

Spini, H., 1978.
Etude géologique de la bordure des chaînes subalpines méridionales au nord de Grasse.
Thèse de doctorat, Université de Nice, 101 p.

Tansi, C. Sorriso-Valvo, M. Greco, R., 2000
Relationships between joint separation and faulting: an initial numerical appraisal. Engineering Geology, 52, (2000), 225-230.

Remerciments:

Tout d'abord je voudrais remercier mon maître de stage, Thomas Lebourg, pour m'avoir permis d'entreprendre ce travail de recherche, m'avoir constamment suivi et pour m'avoir donné de précieux conseils et aidé tout en me laissant suivre mon propre cheminement et développer mes idées de manière autonome.
Un remerciement tout particulier va à mes collègues qui m'ont introduit dans le vaste et merveilleux monde de la Géologie, qui sont devenus de vrais amis dans le parcours de ce stage : Bastien et Swann avec qui j'ai passé d'excellents moments au labo et pendant nos temps libre, Maurin qui m'a hébergé et qui avec sa constante bonne humeur a égayé les journées avec ses nombreuses blagues, Wahib qui m'a aussi accueilli chez lui en un moment de besoin, Samir pour m'avoir donné un précieux aide en faisant les essayes de compression uniaxiales, Remi pour sa agréable compagnie sur la falaise, Julian pour m'avoir aidé avec le four qui ne marchait pas et quand j'ai inondé le labo et enfin Nicolas pour avoir refait quelques essaie triaxial.
Pour la bonne ambiance dans le CNRS je voudrais, à part les personnes déjà cité au dessus, aussi remercier Benoît, Jessica, Perrine, Michelle et Juan Carlos.
Je voudrais remercier aussi mes colocataires ainsi que très bons amis Benjamin et surtout Caroline pour être toujours la pour moi.
Enfin un remerciement générale et impersonnel mais quand même important va à l' Université Sophia Antipolis et au Geoazur du CNRS pour m'avoir donné la possibilité de faire ce stage et ce rapport.

Ringraziamenti

Vorrei ringraziare inanzitutto il Prof. G. Sappa per avermi dato fiducia e lasciato completa libertà nello svolgimento del mio lavoro di tesi all'estero.
Ringrazio i miei gentori per avermi dato la possibilita di passare quest'anno di studi a Nizza, dandomi sempre piena fiducia e liberta ed esserci sempre nel momento del bisogno. Ringrazio mia sorella per i suoi consigli preziosi e la sua 'presenza' , noncurante della lontananza. Ringrazio i miei amici, che amici erano, amici sono ed amici rimarranno e che ritrovo ogni volta che torno da un lungo periodo all'estero.
Ringrazio l'ufficio erasmus di Ingegneria della Sapienza per avermi aiutata a trovare la luce in fondo al mare cartaceo della burocrazia che complica la vita a chi intraprende la strada di una tesi all'estero, Alessandro per avermi fatto passare interminabili ore nell'auletta informatica del sesto piano, ed il Prof. Crespi per incentivare gli studenti ad allargare i propri orizzonti con periodi di studi all'estero e darci ascolto,appoggio e preziosi consigli.

Annex

Annex 1: Schmidt Hammer

Original Schmidt, N Type.
http://www.proceq.com/produits/papierfilm-et-film-plastique/original-schmidt.html?L=3

Caractéristiques :
Modèle N : Les valeurs de rebondissement sont lues à partir d'une échelle pour le calcul ultérieur de la moyenne. Les valeurs de résistance à la compression peuvent être lues à partir d'un courbe de conversion.

Normalisation :

- ISO/DIS 8045
- EN 12 504-2
- ENV 206
- DIN 1048, Partie 2
- BS 1881, Partie 202
- ASTM C 805
- ASTM D 5873 (roches)
- NFP 18-417
- B 15-225
- JGJ/T 23-2001
- JJG 817-1993

Fiche technique :

Modèle	N
Champ de mesure	10-70 N/mm^2 (entre 1 450 et 10 152 psi).
Energie de frappe	2,207 Nm
Bande de papier	Non

Annex 2: Safety factor of the stability calculations:

φ'	C'	F	niv_piez	TEST
10,00	5,00	0,59	0,00	FAUX
12,00	5,00	0,70	0,00	FAUX
14,00	5,00	0,81	0,00	FAUX
16,00	5,00	0,93	0,00	FAUX
18,00	5,00	1,04	0,00	VRAI
20,00	5,00	1,16	0,00	VRAI
22,00	5,00	1,29	0,00	VRAI
24,00	5,00	1,41	0,00	VRAI
26,00	5,00	1,54	0,00	VRAI
28,00	5,00	1,68	0,00	VRAI
30,00	5,00	1,82	0,00	VRAI
32,00	5,00	1,96	0,00	VRAI
34,00	5,00	2,11	0,00	VRAI
36,00	5,00	2,27	0,00	VRAI
38,00	5,00	2,44	0,00	VRAI
40,00	5,00	2,62	0,00	VRAI
10,00	10,00	0,64	0,00	FAUX
12,00	10,00	0,75	0,00	FAUX
14,00	10,00	0,86	0,00	FAUX
16,00	10,00	0,97	0,00	FAUX
18,00	10,00	1,09	0,00	VRAI
20,00	10,00	1,21	0,00	VRAI
22,00	10,00	1,33	0,00	VRAI
24,00	10,00	1,46	0,00	VRAI
26,00	10,00	1,59	0,00	VRAI
28,00	10,00	1,72	0,00	VRAI
30,00	10,00	1,86	0,00	VRAI
32,00	10,00	2,01	0,00	VRAI
34,00	10,00	2,16	0,00	VRAI
36,00	10,00	2,32	0,00	VRAI
38,00	10,00	2,49	0,00	VRAI
40,00	10,00	2,67	0,00	VRAI
10,00	15,00	0,68	0,00	FAUX
12,00	15,00	0,80	0,00	FAUX
14,00	15,00	0,91	0,00	FAUX
16,00	15,00	1,02	0,00	VRAI
18,00	15,00	1,14	0,00	VRAI
20,00	15,00	1,26	0,00	VRAI
22,00	15,00	1,38	0,00	VRAI
24,00	15,00	1,51	0,00	VRAI
26,00	15,00	1,64	0,00	VRAI
28,00	15,00	1,77	0,00	VRAI
30,00	15,00	1,91	0,00	VRAI
32,00	15,00	2,06	0,00	VRAI
34,00	15,00	2,21	0,00	VRAI
36,00	15,00	2,37	0,00	VRAI
38,00	15,00	2,54	0,00	VRAI
40,00	15,00	2,71	0,00	VRAI
10,00	20,00	0,73	0,00	FAUX
12,00	20,00	0,84	0,00	FAUX
14,00	20,00	0,96	0,00	FAUX
16,00	20,00	1,07	0,00	VRAI
18,00	20,00	1,19	0,00	VRAI
20,00	20,00	1,31	0,00	VRAI
22,00	20,00	1,43	0,00	VRAI
24,00	20,00	1,56	0,00	VRAI
26,00	20,00	1,69	0,00	VRAI
28,00	20,00	1,82	0,00	VRAI
30,00	20,00	1,96	0,00	VRAI
32,00	20,00	2,11	0,00	VRAI
34,00	20,00	2,26	0,00	VRAI
36,00	20,00	2,42	0,00	VRAI
38,00	20,00	2,58	0,00	VRAI
40,00	20,00	2,76	0,00	VRAI

φ'	C'	F	niv_piez	TEST
10,00	5,00	0,52	0,25	FAUX
12,00	5,00	0,62	0,25	FAUX
14,00	5,00	0,71	0,25	FAUX
16,00	5,00	0,81	0,25	FAUX
18,00	5,00	0,92	0,25	FAUX
20,00	5,00	1,02	0,25	VRAI
22,00	5,00	1,13	0,25	VRAI
24,00	5,00	1,24	0,25	VRAI
26,00	5,00	1,35	0,25	VRAI
28,00	5,00	1,47	0,25	VRAI
30,00	5,00	1,59	0,25	VRAI
32,00	5,00	1,72	0,25	VRAI
34,00	5,00	1,85	0,25	VRAI
36,00	5,00	1,99	0,25	VRAI
38,00	5,00	2,14	0,25	VRAI
40,00	5,00	2,29	0,25	VRAI
10,00	10,00	0,57	0,25	FAUX
12,00	10,00	0,66	0,25	FAUX
14,00	10,00	0,76	0,25	FAUX
16,00	10,00	0,86	0,25	FAUX
18,00	10,00	0,96	0,25	FAUX
20,00	10,00	1,07	0,25	VRAI
22,00	10,00	1,18	0,25	VRAI
24,00	10,00	1,29	0,25	VRAI
26,00	10,00	1,40	0,25	VRAI
28,00	10,00	1,52	0,25	VRAI
30,00	10,00	1,64	0,25	VRAI
32,00	10,00	1,77	0,25	VRAI
34,00	10,00	1,90	0,25	VRAI
36,00	10,00	2,04	0,25	VRAI
38,00	10,00	2,18	0,25	VRAI
40,00	10,00	2,34	0,25	VRAI
10,00	15,00	0,61	0,25	FAUX
12,00	15,00	0,71	0,25	FAUX
14,00	15,00	0,81	0,25	FAUX
16,00	15,00	0,91	0,25	FAUX
18,00	15,00	1,01	0,25	VRAI
20,00	15,00	1,12	0,25	VRAI
22,00	15,00	1,22	0,25	VRAI
24,00	15,00	1,33	0,25	VRAI
26,00	15,00	1,45	0,25	VRAI
28,00	15,00	1,56	0,25	VRAI
30,00	15,00	1,69	0,25	VRAI
32,00	15,00	1,81	0,25	VRAI
34,00	15,00	1,95	0,25	VRAI
36,00	15,00	2,09	0,25	VRAI
38,00	15,00	2,23	0,25	VRAI
40,00	15,00	2,39	0,25	VRAI
10,00	20,00	0,66	0,25	FAUX
12,00	20,00	0,76	0,25	FAUX
14,00	20,00	0,86	0,25	FAUX
16,00	20,00	0,96	0,25	FAUX
18,00	20,00	1,06	0,25	VRAI
20,00	20,00	1,16	0,25	VRAI
22,00	20,00	1,27	0,25	VRAI
24,00	20,00	1,38	0,25	VRAI
26,00	20,00	1,49	0,25	VRAI
28,00	20,00	1,61	0,25	VRAI
30,00	20,00	1,73	0,25	VRAI
32,00	20,00	1,86	0,25	VRAI
34,00	20,00	1,99	0,25	VRAI
36,00	20,00	2,13	0,25	VRAI
38,00	20,00	2,28	0,25	VRAI
40,00	20,00	2,43	0,25	VRAI

φ'	C'	F	niv_piez	TEST
10,00	5,00	0,45	0,50	FAUX
12,00	5,00	0,53	0,50	FAUX

φ'	C'	Fm	niv_piez	TEST
10,00	5,00	0,39	0,75	FAUX
12,00	5,00	0,46	0,75	FAUX

14,00	5,00	0,62	0,50	FAUX
16,00	5,00	0,70	0,50	FAUX
18,00	5,00	0,79	0,50	FAUX
20,00	5,00	0,88	0,50	FAUX
22,00	5,00	0,97	0,50	FAUX
24,00	5,00	1,07	0,50	VRAI
26,00	5,00	1,16	0,50	VRAI
28,00	5,00	1,26	0,50	VRAI
30,00	5,00	1,37	0,50	VRAI
32,00	5,00	1,48	0,50	VRAI
34,00	5,00	1,59	0,50	VRAI
36,00	5,00	1,71	0,50	VRAI
38,00	5,00	1,84	0,50	VRAI
40,00	5,00	1,97	0,50	VRAI
10,00	10,00	0,50	0,50	FAUX
12,00	10,00	0,58	0,50	FAUX
14,00	10,00	0,67	0,50	FAUX
16,00	10,00	0,75	0,50	FAUX
18,00	10,00	0,84	0,50	FAUX
20,00	10,00	0,93	0,50	FAUX
22,00	10,00	1,02	0,50	VRAI
24,00	10,00	1,11	0,50	VRAI
26,00	10,00	1,21	0,50	VRAI
28,00	10,00	1,31	0,50	VRAI
30,00	10,00	1,42	0,50	VRAI
32,00	10,00	1,52	0,50	VRAI
34,00	10,00	1,64	0,50	VRAI
36,00	10,00	1,76	0,50	VRAI
38,00	10,00	1,88	0,50	VRAI
40,00	10,00	2,01	0,50	VRAI
10,00	15,00	0,55	0,50	FAUX
12,00	15,00	0,63	0,50	FAUX
14,00	15,00	0,71	0,50	FAUX
16,00	15,00	0,80	0,50	FAUX
18,00	15,00	0,89	0,50	FAUX
20,00	15,00	0,98	0,50	FAUX
22,00	15,00	1,07	0,50	VRAI
24,00	15,00	1,16	0,50	VRAI
26,00	15,00	1,26	0,50	VRAI
28,00	15,00	1,36	0,50	VRAI
30,00	15,00	1,46	0,50	VRAI
32,00	15,00	1,57	0,50	VRAI
34,00	15,00	1,69	0,50	VRAI
36,00	15,00	1,80	0,50	VRAI
38,00	15,00	1,93	0,50	VRAI
40,00	15,00	2,06	0,50	VRAI
10,00	20,00	0,59	0,50	FAUX
12,00	20,00	0,68	0,50	FAUX
14,00	20,00	0,76	0,50	FAUX
16,00	20,00	0,85	0,50	FAUX
18,00	20,00	0,93	0,50	FAUX
20,00	20,00	1,02	0,50	VRAI
22,00	20,00	1,11	0,50	VRAI
24,00	20,00	1,21	0,50	VRAI
26,00	20,00	1,31	0,50	VRAI
28,00	20,00	1,41	0,50	VRAI
30,00	20,00	1,51	0,50	VRAI
32,00	20,00	1,62	0,50	VRAI
34,00	20,00	1,73	0,50	VRAI
36,00	20,00	1,85	0,50	VRAI
38,00	20,00	1,98	0,50	VRAI
40,00	20,00	2,11	0,50	VRAI

14,00	5,00	0,53	0,75	FAUX
16,00	5,00	0,60	0,75	FAUX
18,00	5,00	0,68	0,75	FAUX
20,00	5,00	0,75	0,75	FAUX
22,00	5,00	0,83	0,75	FAUX
24,00	5,00	0,91	0,75	FAUX
26,00	5,00	0,99	0,75	FAUX
28,00	5,00	1,08	0,75	VRAI
30,00	5,00	1,17	0,75	VRAI
32,00	5,00	1,26	0,75	VRAI
34,00	5,00	1,35	0,75	VRAI
36,00	5,00	1,45	0,75	VRAI
38,00	5,00	1,56	0,75	VRAI
40,00	5,00	1,67	0,75	VRAI
10,00	10,00	0,43	0,75	FAUX
12,00	10,00	0,50	0,75	FAUX
14,00	10,00	0,58	0,75	FAUX
16,00	10,00	0,65	0,75	FAUX
18,00	10,00	0,72	0,75	FAUX
20,00	10,00	0,80	0,75	FAUX
22,00	10,00	0,88	0,75	FAUX
24,00	10,00	0,96	0,75	FAUX
26,00	10,00	1,04	0,75	VRAI
28,00	10,00	1,12	0,75	VRAI
30,00	10,00	1,21	0,75	VRAI
32,00	10,00	1,30	0,75	VRAI
34,00	10,00	1,40	0,75	VRAI
36,00	10,00	1,50	0,75	VRAI
38,00	10,00	1,61	0,75	VRAI
40,00	10,00	1,72	0,75	VRAI
10,00	15,00	0,48	0,75	FAUX
12,00	15,00	0,55	0,75	FAUX
14,00	15,00	0,62	0,75	FAUX
16,00	15,00	0,69	0,75	FAUX
18,00	15,00	0,77	0,75	FAUX
20,00	15,00	0,84	0,75	FAUX
22,00	15,00	0,92	0,75	FAUX
24,00	15,00	1,00	0,75	VRAI
26,00	15,00	1,08	0,75	VRAI
28,00	15,00	1,17	0,75	VRAI
30,00	15,00	1,26	0,75	VRAI
32,00	15,00	1,35	0,75	VRAI
34,00	15,00	1,45	0,75	VRAI
36,00	15,00	1,55	0,75	VRAI
38,00	15,00	1,65	0,75	VRAI
40,00	15,00	1,76	0,75	VRAI
10,00	20,00	0,53	0,75	FAUX
12,00	20,00	0,60	0,75	FAUX
14,00	20,00	0,67	0,75	FAUX
16,00	20,00	0,74	0,75	FAUX
18,00	20,00	0,81	0,75	FAUX
20,00	20,00	0,89	0,75	FAUX
22,00	20,00	0,97	0,75	FAUX
24,00	20,00	1,05	0,75	VRAI
26,00	20,00	1,13	0,75	VRAI
28,00	20,00	1,21	0,75	VRAI
30,00	20,00	1,30	0,75	VRAI
32,00	20,00	1,40	0,75	VRAI
34,00	20,00	1,49	0,75	VRAI
36,00	20,00	1,59	0,75	VRAI
38,00	20,00	1,70	0,75	VRAI
40,00	20,00	1,81	0,75	VRAI

φ'	**C'**	**F**	**niv_piez**	**TEST**
10,00	5,00	0,32	1,00	FAUX

12,00	5,00	0,38	1,00	FAUX
14,00	5,00	0,44	1,00	FAUX
16,00	5,00	0,49	1,00	FAUX
18,00	5,00	0,55	1,00	FAUX
20,00	5,00	0,62	1,00	FAUX
22,00	5,00	0,68	1,00	FAUX
24,00	5,00	0,74	1,00	FAUX
26,00	5,00	0,81	1,00	FAUX
28,00	5,00	0,88	1,00	FAUX
30,00	5,00	0,95	1,00	FAUX
32,00	5,00	1,02	1,00	VRAI
34,00	5,00	1,10	1,00	VRAI
36,00	5,00	1,18	1,00	VRAI
38,00	5,00	1,27	1,00	VRAI
40,00	5,00	1,36	1,00	VRAI
10,00	10,00	0,37	1,00	FAUX
12,00	10,00	0,42	1,00	FAUX
14,00	10,00	0,48	1,00	FAUX
16,00	10,00	0,54	1,00	FAUX
18,00	10,00	0,60	1,00	FAUX
20,00	10,00	0,66	1,00	FAUX
22,00	10,00	0,72	1,00	FAUX
24,00	10,00	0,79	1,00	FAUX
26,00	10,00	0,86	1,00	FAUX
28,00	10,00	0,92	1,00	FAUX
30,00	10,00	1,00	1,00	FAUX
32,00	10,00	1,07	1,00	VRAI
34,00	10,00	1,15	1,00	VRAI
36,00	10,00	1,23	1,00	VRAI
38,00	10,00	1,31	1,00	VRAI
40,00	10,00	1,41	1,00	VRAI
10,00	15,00	0,41	1,00	FAUX
12,00	15,00	0,47	1,00	FAUX
14,00	15,00	0,53	1,00	FAUX
16,00	15,00	0,59	1,00	FAUX
18,00	15,00	0,65	1,00	FAUX
20,00	15,00	0,71	1,00	FAUX
22,00	15,00	0,77	1,00	FAUX
24,00	15,00	0,83	1,00	FAUX
26,00	15,00	0,90	1,00	FAUX
28,00	15,00	0,97	1,00	FAUX
30,00	15,00	1,04	1,00	VRAI
32,00	15,00	1,12	1,00	VRAI
34,00	15,00	1,19	1,00	VRAI
36,00	15,00	1,27	1,00	VRAI
38,00	15,00	1,36	1,00	VRAI
40,00	15,00	1,45	1,00	VRAI
10,00	20,00	0,46	1,00	FAUX
12,00	20,00	0,52	1,00	FAUX
14,00	20,00	0,57	1,00	FAUX
16,00	20,00	0,63	1,00	FAUX
18,00	20,00	0,69	1,00	FAUX
20,00	20,00	0,75	1,00	FAUX
22,00	20,00	0,82	1,00	FAUX
24,00	20,00	0,88	1,00	FAUX
26,00	20,00	0,95	1,00	FAUX
28,00	20,00	1,02	1,00	VRAI
30,00	20,00	1,09	1,00	VRAI
32,00	20,00	1,16	1,00	VRAI
34,00	20,00	1,24	1,00	VRAI
36,00	20,00	1,32	1,00	VRAI
38,00	20,00	1,41	1,00	VRAI
40,00	20,00	1,50	1,00	VRAI

Annex 3: Coordinates of the individuals on the new axes F1, F2 for the PCA of the hard layer

Individuals	F1	F2
1	-0,088428677	-0,967878322
2	-0,095228927	-0,718248237
3	0,565197339	-1,01043113
4	2,407037736	-0,958274999
5	2,302426602	-0,507839733
6	0,398889242	-1,125129901
7	0,652273718	2,255765422
8	-0,027808408	2,363444172
9	1,148885689	2,102222594
10	3,272257323	-0,44470056
11	0,076117695	-0,949626855
12	-2,776725721	-2,197211016
13	-2,567846265	-0,506071791
14	-1,913665473	0,032741338
15	-1,794731151	1,448145843
16	-1,651823427	0,821480451
17	-0,839689631	1,377662175
18	0,327828151	1,378324301
19	-0,074801772	-1,324035194
20	0,679835956	-1,070338559